

Washington University in St. Louis

Washington University Open Scholarship

Arts & Sciences Electronic Theses and
Dissertations

Arts & Sciences

Spring 5-15-2016

Metal Selectivity and Acquisition by the Yersiniabactin Metallophore System in Escherichia coli

Eun-Ik Koh

Washington University in St. Louis

Follow this and additional works at: https://openscholarship.wustl.edu/art_sci_etds



Part of the [Biochemistry Commons](#), and the [Microbiology Commons](#)

Recommended Citation

Koh, Eun-Ik, "Metal Selectivity and Acquisition by the Yersiniabactin Metallophore System in Escherichia coli" (2016). *Arts & Sciences Electronic Theses and Dissertations*. 790.

https://openscholarship.wustl.edu/art_sci_etds/790

This Dissertation is brought to you for free and open access by the Arts & Sciences at Washington University Open Scholarship. It has been accepted for inclusion in Arts & Sciences Electronic Theses and Dissertations by an authorized administrator of Washington University Open Scholarship. For more information, please contact digital@wumail.wustl.edu.

WASHINGTON UNIVERSITY IN ST. LOUIS

Division of Biology and Biomedical Sciences
Molecular Microbiology and Microbial Pathogenesis

Dissertation Examination Committee:

Jeffrey P. Henderson, Chair

Peter M. J. Burgers

Michael G. Caparon

James Fleckenstein

Jennifer K. Lodge

Timothy A. Wencewicz

Metal Selectivity and Acquisition by the Yersiniabactin Metallophore System in *Escherichia coli*

By

Eun-Ik Koh

A dissertation presented to the
Graduate School of Arts & Sciences
of Washington University in
partial fulfillment of the
requirements for the degree
of Doctor of Philosophy

May 2016
St. Louis, Missouri

© 2016, Eun-Ik Koh

TABLE OF CONTENTS

	PAGE
List of Figures	iii
List of Tables	v
Acknowledgements	vi
Abstract of the Dissertation	viii
1. Introduction: Microbial copper-binding siderophores at the host-pathogen interface	1
1.1 Siderophores	2
1.2 Uropathogenic <i>E. coli</i> siderophores	3
1.3 Cupric yersiniabactin in human infections	5
1.4 Structural features of biological copper-binding molecules	6
1.5 Copper-binding siderophores as a defense against host-derived copper toxicity	9
1.6 Copper-binding siderophores as a countermeasure against superoxide-based host defenses	11
1.7 Questions and hypotheses	14
2. Metal selectivity by the virulence-associated yersiniabactin metallophore system	30
3. The yersiniabactin-associated ATP binding cassette proteins YbtP and YbtQ enhance <i>E. coli</i> fitness during high titer cystitis	74
4. Metal acquisition by the virulence-associated yersiniabactin metallophore system	109
5. Conclusions, Perspectives and Implications	149
5.1 Summary of the Thesis	150
5.2 Perspectives on metal availability in the urinary tract	151
5.3 Implications and outcomes of metallophore transport	152
5.4 Methodology development and applications	155
5.5 Concluding remarks	156
Curriculum Vitae	165

LIST OF FIGURES

FIGURE		PAGE
CHAPTER ONE		
1	Uropathogenic <i>Escherichia coli</i> siderophores	15
2	Extracellular copper binding molecules	16
3	Copper-binding siderophore functions at the host-pathogen interface	17
CHAPTER TWO		
1	Mass spectrometric neutral loss screen reveals multiple stable metal-Ybt complexes	52
2	MS and MS/MS spectral analyses reveal non-ferric metal-Ybt complexes	53
3	Density function theory (DFT) models structurally differentiate Cu(II)-Ybt complexes	54
4	FyuA and YbtPQ are necessary for Fe(III)-Ybt-dependent growth in pathogenic (UTI89) and non-pathogenic (MG1655) <i>E. coli</i>	55
5	Direct LC-MS/MS detection of cell-associated Fe(III)-Ybt in FyuA-expressing UTI89 and MG1655	56
6	FyuA and TonB-dependent uptake of Cu(II)-Ybt and other non-ferric complexes	57
7	Cu(II)-Ybt does not competitively inhibit Fe(III)-Ybt uptake	59
8	Metal-Ybt transport model	61
S1	Fe(III)-Ybt and <i>apo</i> -Ybt levels do not decrease in presence of excess zinc ions	62
S2	Structural confirmation of metal-Ybt complexes by stable isotope labeling	63
S3	Comparison of neutral Fe(III)-Ybt complexes	64
S4	FyuA and YbtPQ are necessary for Fe(III)-Ybt-dependent growth in UPEC	65
CHAPTER THREE		
1	Genetic organization of UTI89 <i>Yersinia</i> High Pathogenicity Island (HPI)	91
2	YbtPQ is required for Fe(III)-Ybt-dependent growth in UPEC	92
3	YbtPQ is not required for Ybt synthesis in UPEC	93
4	<i>In vivo</i> single strain infections in C3H/HeN mice background	94
5	Bladder intracellular bacterial communities at 6 hours post infection in C3H/HeN mice	95
6	<i>In vivo</i> competitive infection in C3H/HeN mice and <i>in vitro</i> co-culture growth	96
7	<i>In vivo</i> competitive infections in C3H/HeN mice show correlation with bacterial levels	97
8	<i>In vivo</i> competitive infection with C3H/HeOuJ mice	98
9	<i>In vivo</i> single strain infections in C3H/HeOuJ mice backgrounds	99

CHAPTER FOUR		
1	FyuA and YbtPQ are required and sufficient for Fe(III)-Ybt-dependent growth in UPEC	129
2	Direct LC-MS/MS detection of supernatant and cell-associated Fe(III)- and <i>apo</i> -Ybt in FyuA and YbtPQ-expressing UTI89	130
3	Growth of pathogenic <i>E. coli</i> strains under Fe(III)-Ybt-dependent conditions	132
4	Direct LC-MS/MS detection of Fe(III)- and <i>apo</i> -Ybt from pathogenic <i>E. coli</i> culture supernatant	133
5	<i>In vitro</i> iron release from Fe(III)-Ybt complexes	134
6	Direct LC-MS/MS detection of supernatant and cell-associated Ga(III)- and <i>apo</i> -Ybt in FyuA and YbtPQ-expressing UTI89	135
7	Direct LC-MS/MS detection of supernatant and cell-associated Cu(II)-, Ni(II)- and <i>apo</i> -Ybt in FyuA and YbtPQ-expressing UTI89	137
8	Direct detection of ⁶⁴ Cu from cellular ⁶⁴ Cu(II)-Ybt	139
CHAPTER FIVE		
1	Metal transport and delivery by the yersiniabactin metallophore system	158

LIST OF TABLES

TABLE		PAGE
	CHAPTER TWO	
1	Calculated metal-Ybt extinction coefficient values	66
	CHAPTER THREE	
1	UTI89 mutant strains used in this study	100

ACKNOWLEDGEMENTS

This dissertation along with all the scientific and personal growth would not have been possible without the support and encouragement of many individuals. First and foremost, I am extremely grateful to my thesis mentor, Dr. Jeff Henderson. It is difficult to describe all the positive contributions Jeff has made to my development as a scientist. From the very beginning, Jeff has brought patience and enthusiasm to allow me to find confidence and think critically in the lab. He has always been available with helpful advice and has actively opened new opportunities and resources to help pursue my scientific goals. I am truly honored to have been his student.

I am grateful to members of the scientific community at Washington University for their expert guidance and support. I thank my thesis committee for their important contributions to this dissertation and my scientific career. This dissertation would also not have been possible without the kindness and support of the fantastic people I have worked with in the lab. I would especially like to thank Dr. Chia Hung for his humor and guidance from the very beginning. I am also thankful to Jan Crowley, Hung Tran, Dr. Jonas Marschall, Dr. Kaveri Parker, Dr. Robin Shields-Cutler and Shannon Ohlemacher for their enthusiasm, kindness and support. I would also like to acknowledge the expertise and kindness of collaborators, Dr. Daryl Giblin, Dr. Nilantha Bandara and Dr. Buck Rogers. And to my classmates in the Division of Biology and Biomedical Sciences, I am grateful for our friendship over the years.

I would also like to thank mentors and teachers prior to graduate school whose valuable encouragements built the foundations for this thesis. David Hoover and John McCandless encouraged me to develop my scientific thinking in high school. Dr. Steven Blanke and Dr.

Manfredo Seufferheld introduced me to microbial research and provided valuable scientific experiences during my undergraduate years.

I am eternally grateful to my parents, Kwang Ok Koh and Mi Soon Song, and my sister, Eunjin Koh for their love and support. I would not be the person who I am today without my family. Lastly, I would like to thank my wife, Yu Sun Chung. She has been my greatest source of support, friendship and love over the years. I am grateful to share our life journey together.

Eun-Ik Koh

Washington University in St. Louis

May 2016

ABSTRACT FOR THE DISSERTATION

Metal Selectivity and Acquisition by the Yersiniabactin Metallophore System in *Escherichia coli*

By

Eun-Ik Koh

Doctor of Philosophy in Biology and Biomedical Sciences

Molecular Microbiology and Microbial Pathogenesis

Washington University in St. Louis, 2016

Professor Jeffrey P. Henderson, Chair

Urinary tract infections (UTI) are one of the most common bacterial infections, of which, the majority are caused by uropathogenic *Escherichia coli* (UPEC). Many bacterial pathogens including UPEC synthesize and secrete chemically diverse metabolites called siderophores, which are classically defined by their ability of bind and deliver iron(III), an essential nutrient, to pathogens during infections. UPEC isolates can express multiple siderophore systems, of which, the virulence-associated siderophore yersiniabactin (Ybt) binds to both iron(III) and copper(II) during urinary tract infections. In this thesis we show that Ybt interacts with multiple physiologic transition metals and acts as a metallophore system to deliver select metal ions to UPEC. We show Ybt transporters promote bacterial fitness during urinary tract infections, consistent with a pathogenic gain-of-function conferred by the Ybt system to UPEC.

Direct detection of both iron(III) and copper(II) complexes with Ybt during UTI led to the hypotheses that Ybt may interact with additional physiologic transition metals and that these complexes are transport substrates for the Ybt import system. Using a mass spectrometry based

screen, we identified stable trivalent and divalent metal-Ybt complexes that were predicted to use similar coordination sites as iron(III)-Ybt. We used bacterial genetic and quantitative mass spectrometric approaches to show that these complexes are imported into UPEC by the TonB-dependent outer membrane transporter FyuA. Of the metal-Ybt complexes examined, copper(II)-Ybt was predicted to be structurally unique and was the only complex to not competitively inhibit iron(III)-Ybt transport. These results suggest that Ybt can preferentially transport iron in copper-rich environments where copper(II)-Ybt concentrations may exceed those of iron(III)-Ybt.

While the Ybt transport system has been shown to be critical for several Gram-negative pathogens, its role in UPEC during UTI has been unclear. We used bacterial genetics and quantitative mass spectrometric approaches to show that ATP-binding cassette transporters YbtP and YbtQ are necessary for iron(III)-Ybt dependent growth but not Ybt synthesis in UPEC. Using an experimental murine cystitis model and standard liquid culture conditions, we compared the outcome of isogenic wild type and *ybtPQ* mutant strains and found UPEC lacking *ybtPQ* to exhibit significant competitive fitness defect only during high titer infections. These results support a model in which YbtP and Q play an important role in the bladder microenvironment during UPEC pathogenesis.

Combining our findings with metal-Ybt import through FyuA and the importance of YbtP and Q during UPEC infections, we sought to investigate metal-Ybt import through YbtPQ and the fate of intracellular metal-Ybt complexes. Using a combination of bacterial genetics, quantitative mass spectrometry and radiolabeling approaches, we observed that in *fyuA* and *ybtPQ*-expressing

E. coli, both iron and copper are released from their respective intracellular metal-Ybt complex through reduction, with metal-free *apo*-Ybt recycled to the extracellular medium. This was in contrast to intracellular gallium(III)-Ybt, which remained stable with no detectable *apo*-Ybt recycling. These findings are consistent with our model of Ybt as a metallophore system that delivers physiologic transition metals to UPEC. The requirements for iron and copper by UPEC metalloenzymes may therefore be targets for future investigations and therapeutic development.

Together, the work presented in this thesis describes the Ybt system as a multi-level virulence strategy used by UPEC to overcome varying host environments and challenges to metal homeostasis.

CHAPTER ONE

Introduction: Microbial copper-binding siderophores at the host-pathogen interface

1.1 Siderophores

Siderophores (Greek for iron carrier) are a diverse group of specialized ferric iron(III)-binding metabolites that function to supply iron to the microbe and are the subject of classic works in microbial metabolism (1-3). Iron is an essential metal for most bacteria; acting as an essential cofactor in diverse physiological processes including respiration, deoxynucleotide biosynthesis, and DNA replication (4). The evolution of siderophores is viewed as a response to the appearance of O₂ in the early atmosphere which resulted in oxidation of soluble ferrous iron (Fe(II)) to its relatively insoluble ferric form (Fe(III)) (5).

Siderophores are widely synthesized among microbes, with over 500 different siderophores described. These specialized metabolites use a chemically diverse array of metal-binding prosthetic groups, often deployed in varying combinations within a single siderophore. Bacterial siderophore biosynthesis and transporter proteins are translated when intracellular iron is low, classically following transcriptional derepression by the global iron regulator, Fur (ferric uptake repressor) (6, 7). Siderophore biosynthetic pathways can be classified as nonribosomal peptide synthetase/polyketide synthase (NRPS/PKS) dependent or independent systems. NRPS/PKS are large (>350 kD for the yersiniabactin biosynthesis protein *irp1* (8)) multienzyme complexes that use a wide range of cellular substrates to synthesize various metabolites including catecholate and phenolate type siderophores.

Once secreted into the extracellular space, siderophores can bind oxidized metal ions with remarkably high affinities (9). Ferric siderophore complexes are subsequently recognized and internalized through siderophore-specific transport machinery in bacterial inner and outer

membranes. Transport through the Gram-negative outer membrane transporters occurs through specialized proteins associated with the TonB protein complex, which transduces energy from the cytoplasmic proton motive force (3, 10, 11). Inner membrane ATP-binding cassette transporters in both Gram-negative and Gram-positive organisms transport ferric siderophore complexes, or the iron released from them, to the cytoplasm (12-16). Once ferric siderophores are internalized, their intracellular fate varies between different siderophores, with reported examples of Fe(III) reduction to Fe(II) or Fe(III)-siderophore hydrolysis. All or part of the siderophore may be recycled and used again after releasing its metal ion cargo (17, 18).

Although pathogens often carry multiple iron acquisition systems that are redundant in laboratory culture conditions, siderophore-dependent systems appear to play specialized roles at the host-pathogen interface (16, 17, 19, 20). Specifically, siderophores have been ascribed roles in liberating ferric ions bound to host iron storage proteins or sequestered away from pathogens within distinctive compartments. As such, siderophores have long been considered a microbial solution to low iron availability imposed by microenvironments in the infected host (21).

1.2 Uropathogenic *E. coli* siderophores

E. coli recovered from infected patients or animals often synthesize different siderophores types spanning three chemical families in addition to the prototypical, genetically-conserved enterobactin siderophore system (Fig. 1) (22). Although unnecessary for growth in standard culture conditions, multiple siderophore genes are upregulated during *E. coli* urinary tract infections (23, 24) and siderophore biosynthesis in this disease has been demonstrated by direct mass spectrometric detection (25). The multiplicity of siderophores synthesized by these

uropathogenic *E. coli* strains raises the question of why bacteria would commit scarce cellular resources to synthesize chemically distinctive siderophores with a common recognized function (26).

One reason pathogenic bacteria may synthesize multiple siderophore types emerged from the finding that the inflammation-associated protein siderocalin (SCN, also known as lipocalin 2 [Lcn2], NGAL, or 24p3) can tightly bind the ferric complex of the prototypical *E. coli* siderophore enterobactin, rendering its iron cargo inaccessible to bacteria (27). In contrast, functional data with siderophores synthesized from the three genetically non-conserved *E. coli* siderophore systems (salmochelin, yersiniabactin and aerobactin) suggests that these do not bind to SCN, leading to their categorization as “stealth siderophores” along with other *non-E. coli* siderophores with this property. SCN-deficient mice exhibit increased susceptibility to bloodstream infections with *E. coli* that produce enterobactin as its sole siderophore, consistent with a physiologic role for this SCN-enterobactin binding interaction (28, 29). In the human urinary environment this situation can be reversed, with enterobactin becoming necessary to liberate iron from SCN-bound ferric complexes that form with urinary catechol metabolites (30).

An additional rationale for synthesizing salmochelin (a more polar, glucose conjugated version of enterobactin) is suggested by measurements showing that this siderophore partitions into cellular membranes less than enterobactin, which may allow it to more effectively scavenge ferric ions in membrane rich host environments (31). Finally, using siderophores with different pH optima for ferric ion binding may allow uropathogenic *E. coli* to adapt to a wider range of host environments. Aerobactin, for example, may be a better iron scavenger in low pH

environments where protonation diminishes the ferric ion affinity of catecholate siderophores (32, 33). Together, these findings suggest that siderophores' remarkable chemical diversity – even within a single bacterial strain – may represent chemical co-evolutionary responses to numerous selective pressures within vertebrate hosts.

1.3 Cupric yersiniabactin in human infections

The phenolate/thiazoline-based yersiniabactin (Ybt) siderophore system was first described in pathogenic *Yersinia* species and subsequently found to be the most frequently-expressed, genetically non-conserved siderophore system in uropathogenic *E. coli* (22, 34-36). Ybt is synthesized by a large NRPS/PKS complex that has been successfully reconstituted *in vitro* and assembles Ybt through a succession of phosphopantethiene-bound intermediates (37, 38). These biosynthetic genes are encoded alongside metabolic, transport, and transcription factor genes in the genetically mobile, multi-operon *Yersinia* High Pathogenicity Island (11, 39).

Although siderophores are known for ferric metal binding, *in vitro* binding of non-ferric metal ions has been widely noted (40-44). To identify the metals that bind Ybt in a biologically relevant environment, *Chaturvedi et al.* devised a liquid chromatography-constant neutral loss (LC-CNL) mass spectrometric screen using a yersiniabactin-specific MS/MS fragmentation pathway. When Ybt was mixed with pooled urine samples from healthy human donors, LC-CNL screen identified a chromatographic peak corresponding to a new metal-yersiniabactin complex. Accurate mass values and isotope pattern matched that of a cupric yersiniabactin (Cu(II)-Ybt) complex. This complex was replicated using defined components *in vitro* when Ybt was titrated with cupric sulfate solution, producing a visibly blue-colored complex. LC-MS/MS analysis

detected Cu(II)-Ybt in urine from urinary tract infection patients infected with yersiniabactin-producing *E. coli*, demonstrating the physiologic relevance of copper binding by yersiniabactin. Cu(II)-Ybt was also detected in urine and bladder tissue from mice experimentally infected with UTI89, a model yersiniabactin-producing uropathogenic *E. coli* strain. Interestingly, the Cu(II)-Ybt/Fe(III)-Ybt molar ratio in both human and mouse specimens was consistently greater than 1, suggesting that Ybt binds host-derived copper at least as extensively as Fe(III) during infections (25).

These findings provide direct mass spectrometric evidence that yersiniabactin is produced during human urinary tract infections and that metal availability and yersiniabactin metal affinities are such that copper complexes exceed iron complexes. The observed excess copper complexes may reflect host responses that limit siderophore-accessible iron (nutritional immunity) as well as inflammation-associated processes that increase copper availability at the host-pathogen interface (19, 45, 46). The presence of a virulence-associated, copper-binding siderophore in *E. coli* may reflect an adaptive response to the distinctive physiologic metal composition that arises in infection microenvironments (21). Yersiniabactin may play a similar role in *Yersinia pestis*, where it is linked to virulence in experimental animal models (12, 47). Common structural features of yersiniabactin and other biological copper-binding molecules may facilitate identification of analogous biological copper carriers in other microbial pathogens.

1.4 Structural features of biological copper-binding molecules

Although yersiniabactin is currently the best-described example of a siderophore shown to bind copper in the host, other examples may await discovery. Structural features of well-known

extracellular copper carriers may assist identification of currently unappreciated copper binders among pathogen-associated siderophores. In the mammalian host, the prototypical extracellular copper carrier is ceruloplasmin, which carries up to 95% of circulating copper and rises and falls with copper excess and deficiency, respectively (48). A ~2kD urinary copper-binding molecule has also been observed in copper-overloaded mice but has not been structurally characterized (49). Copper ions bound to ceruloplasmin are critical components of its multicopper oxidase function, which is essential for normal mammalian iron homeostasis. Ceruloplasmin harbors 6 copper atoms in three distinct copper sites as is typical of the conserved multicopper oxidase family (50). Ceruloplasmin contains three type I “blue copper” sites, two of which coordinate a single copper ion using a cysteine residue, a methionine residue and two histidine residues (Fig. 2a). The other three copper ions form a histidine-rich trinuclear copper cluster in which four histidine imidazole nitrogens coordinate one Type II copper and three histidine residues coordinate two Type III copper ions (51). These six copper atoms are required to achieve the final conformation-driven state, and are incorporated during ceruloplasmin biosynthesis late in the secretory pathway (52). Although an array of negatively charged groups might effectively coordinate copper, it is notably that cuproproteins often use histidine imidazole nitrogens for this purpose. Indeed this is a useful basis for identifying new cuproproteins from genomic databases (53, 54). Incorporation of analogous nitrogen-containing heterocycles into protein and non-protein microbial products may confer a similar copper binding preference.

Among prokaryotes, a new family of copper binding, siderophore-like, natural products has recently been described among methanotrophic Gram-negative bacteria from environmental sources. Methanobactins (Mb) are a family of small molecules secreted into the extracellular

space to scavenge copper for nutritional purposes (for detailed review, see (42)). These chalkophores (Greek for copper carriers) help satisfy the high copper demand resulting from biosynthesis of particulate methane monooxygenase, which permits methanotrophs to use methane as their sole carbon source (55, 56). There are numerous similarities between Mb and Gram-negative bacterial siderophores systems. Gram-negative siderophores and Mb are actively transported through the outer membrane by TonB-dependent transporters, and possess distinctive heterocyclic structural elements involved in metal binding (43, 57). As in most cuproproteins, biophysical studies of Mb implicate heterocyclic nitrogens (oxazolones for Mb) in copper ion coordination (Fig. 2b). Use of these chemical groups to bind copper in Mb raise the possibility that previously-described mechanisms for nitrogen heterocycle incorporation into other peptides and natural products (reviewed by Walsh *et al.* (58)) may facilitate copper binding in some of these molecules.

Yersiniabactin is a nonribosomal peptide synthase/polyketide synthase (NRPS/PKS) product that lacks the peptide backbone of Mb and possesses three nitrogen-sulfur heterocycles whose nitrogens participate in co-planar ferric ion binding identified in crystallographic structures (59, 60). Quantum mechanical modeling using density functional theory (DFT) predicts similar coordination environment for Cu(II)-Ybt, in which the three heterocyclic nitrogens (two thiazoline and one thiazolidine) and the phenolate oxygen contribute to a typical square planar configuration around Cu(II) (Fig. 2c). However in contrast to other metal-Ybt complexes, Cu(II)-Ybt is predicted to exist as two closely related linkage isomers with one having an open penta-coordinate site arising from differential interaction with the terminal carboxylic acid group (61, 62). A similar phenolate-thiazoline role in copper-binding may occur with pyochelin, a related

siderophore from the opportunistic pathogen *Pseudomonas aeruginosa*, in which UV/visible analysis indicates formation of an *in vitro* Cu(II) complex (41). The consistent appearance of nitrogen-containing heterocycles in ceruloplasmin, methanobactin, and yersiniabactin metal-binding sites suggests a particularly important role for this structural element in binding copper. More examples of copper-binding molecules are necessary to properly evaluate this association and to predict biologically meaningful copper binding activity among microbial siderophores.

1.5 Copper-binding siderophores as a defense against host-derived copper toxicity

Secreted copper-binding molecules may have evolved in pathogens to neutralize the antibacterial activity of copper (for recent reviews, see (46, 63, 64)). While inflammatory responses classically limit transition metal bioavailability, copper appears to be a notable exception. Several works report unchanged or increased systemic and local copper availability during infections (65-68). More recently, *White et al.*, have shown ATP7A-mediated copper trafficking from the Golgi apparatus to *E. coli*-containing phagosomes, consistent with a bactericidal system that targets phagocytosed microorganisms (45). Within this restricted phagosomal space, ($\sim 1.2 \times 10^{-15}$ L (69)) toxic levels of copper sufficient to kill microbes may be rapidly achieved.

Consistent with an important role for copper-based host defenses, uropathogenic *E. coli* isolates have been observed to exhibit greater copper resistance than intestinal isolates in urinary tract infection patients. Yersiniabactin synthesis was associated with copper resistance in these isolates and a causative association was supported by a significant decrease in resistance by yersiniabactin-null mutants and a significant increase in resistance following supplementation with purified yersiniabactin (25). A similar relationship was observed in *Pseudomonas*

aeruginosa, where synthesis of the virulence-associated siderophores pyochelin and pyoverdine (70, 71) increased copper resistance (72). Furthermore *Pseudomonas aeruginosa* with deficiency in copper detoxification system showed reduced virulence, though connections with pyochelin and pyoverdine were unexplored (73). Further studies will be necessary to examine how Cu(I) in the phagosome is oxidized to Cu(II) for yersiniabactin binding. The bacterial periplasmic multi-copper oxidase, CueO, has been suggested to oxidize Cu(I) to Cu(II) (74, 75). These copper defense systems may thus work in tandem with yersiniabactin and related siderophores to sequester Cu(II) ions.

Not all siderophores protect against copper toxicity. Catecholate siderophores in *E. coli* sensitized them to copper toxicity, an effect linked to Cu(II) reduction by catechols to the more cytotoxic Cu(I) ion (25, 74, 76). When bound to yersiniabactin, catechols were unable to reduce Cu(II) (25). In the presence of copper ions, yersiniabactin may thus protect *E. coli* by preventing enterobactin-mediated Cu(I) formation (Fig. 3). It is however unclear whether aerobactin is similarly involved in strains that produce this siderophore.

The mechanism of copper toxicity in bacteria is incompletely understood. Cu(I) toxicity through Fenton reaction-mediated hydroxyl radical (OH[•]) generation has long been proposed to be an important mechanism, although observations that copper-loaded *E. coli* are more – not less – resistant to hydrogen peroxide suggests that Fenton chemistry alone is an inadequate explanation (77). Recent works instead point to a major role for cytoplasmic Cu(I) in dissociating iron-sulfur clusters and thereby interfering with multiple metabolic processes including heme and branched chain amino biosynthesis (78-80). This mechanism finds additional support from the finding that

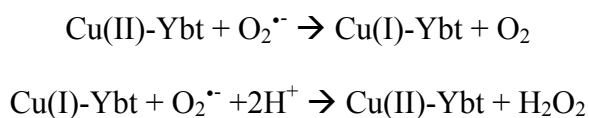
metal ions that do not act as Fenton reagents but also disrupt iron-sulfur clusters exert similar toxicity (81, 82). While further studies are needed to dissect the toxic activities of copper, these results point to the ability of yersiniabactin to prevent free copper from reaching the cytoplasm as an important virulence function.

A pathogenic role for yersiniabactin copper binding was assessed in a version of the macrophage survival assay first described by *White et al.* (45). In this study, a yersiniabactin-deficient uropathogenic *E. coli* was profoundly sensitized to intracellular killing by macrophage-like RAW264.7 cells relative to its yersiniabactin-proficient isogenic wild type control (61). The yersiniabactin-null phenotype was abolished when copper-deficient RAW264.7 cells were used. This sensitization phenotype was similar to that observed for a K12 *E. coli* strain lacking the copper efflux pump CopA (83). Overall, these results are consistent with yersiniabactin sequestration of phagosomal copper ions as a contributor to intracellular survival. Together, these findings support a role for non-reducing, copper-binding siderophores in protecting pathogens from copper-based host defenses.

1.6 Copper-binding siderophores as a countermeasure against superoxide-based host defenses

Phagocytes are a classic host defense against invading microbial pathogens and the copper-dependent ATP7A bactericidal system described by *White et al.* is one of several chemical defenses deployed by these cells (45). Also notable among these defenses is the “respiratory burst”, in which a membrane-bound NADPH oxidase generates superoxide anion ($O_2^{\bullet-}$) within the phagosome (84).

Yersiniabactin synthesis was implicated in resisting superoxide-dependent host defenses through the observation that the yersiniabactin-dependent intracellular survival phenotype requires both copper and NADPH oxidase activity (61). Subsequent studies identified a soluble superoxide dismutase-like activity in UPEC-conditioned media that was similarly dependent upon yersiniabactin biosynthesis and copper supplementation. Chromatographic fractionation and mass spectrometric analysis associated this soluble SOD-like activity to Cu(II)-Ybt. Purified Cu(II)-Ybt exhibited SOD-like activity that was also observed upon substitution of Cu(II) with Fe(III) but not with non-redox active gallium (III), consistent with a catalytic requirement for redox active metal. Unlike previously-described cupric salicylate complexes with SOD-like activity, Cu(II)-Ybt retained its activity in the presence of protein, which acts as a competitive copper chelator (61). These data are consistent with the ability of non-protein Cu(II)-Ybt complexes to catalyze superoxide dismutation as follows:



Density functional theory-based quantum simulations of this catalytic cycle supported a key role for copper redox cycling during coordination by the phenolate, thiazoline, and thiazolidine groups in yersiniabactin (61). There is evidence that the thiolate and heteroaromatic ring coordination sites of methanobactin may support a similar catalytic cycle (85). Although the catalytic activity of Cu(II)-Ybt does not exceed that of periplasmic Cu, Zn-SOD, the extracellular localization of yersiniabactin would be expected to place it in closer proximity to

the superoxide source (the host NADPH oxidase complex) where it may be more effective. Cu(II)-Ybt catalysis may further benefit the pathogen through its lower metabolic cost of production and its likely ability to avoid proteolysis, which may permit substantial accumulation within the phagosome. Siderophore-based catalysts that take advantage of host-supplied copper may therefore be well-suited to this distinctive host environment (86) (Fig. 3).

An analogous protective role for an extracellular copper-binding protein was recently suggested by *Gleason et al.*, in the human fungal pathogen *Candida albicans* (87). Candidal SOD5 was found to possess an open active site that readily captures extracellular copper for its activity.

Although it lacks the zinc-binding site, it is otherwise structurally homologous to Cu, Zn-SODs and rapidly reacts with superoxide with rates approaching the dismutase limit (87).

Yersiniabactin and SOD5 may thus use similar strategies to catalyze superoxide dismutation through spontaneous capture and immobilization of host-supplied, extracellular copper. A more detailed investigation of copper-based dismutation catalysts in this context will require an improved biochemical understanding of the role of superoxide in microbial killing. Nevertheless, it appears likely that additional examples of this survival strategy await discovery among invasive, disease-associated microorganisms.

The surprising ability of yersiniabactin production to modulate copper-dependent intracellular survival underscores that there is still much to learn about transition metal interactions at the host-pathogen interface. As the phagosome matures, metal content, pH, and redox potential may change dramatically (for recent reviews, see (88, 89)). Future measurements of the binding

affinity of yersiniabactin for Cu(II) and Cu(I), both of which may be present within the phagosome, would aid these investigations.

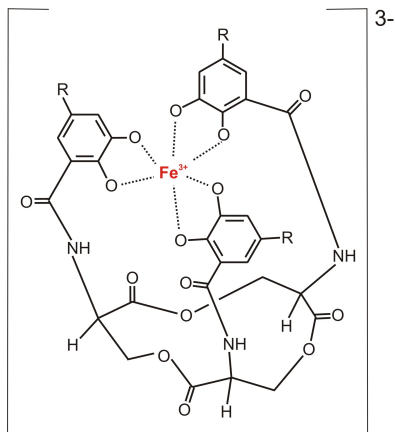
1.7 Questions and hypotheses

While Ybt's interactions with copper has largely focused on its extracellular protective roles, the role of Ybt in delivering copper to pathogens has been unclear. Methanobactin is a notable precedent for a siderophore-like small molecule that scavenges and delivers copper (a chalkophore) to bacteria. While methanotrophic Gram-negative bacteria use methanobactin to support exceptional copper demands associated with particulate methane monooxygenase biosynthesis (56, 57), it remains unclear whether pathogenic bacteria benefit from a similar strategy. Copper is an important cofactor in multiple bacterial enzymes including NADH dehydrogenase, cytochrome oxidase and copper, zinc superoxide dismutases (53). Furthermore, Gram-negative cuproenzymes such as Cu, Zn-SOD have been described to receive copper in the periplasmic compartment (90). Therefore we hypothesized that Ybt may act as a metallophore to deliver iron and copper to uropathogenic *E. coli*. To investigate this hypothesis, this thesis examines the following questions:

1. Does Ybt interact with other physiologic metals in addition to iron(III) and copper(II)?
2. Are non-iron metal-Ybt complexes transport substrates of the Ybt import system? If so, what is the fate of intracellular metal-Ybt complexes?
3. How does the Ybt transport system affect uropathogenic *E. coli* pathogenesis?

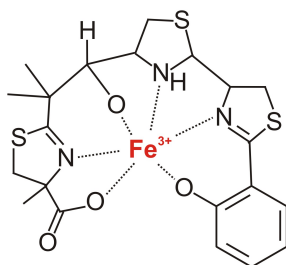
CHAPTER ONE: FIGURES

Catecholate Type



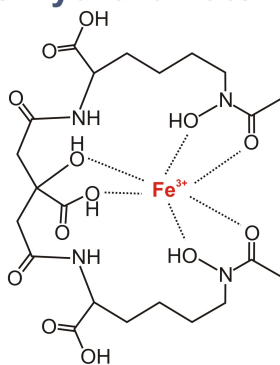
Enterobactin **R** = H
Salmochelin **R** = Glucose

Phenolate-Thiazoline Type



Yersiniabactin

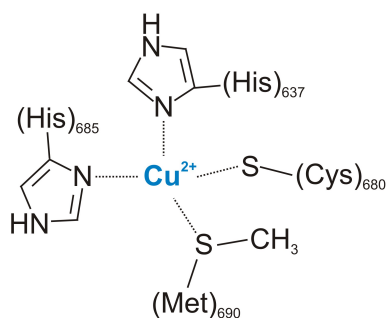
Citrate-Hydroxamate Type



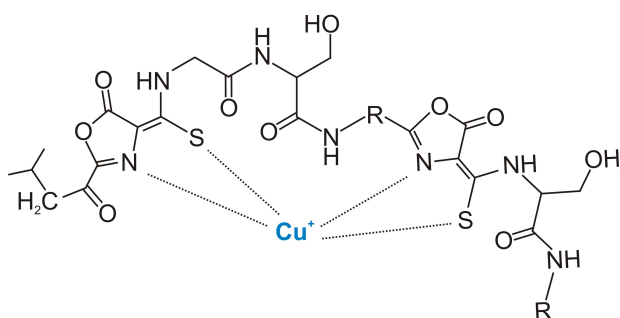
Aerobactin

Figure 1. Uropathogenic *Escherichia coli* siderophores. Pathogenic *E. coli* isolates synthesize multiple siderophore types known to coordinate Fe(III) with a variety of functional groups (22).

a Ceruloplasmin - Type I copper center



b Methanobactin



c Yersiniabactin

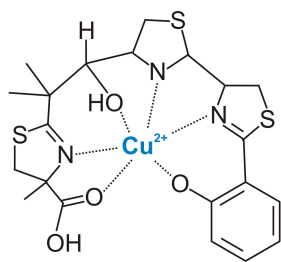


Figure 2. Extracellular copper binding molecules. **a)** Ceruloplasmin has six copper-binding sites of which three are type I copper centers coordinated with two histidine residues, a cysteine residue and a methionine residue (48). **b)** Methanobactin structures contain a recognizable peptide backbone with distinctive oxazolone heterocycles, which are implicated in copper ion coordination (43). **c)** Yersiniabactin has three heterocyclic nitrogens (two thiazoline and one thiazolidine) that contribute to a square planar configuration around Cu(II) alongside the phenolate oxygen (61).

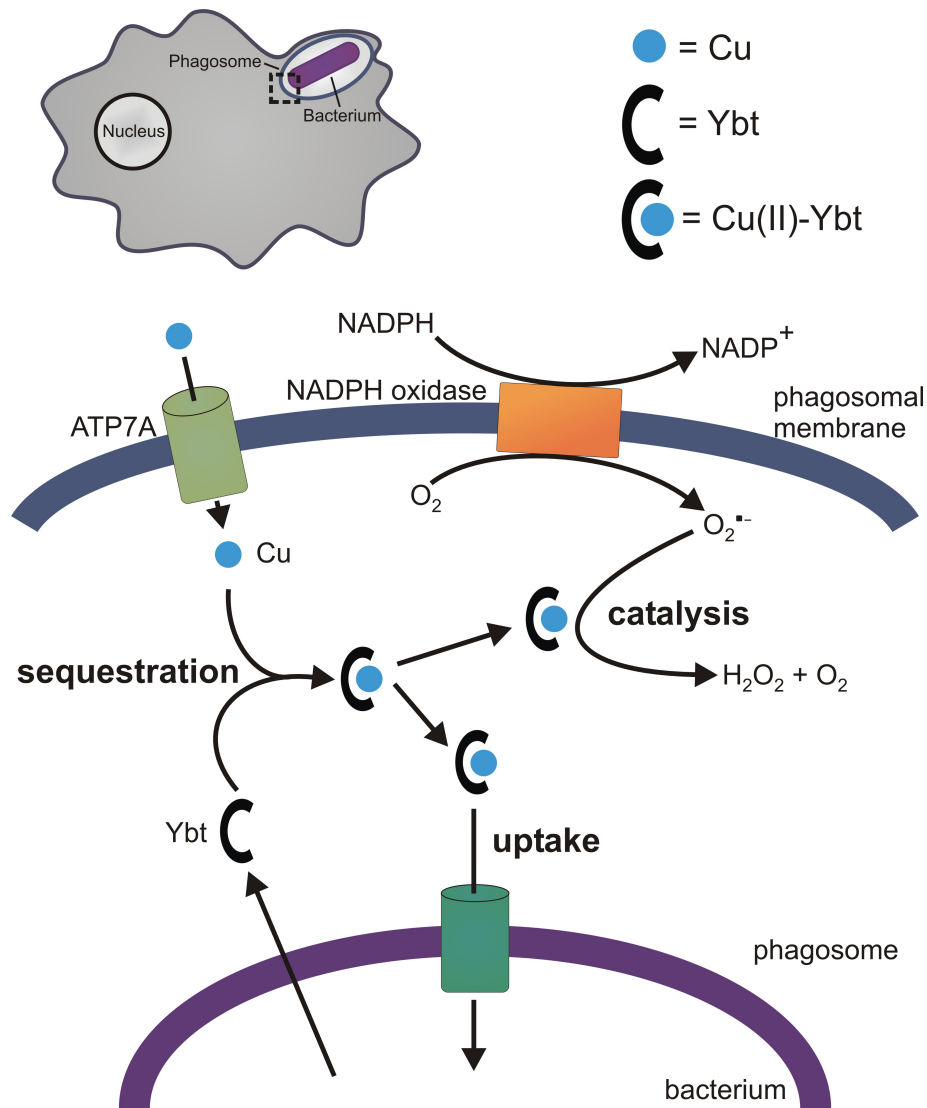


Figure 3. Copper-binding siderophore functions at the host-pathogen interface. Within the phagosomal compartments of host phagocytic cells (upper left), yersiniabactin may protect bacterial pathogens by sequestering toxic copper ions translocated by ATP7A into the phagosome (25,45). The resulting Cu(II)-Ybt complex may further protect the host by catalyzing superoxide dismutation to counter superoxide-based host defenses (61). In phagosomal or non-phagosomal environments characterized instead by copper scarcity, *E. coli* may import Cu(II)-Ybt as a nutritional copper source.

CHAPTER ONE: REFERENCES

1. Neilands, J. B. (1995) Siderophores: structure and function of microbial iron transport compounds. *The Journal of biological chemistry* **270**, 26723-26726
2. Miethke, M., and Marahiel, M. A. (2007) Siderophore-based iron acquisition and pathogen control. *Microbiology and Molecular Biology Reviews* **71**, 413-451
3. Chu, B. C., Garcia-Herrero, A., Johanson, T. H., Krewulak, K. D., Lau, C. K., Peacock, R. S., Slavinskaya, Z., and Vogel, H. J. (2010) Siderophore uptake in bacteria and the battle for iron with the host; a bird's eye view. *Biometals* **23**, 601-6111
4. Andreini, C., Bertini, I., Cavallaro, G., Holliday, G. L., and Thornton, J. M. (2008) Metal ions in biological catalysis: from enzyme databases to general principles. *Journal of biological inorganic chemistry : JBIC : a publication of the Society of Biological Inorganic Chemistry* **13**, 1205-1218
5. Neilands, J. B. (1981) Microbial iron compounds. *Annu. Rev. Biochem.* **50**, 715-731
6. Bagg, A., and Neilands, J. B. (1987) Ferric uptake regulation protein acts as a repressor, employing iron (II) as a cofactor to bind the operator of an iron transport operon in *Escherichia coli*. *Biochemistry* **26**, 5471-5477
7. Fetherston, J. D., Bearden, S. W., and Perry, R. D. (1996) YbtA, an AraC-type regulator of the *Yersinia pestis* pesticin/yersiniabactin receptor. *Mol. Microbiol.* **22**, 315-325
8. Gehring, A. M., DeMoll, E., Fetherston, J. D., Mori, I., Mayhew, G. F., Blattner, F. R., Walsh, C. T., and Perry, R. D. (1998) Iron acquisition in plague: modular logic in enzymatic biogenesis of yersiniabactin by *Yersinia pestis*. *Chem. Biol.* **5**, 573-586
9. Harris, W. R., Carrano, C. J., Cooper, S. R., Sofen, S. R., Avdeef, A. E., McArdle, J. V., and Raymond, K. N. (1979) Coordination chemistry of microbial iron transport

- compounds. 19. Stability constants and electrochemical behavior of ferric enterobactin and model complexes. *J. Am. Chem. Soc.* **101**
10. Noinaj, N., Guillier, M., Barnard, T. J., and Buchanan, S. K. (2010) TonB-Dependent Transporters: Regulation, Structure, and Function. *Annu. Rev. Microbiol.*, 43-60
 11. Perry, R. D., and Fetherston, J. D. (2011) Yersiniabactin iron uptake: mechanisms and role in *Yersinia pestis* pathogenesis. *Microbes and infection / Institut Pasteur* **13**, 808-817
 12. Fetherston, J. D., Bertolino, V. J., and Perry, R. D. (1999) YbtP and YbtQ: two ABC transporters required for iron uptake in *Yersinia pestis*. *Mol. Microbiol.* **32**, 289-299
 13. Raymond, K. N., Dertz, E. A., and Kim, S. S. (2003) Enterobactin: an archetype for microbial iron transport. *Proc. Natl. Acad. Sci. U. S. A.* **100**, 3584-3588
 14. Schalk, I. J. (2008) Metal trafficking via siderophores in Gram-negative bacteria: specificities and characteristics of the pyoverdine pathway. *J. Inorg. Biochem.* **102**, 1159-1169
 15. Brem, D., Pelludat, C., Rakin, A., Jacobi, C. A., and Heesemann, J. (2001) Functional analysis of yersiniabactin transport genes of *Yersinia enterocolitica*. *Microbiology* **147**, 1115-1127
 16. Rodriguez, G. M., and Smith, I. (2006) Identification of an ABC transporter required for iron acquisition and virulence in *Mycobacterium tuberculosis*. *J. Bacteriol.* **188**, 424-430
 17. Miethke, M., and Marahiel, M. A. (2007) Siderophore-based iron acquisition and pathogen control. *Microbiology and molecular biology reviews : MMBR* **71**, 413-451
 18. Brickman, T. J., and McIntosh, M. A. (1992) Overexpression and purification of ferric enterobactin esterase from *Escherichia coli*. Demonstration of enzymatic hydrolysis of enterobactin and its iron complex. *The Journal of biological chemistry* **267**, 12350-12355

19. Hood, M. I., and Skaar, E. P. (2012) Nutritional immunity: transition metals at the pathogen–host interface. *Nature Reviews Microbiology* **10**, 525-537
20. Fetherston, J. D., Kirillina, O., Bobrov, A. G., Paulley, J. T., and Perry, R. D. (2010) The yersiniabactin transport system is critical for the pathogenesis of bubonic and pneumonic plague. *Infect. Immun.* **78**, 2045-2052
21. Prentice, A. M., Ghattas, H., and Cox, S. E. (2007) Host-Pathogen Interactions: Can Micronutrients Tip the Balance? *The Journal of Nutrition*, 1334-1337
22. Henderson, J. P., Crowley, J. R., Pinkner, J. S., Walker, J. N., Tsukayama, P., Stamm, W. E., Hooton, T. M., and Hultgren, S. J. (2009) Quantitative Metabolomics Reveals an Epigenetic Blueprint for Iron Acquisition in Uropathogenic Escherichia coli. *PLoS Pathog.* **5**
23. Hagan, E. C., Lloyd, A. L., Rasko, D. A., Faerber, G. J., and Mobley, H. L. T. (2010) Escherichia coli Global Gene Expression in Urine from Women with Urinary Tract Infection. *PLoS Pathog.* **6**
24. Reigstad, C. S., Hultgren, S. J., and Gordon, J. I. (2007) Functional genomic studies of uropathogenic Escherichia coli and host urothelial cells when intracellular bacterial communities are assembled. *The Journal of biological chemistry* **282**, 21259-21267
25. Chaturvedi, K. S., Hung, C. S., Crowley, J. R., Stapleton, A. E., and Henderson, J. P. (2012) The siderophore yersiniabactin binds copper to protect pathogens during infection. *Nat. Chem. Biol.*
26. Lv, H., Hung, C. S., and Henderson, J. P. (2014) Metabolomic analysis of siderophore cheater mutants reveals metabolic costs of expression in uropathogenic Escherichia coli. *J. Proteome Res.* **13**, 1397-1404

27. Goetz, D. H., Holmes, M. A., Borregaard, N., Bluhm, M. E., Raymond, K. N., and Strong, R. K. (2002) The neutrophil lipocalin NGAL is a bacteriostatic agent that interferes with siderophore-mediated iron acquisition. *Mol. Cell* **10**, 1033-1043
28. Berger, T., Togawa, A., Duncan, G. S., Elia, A. J., You-Ten, A., Wakeham, A., Fong, H. E., Cheung, C. C., and Mak, T. W. (2006) Lipocalin 2-deficient mice exhibit increased sensitivity to *Escherichia coli* infection but not to ischemia-reperfusion injury. *Proc. Natl. Acad. Sci. U. S. A.* **103**, 1834-1839
29. Flo, T. H., Smith, K. D., Sato, S., Rodriguez, D. J., Holmes, M. A., Strong, R. K., Akira, S., and Aderem, A. (2004) Lipocalin 2 mediates an innate immune response to bacterial infection by sequestering iron. *Nature* **432**, 917-921
30. Shields-Cutler, R. R., Crowley, J. R., Hung, C. S., Stapleton, A. E., Aldrich, C. C., Marschall, J., and Henderson, J. P. (2015) Human Urinary Composition Controls Siderocalin's Antibacterial Activity. *J. Biol. Chem.*
31. Luo, M., Lin, H., Fischbach, M. A., Liu, D. R., Walsh, C. T., and Groves, J. T. (2006) Enzymatic tailoring of enterobactin alters membrane partitioning and iron acquisition. *ACS Chem. Biol.* **1**, 29-32
32. Valdebenito, M., Crumbliss, A. L., Winkelmann, G., and Hantke, K. (2006) Environmental factors influence the production of enterobactin, salmochelin, aerobactin, and yersiniabactin in *Escherichia coli* strain Nissle 1917. *International journal of medical microbiology : IJMM* **296**, 513-520
33. Abergel, R. J., Warner, J. A., Shuh, D. K., and Raymond, K. N. (2006) Enterobactin protonation and iron release: structural characterization of the salicylate coordination shift in ferric enterobactin. *J. Am. Chem. Soc.* **128**, 8920-8931

34. Haag, H., Hantke, K., Drechsel, H., Stojiljkovic, I., Jung, G., and Zahner, H. (1993) Purification of yersiniabactin: a siderophore and possible virulence factor of *Yersinia enterocolitica*. *J. Gen. Microbiol.* **139**, 2159-2165
35. Heesemann, J., Hantke, K., Vocke, T., Saken, E., Rakin, A., Stojiljkovic, I., and Berner, R. (1993) Virulence of *Yersinia enterocolitica* is closely associated with siderophore production, expression of an iron-repressible outer membrane polypeptide of 65,000 Da and pesticin sensitivity. *Mol. Microbiol.* **8**, 397-408
36. Mabbetta, A. N., Uletta, G. C., Watts, R. E., Treea, J. J., Totsikaa, M., Onga, C.-I. Y., Wooda, J. M., Monaghanb, W., Lookec, D. F., Nimmod, G. R., Svanborge, C., and Schembria, M. A. (2009) Virulence properties of asymptomatic bacteriuria *Escherichia coli*. *Int. J. Med. Microbiol.*
37. Mazur, M. T., Walsh, C. T., and Kelleher, N. L. (2003) Site-specific observation of acyl intermediate processing in thiotemplate biosynthesis by fourier transform mass spectrometry: the polyketide module of yersiniabactin synthetase. *Biochemistry* **42**, 13393-13400
38. Miller, D. A., Luo, L., Hillson, N., Keating, T. A., and Walsh, C. T. (2002) Yersiniabactin synthetase: a four-protein assembly line producing the nonribosomal peptide/polyketide hybrid siderophore of *Yersinia pestis*. *Chem. Biol.* **9**, 333-344
39. Benedek, O., and Schubert, S. (2007) Mobility of the *Yersinia* High-Pathogenicity Island (HPI): transfer mechanisms of pathogenicity islands (PAIS) revisited (a review). *Acta Microbiol. Immunol. Hung.* **54**, 89-105
40. Hannauer, M., Braud, A., Hoegy, F., Ronot, P., Boos, A., and Schalk, I. J. (2012) The PvdRT-OpmQ efflux pump controls the metal selectivity of the iron uptake pathway

- mediated by the siderophore pyoverdine in *Pseudomonas aeruginosa*. *Environ. Microbiol.* **14**, 1696-1708
41. Brandel, J., Humbert, N., Elhabiri, M., Schalk, I. J., Mislin, G. L., and Albrecht-Gary, A. M. (2012) Pyochelin, a siderophore of *Pseudomonas aeruginosa*: physicochemical characterization of the iron(III), copper(II) and zinc(II) complexes. *Dalton transactions* **41**, 2820-2834
 42. Kenney, G. E., and Rosenzweig, A. C. (2012) Chemistry and biology of the copper chelator methanobactin. *ACS Chem. Biol.* **7**, 260-268
 43. Kim, H. J., Graham, D. W., DiSpirito, A. A., Alterman, M. A., Galeva, N., Larive, C. K., Asunskis, D., and Sherwood, P. M. (2004) Methanobactin, a copper-acquisition compound from methane-oxidizing bacteria. *Science* **305**, 1612-1615
 44. Ecker, D. J., and Emery, T. (1983) Iron uptake from ferrichrome A and iron citrate in *Ustilago sphaerogena*. *J. Bacteriol.* **155**, 616-622
 45. White, C., Lee, J., Kambe, T., Fritsche, K., and Petris, M. J. (2009) A role for the ATP7A copper-transporting ATPase in macrophage bactericidal activity. *The Journal of biological chemistry* **284**, 33949-33956
 46. Fu, Y., Chang, F. M., and Giedroc, D. P. (2014) Copper transport and trafficking at the host-bacterial pathogen interface. *Acc. Chem. Res.* **47**, 3605-3613
 47. Bearden, S. W., Fetherston, J. D., and Perry, R. D. (1997) Genetic organization of the yersiniabactin biosynthetic region and construction of avirulent mutants in *Yersinia pestis*. *Infect. Immun.* **65**, 1659-1668
 48. Hellman, N. E., and Gitlin, J. D. (2002) Ceruloplasmin metabolism and function. *Annu. Rev. Nutr.* **22**, 439-458

49. Gray, L. W., Peng, F., Molloy, S. A., Pendyala, V. S., Muchenditsi, A., Muzik, O., Lee, J., Kaplan, J. H., and Lutsenko, S. (2012) Urinary copper elevation in a mouse model of Wilson's disease is a regulated process to specifically decrease the hepatic copper load. *PLoS One* **7**, e38327
50. Messerschmidt, A., and Huber, R. (1990) The blue oxidases, ascorbate oxidase, laccase and ceruloplasmin. Modelling and structural relationships. *European journal of biochemistry / FEBS* **187**, 341-352
51. Zaitseva, I., Zaitsev, V., Card, G., Moshkov, K., Bax, B., Ralph, A., and Lindley, P. (1996) The X-ray structure of human serum ceruloplasmin at 3.1 Å: nature of the copper centres. *JBIC Journal of Biological Inorganic Chemistry* **1**, 15-23
52. Hellman, N. E., Kono, S., Mancini, G. M., Hoogeboom, A. J., De Jong, G. J., and Gitlin, J. D. (2002) Mechanisms of copper incorporation into human ceruloplasmin. *The Journal of biological chemistry* **277**, 46632-46638
53. Ridge, P. G., Zhang, Y., and Gladyshev, V. N. (2008) Comparative genomic analyses of copper transporters and cuproproteomes reveal evolutionary dynamics of copper utilization and its link to oxygen. *PLoS One* **3**, e1378
54. Zhang, Y., and Gladyshev, V. N. (2011) Comparative genomics of trace element dependence in biology. *The Journal of biological chemistry* **286**, 23623-23629
55. Balasubramanian, R., Smith, S. M., Rawat, S., Yatsunyk, L. A., Stemmler, T. L., and Rosenzweig, A. C. (2010) Oxidation of methane by a biological dicopper centre. *Nature* **465**, 115-119

56. Knapp, C. W., Fowle, D. A., Kulczycki, E., Roberts, J. A., and Graham, D. W. (2007) Methane monooxygenase gene expression mediated by methanobactin in the presence of mineral copper sources. *Proc. Natl. Acad. Sci. U. S. A.* **104**, 12040-12045
57. Balasubramanian, R., Kenney, G. E., and Rosenzweig, A. C. (2011) Dual pathways for copper uptake by methanotrophic bacteria. *The Journal of biological chemistry* **286**, 37313-37319
58. Walsh, C. T., Haynes, S. W., and Ames, B. D. (2012) Aminobenzoates as building blocks for natural product assembly lines. *Nat. Prod. Rep.* **29**, 37-59
59. Miller, M. C., Parkin, S., Fetherston, J. D., Perry, R. D., and Demoll, E. (2006) Crystal structure of ferric-yersiniabactin, a virulence factor of *Yersinia pestis*. *J. Inorg. Biochem.* **100**, 1495-1500
60. Lukacik, P., Barnard, T. J., Keller, P. W., Chaturvedi, K. S., Seddiki, N., Fairman, a. W., Noinaj, N., Kirby, T. L., Henderson, J. P., Steven, A. C., Hinnebusch, B. J., and Buchanan, S. K. (2012) Structural engineering of a phage lysin that targets Gram-negative pathogens. *PNAS* **109**, 9857-9862
61. Chaturvedi, K. S., Hung, C. S., Giblin, D. E., Urushidani, S., Austin, A. M., Dinauer, M. C., and Henderson, J. P. (2013) Cupric Yersiniabactin Is a Virulence-Associated Superoxide Dismutase Mimic. *ACS Chem. Biol.* **9**, 551-561
62. Koh, E. I., Hung, C. S., Parker, K. S., Crowley, J. R., Giblin, D. E., and Henderson, J. P. (2015) Metal selectivity by the virulence-associated yersiniabactin metallophore system. *Metallomics*
63. Chaturvedi, K. S., and Henderson, J. P. (2014) Pathogenic adaptations to host-derived antibacterial copper. *Frontiers in cellular and infection microbiology* **4**, 3

64. Hodgkinson, V., and Petris, M. J. (2012) Copper homeostasis at the host-pathogen interface. *The Journal of biological chemistry* **287**, 13549-13555
65. Crocker, A., Lee, C., Aboko-Cole, G., and Durham, C. (1992) Interaction of nutrition and infection: effect of copper deficiency on resistance to *Trypanosoma lewisi*. *J. Natl. Med. Assoc.* **84**, 697-706
66. Matousek de Abel de la Cruz, A. J., Burguera, J. L., Burguera, M., and Anez, N. (1993) Changes in the total content of iron, copper, and zinc in serum, heart, liver, spleen, and skeletal muscle tissues of rats infected with *Trypanosoma cruzi*. *Biol. Trace Elem. Res.* **37**, 51-70
67. Ilback, N. G., Benyamin, G., Lindh, U., and Friman, G. (2003) Sequential changes in Fe, Cu, and Zn in target organs during early Coxsackievirus B3 infection in mice. *Biol. Trace Elem. Res.* **91**, 111-124
68. Tufft, L. S., Nockels, C. F., and Fettman, M. J. (1988) Effects of *Escherichia coli* on iron, copper, and zinc metabolism in chicks. *Avian Dis.* **32**, 779-786
69. Winterbourn, C. C., Hampton, M. B., Livesey, J. H., and Kettle, A. J. (2006) Modeling the reactions of superoxide and myeloperoxidase in the neutrophil phagosome: implications for microbial killing. *The Journal of biological chemistry* **281**, 39860-39869
70. Wang, J., Mushegian, A., Lory, S., and Jin, S. (1996) Large-scale isolation of candidate virulence genes of *Pseudomonas aeruginosa* by in vivo selection. *Proc. Natl. Acad. Sci. U. S. A.* **93**, 10434-10439
71. Lamont, I. L., Beare, P. A., Ochsner, U., Vasil, A. I., and Vasil, M. L. (2002) Siderophore-mediated signaling regulates virulence factor production in *Pseudomonas aeruginosa*. *Proc. Natl. Acad. Sci. U. S. A.* **99**, 7072-7077

72. Braud, A., Geoffroy, V., Hoegy, F., Mislin, G. L., and Schalk, I. J. (2010) Presence of the siderophores pyoverdine and pyochelin in the extracellular medium reduces toxic metal accumulation in *Pseudomonas aeruginosa* and increases bacterial metal tolerance. *Environ. Microbiol. Rep.* **2**, 419-425
73. Schwan, W. R., Warrenner, P., Keunz, E., Stover, C. K., and Folger, K. R. (2005) Mutations in the *cueA* gene encoding a copper homeostasis P-type ATPase reduce the pathogenicity of *Pseudomonas aeruginosa* in mice. *Int. J. Med. Microbiol.* **295**, 237-242
74. Grass, G., Thakali, K., Klebba, P. E., Thieme, D., Müller, A., Wildner, G. n. F., and Rensing, C. (2004) Linkage between Catecholate Siderophores and the Multicopper Oxidase CueO in *Escherichia coli*. *J. Bacteriol.* **186**, 5826-5833
75. Outten, F. W., Huffman, D. L., Hale, J. A., and O'Halloran, T. V. (2001) The independent *cue* and *cus* systems confer copper tolerance during aerobic and anaerobic growth in *Escherichia coli*. *J. Biol. Chem.* **276**, 30670-30677
76. Beswick, P. H., Hall, G. H., Hook, A. J., Little, K., McBrien, D. C., and Lott, K. A. (1976) Copper toxicity: evidence for the conversion of cupric to cuprous copper in vivo under anaerobic conditions. *Chem. Biol. Interact.* **14**, 347-356
77. Macomber, L., Rensing, C., and Imlay, J. A. (2007) Intracellular copper does not catalyze the formation of oxidative DNA damage in *Escherichia coli*. *J. Bacteriol.* **189**, 1616-1626
78. Macomber, L., and Imlay, J. A. (2009) The iron-sulfur clusters of dehydratases are primary intracellular targets of copper toxicity. *Proc. Natl. Acad. Sci. U. S. A.* **106**, 8344-8349

79. Chillappagari, S., Seubert, A., Trip, H., Kuipers, O. P., Marahiel, M. A., and Miethke, M. (2010) Copper stress affects iron homeostasis by destabilizing iron-sulfur cluster formation in *Bacillus subtilis*. *J. Bacteriol.* **192**, 2512-2524
80. Djoko, K. Y., and McEwan, A. G. (2013) Antimicrobial action of copper is amplified via inhibition of heme biosynthesis. *ACS Chem. Biol.* **8**, 2217-2223
81. Jozefczak, M., Remans, T., Vangronsveld, J., and Cuypers, A. (2012) Glutathione is a key player in metal-induced oxidative stress defenses. *Int. J. Mol. Sci.* **13**, 3145-3175
82. Xu, F. F., and Imlay, J. A. (2012) Silver(I), mercury(II), cadmium(II), and zinc(II) target exposed enzymic iron-sulfur clusters when they toxify *Escherichia coli*. *Appl. Environ. Microbiol.* **78**, 3614-3621
83. Rensing, C., Fan, B., Sharma, R., Mitra, B., and Rosen, B. P. (2000) CopA: An *Escherichia coli* Cu(I)-translocating P-type ATPase. *Proc. Natl. Acad. Sci. U. S. A.* **97**, 652-656
84. Beaman, L., and Beaman, B. L. (1984) The role of oxygen and its derivatives in microbial pathogenesis and host defense. *Annu. Rev. Microbiol.* **38**, 27-48
85. Choi, D. W., Semrau, J. D., Antholine, W. E., Hartsel, S. C., Anderson, R. C., Carey, J. N., Dreis, A. M., Kenseth, E. M., Renstrom, J. M., Scardino, L. L., Van Gorden, G. S., Volkert, A. A., Wingad, A. D., Yanzer, P. J., McEllistrem, M. T., de la Mora, A. M., and DiSpirito, A. A. (2008) Oxidase, superoxide dismutase, and hydrogen peroxide reductase activities of methanobactin from types I and II methanotrophs. *J. Inorg. Biochem.* **102**, 1571-1580

86. Kim, B., Richards, S. M., Gunn, J. S., and Slauch, J. M. (2010) Protecting against antimicrobial effectors in the phagosome allows SodCII to contribute to virulence in *Salmonella enterica* serovar Typhimurium. *J. Bacteriol.* **192**, 2140-2149
87. Gleason, J. E., Galalaldein, A., Peterson, R. L., Taylor, A. B., Holloway, S. P., Waninger-Saroni, J., Cormack, B. P., Cabelli, D. E., Hart, P. J., and Culotta, V. C. (2014) *Candida albicans* SOD5 represents the prototype of an unprecedented class of Cu-only superoxide dismutases required for pathogen defense. *Proc. Natl. Acad. Sci. U. S. A.* **111**, 5866-5871
88. Soldati, T., and Neyrolles, O. (2012) Mycobacteria and the intraphagosomal environment: take it with a pinch of salt(s)! *Traffic* **13**, 1042-1052
89. Nunes, P., Demaurex, N., and Dinauer, M. C. (2013) Regulation of the NADPH oxidase and associated ion fluxes during phagocytosis. *Traffic* **14**, 1118-1131
90. Osman, D., Patterson, C. J., Bailey, K., Fisher, K., Robinson, N. J., Rigby, S. E., and Cavet, J. S. (2013) The copper supply pathway to a *Salmonella* Cu,Zn-superoxide dismutase (SodCII) involves P(1B)-type ATPase copper efflux and periplasmic CueP. *Mol. Microbiol.* **87**, 466-477

CHAPTER TWO

Metal selectivity by the virulence-associated yersiniabactin metallophore system

ABSTRACT

Uropathogenic *Escherichia coli* secrete siderophores during human infections. Although siderophores are classically defined by their ability to bind ferric ions, the virulence-associated siderophore yersiniabactin was recently found to bind divalent copper ions during urinary tract infections. Here we use a mass spectrometric approach to determine the extent of non-ferric metal interactions by yersiniabactin and its TonB-dependent outer membrane importer FyuA. In addition to copper, iron and gallium ions, yersiniabactin was also observed to form stable nickel, cobalt, and chromium ion complexes. In *E. coli*, copper(II) and all other non-ferric yersiniabactin complexes were imported by FyuA in a TonB-dependent manner. Among metal-yersiniabactin complexes, copper(II) yersiniabactin is predicted to be structurally distinctive and was the only complex not to competitively inhibit ferric yersiniabactin import. These results are consistent with yersiniabactin as part of a metallophore system able to prioritize ferric complex uptake in high copper environments.

INTRODUCTION

Numerous bacterial pathogens synthesize and secrete chemically diverse specialized metabolites called siderophores, which are defined by their ability to bind ferric iron (Fe(III)) and counter the effects of nutritional immunity by the host (1, 2). Most Gram-negative bacteria must first actively transport ferric-siderophore complexes to the periplasm through dedicated outer membrane transporters powered by the TonB complex, which transduces energy from the cytoplasmic proton motive force (3–5). These ferric siderophore complexes, or the iron released from them, are subsequently transported to the cytoplasm through inner membrane ATP-binding cassette transporters (6–9).

Although only a single siderophore system is necessary for iron-dependent growth in iron-chelated culture conditions, uropathogenic *E. coli* (UPEC) isolates can express multiple siderophore systems consisting of enterobactin (which is genetically conserved in all *E. coli*) in combination with salmochelin, aerobactin and/or yersiniabactin (10). Among these, the yersiniabactin (Ybt) siderophore system is the most frequently-carried, non-conserved siderophore system in UPEC (10, 11). Genes encoding Ybt biosynthetic proteins, an outer membrane import protein (*fyuA*), putative inner membrane transporters (*ybtP,Q*), and a transcription factor (*ybtA*) are present on the non-conserved 30 kilobase multi-operon *Yersinia* High Pathogenicity Island (HPI) (6, 12, 13). *Yersinia* HPI genes are dramatically upregulated during experimental mouse cystitis and Ybt has also been directly detected in the urine of UTI patients infected with Ybt-expressing pathogens (14–16). Together these findings are consistent with a pathogenic gain-of-function conferred by yersiniabactin siderophore system expression.

Recent observations demonstrating that Ybt binds both copper and iron ions during both human and experimental animal cystitis suggest that the Ybt system confers a gain-of-function through interactions with non-ferric metal ions (16, 17). Chemical diversity among siderophores may thus reflect differential “tuning” of these chelators to bind metal ions other than Fe(III), including divalent ions such as Cu(II). In intracellular compartments where copper is used as an antibacterial agent, Ybt may protect pathogenic bacteria by sequestering copper and catalyzing superoxide dismutation (17, 18). To date, it has been unclear whether Cu(II)-Ybt is also an additional transport substrate for FyuA, the TonB-dependent outer membrane Fe(III)-Ybt importer (4, 6, 19). If non-iron yersiniabactin complexes with physiologic metals are imported, yersiniabactin may possess a previously unappreciated metallophore function beyond its classic iron scavenging activity.

In this study, we used a liquid chromatography mass spectrometry (LC-MS) based screen to unambiguously identify stable Ybt complexes with non-ferric metal ions. We found that Ybt forms stable complexes with multiple physiologically relevant trivalent and divalent metal ions that are predicted to use similar coordination sites. A combined bacterial genetic and quantitative mass spectrometric approach showed that these complexes can be imported into *E. coli* by the TonB-dependent transporter FyuA. Of the non-ferric complexes examined, only Cu(II)-Ybt did not competitively inhibit Fe(III)-Ybt uptake. Together these results are consistent with a metallophore-like function for the yersiniabactin system that prioritizes iron uptake in copper-rich intracellular compartments where Cu(II)-Ybt may reach high concentrations.

EXPERIMENTAL PROCEDURES

Bacterial strains, plasmids and culture conditions

The uropathogenic *E. coli* isolate UTI89 and the non-uropathogenic K-12 *E. coli* isolate MG1655 were used in this study (20, 21). Strains were grown in LB agar (Becton, Dickson and Company), LB broth (Becton, Dickson and Company), YESCA (Yeast extract-Casamino acids) broth or M63 minimal media (10) with antibiotics as appropriate. Ampicillin (100 µg/mL, Goldbio), kanamycin (50 µg/mL, Goldbio) were used for plasmid selection. In-frame deletions in UTI89 and MG1655 were made using the standard red recombinase method, using pKD4 or pKD13 as a template (22). Deletions were confirmed using PCR with flanking primers.

Antibiotic resistance insertions were removed by transforming the strains with pCP20 expressing the FLP recombinase. Plasmids were made using the pTrc99a vector (23) and cloning in genes using standard PCR and recombination techniques.

Yersiniabactin and ¹³C-Yersiniabactin preparation

Apo-Ybt was generated from UTI89 Δ *entB* grown in M63 minimal medium supplemented with 0.2% glycerol (v/v) and 10mg/ml niacin (Sigma) as previously described (16). ¹³C-Ybt was produced by growing the UTI89 Δ *fur* strain in media supplemented with ¹³C-labeled glycerol as previously described (16). Metal-Ybt complexes were generated by adding metals salts to culture supernatant to a final concentration of 10mM. The metal salts added were iron(III) chloride, copper(II) sulfate, nickel(II) nitrate, cobalt(II) chloride, chromium(II) chloride, gallium(III) nitrate, zinc(II) sulfate or manganese(II) chloride (Sigma), respectively. Metal-treated supernatants were incubated for 2 hours at 4 degrees and then applied to a methanol conditioned C18 silica column (Sigma). Samples were eluted with 80% methanol. Lyophilizer was used to

concentrate the eluate overnight. Dried samples were resuspended in 20% methanol and further purified through high-performance liquid chromatography using C18 silica column (Whatman Partisil). The following gradient was used: Solvent A (0.1% (v/v) formic acid) was held constant at 80%, and solvent B (100% (v/v) acetonitrile in 0.1% formic acid (v/v)) was held constant at 20% for 2 min, then solvent B was increased to 100% by 20 min. Metal-Ybt containing fractions were collected, dried down using a lyophilizer and resuspended in deionized water. Isotope labeled metal-Ybt complexes were confirmed by LC-MS at corresponding masses.

Complex validation by ICP-MS

HPLC-purified metal-Ybt complexes were dried down using a lyophilizer and resuspended in ultrapure water and trace metal grade nitric acid (Fisher). Final concentration of nitric acid was 2% v/v. Samples were diluted 1:10 using 2% nitric acid solution, and metal concentrations were analyzed by high resolution ICP-MS (Agilent 7500 ICP-MS). Machine was calibrated using Environmental calibration standard (Agilent) and PerkinElmer Pure Plus ICP-MS standard (PerkinElmer).

Yersiniabactin complex preparations

Absorption spectra were measured using a quartz cuvette on a standard UV/Vis spectrometer (Beckman Coulter DU800). The Fe(III)-Ybt absorption spectra local maximum observed at 385 nm matched the previously reported local maximum (24). Extinction coefficients using Beer's law for each Ybt complex were determined using their distinctive local absorption maxima (Table 1) relative to absolute concentration determined by ICP-MS assuming the observed 1:1

(metal:Ybt) stoichiometry. These extinction coefficient values were used to determine metal-Ybt complex concentrations.

Liquid chromatography-mass spectrometry

LC-MS analyses were conducted using a Shimadzu UFLC-equipped AB-Sciex 4000 QTrap operated in positive ion mode using the Turbo V ESI ion source and a Thermo LCQ Deca as previously described (16). The samples were injected onto a Fused-core phenylhexyl column (100 × 2 mm, 2.7- μ m particle, Ascentis Express, Supelco) with a flow rate of 0.4 ml per min. The following gradient was used: Solvent A (0.1% (v/v) formic acid) was held constant at 98%, and solvent B (90% (v/v) acetonitrile in 0.1% formic acid (v/v)) was held constant at 2% for 2 min, then solvent B was increased to 65% by 10 min and then to 98% by 12 min. The ion spray voltage was set to 5 kV. The heater temperature was 500 °C. The declustering potential, nebulizer gas (G1), auxiliary gas (G2) and collision energy were set at 110V, 40V, 35V and 35V, respectively.

Liquid chromatography-constant neutral loss analysis

The UFLC-4000 QTrap was used with settings described above to identify compounds with a common neutral fragment loss of 187 m/z units as shown previously (16). The collision energy was set to 35 V, and the first mass analyzer (Q1) was set to scan from m/z 200 to 800 a.m.u., whereas the second mass analyzer (Q3) simultaneously scanned at 187 m/z units less than Q1. To identify ^{13}C -labeled metal-Ybt samples, settings were changed to scan for 195-a.m.u. neutral loss.

Theoretical calculations

Theoretical calculations were conducted in collaboration with Dr. Daryl Giblin at the Department of Chemistry at Washington University in St. Louis. Theoretical calculations were performed to characterize the potential-energy surface (PES) associated with fragmentation and reaction as previously described (17). Conformer spaces for precursors (cupric and ferric complexes with Ybt), and intermediates were explored by Monte Carlo/MMFF molecular mechanisms/dynamics methods. From these results, structures of precursors, intermediates, and scans for associated transition states were explored by using the PM3 semi-empirical algorithm (25), both in Spartan (26), for Linux v. Two (Wave function, Inc.). DFT (Density Functional Theory, part of Gaussian 03 and 09 suites, Gaussian Inc.) calculations were performed by using the PBE0 functional (27, 28) (PBE1PBE in Gaussian parlance) with basis sets Def2-SVP and Def2-TZVP (29). Minima and transition states were optimized at the level PBE1PBE/Def2-SVP and confirmed by vibrational frequency analysis. In addition, connections of transition states to minima were examined by inspection, projections along normal reaction coordinates, and path calculations as necessary. Single-point energies were calculated at level PBE1PBE/Def2-TZVP, and scaled thermal-energy corrections were applied using scaling factors for B3LYP/6-31G(d,p) (30). Solvent-based single-point energies were calculated at the same level by using the CPCM polarizable conductor calculation model for water and using the Universal Force Field for atomic radii (31). The hybrid functional and basis sets were chosen on basis of performance with transition metal complexes (32, 33). DFT was selected for high-level calculations on pragmatic reasons because it requires overall less computational overhead than ab initio methods and performs adequately (34–36). All results are reported in kcal/mol as enthalpies of formation relative to a selected, suitable precursor.

Yersiniabactin neutral has 4 labile protons and 12 Lewis base sites: 3N, 3S, 4O, and 2 classes of positions on the terminal salicylate moiety. The N, S, and O atoms are potential complexation sites with the metal ion. Yersiniabactin can interact with the metal ions using combinations of the Lewis base sites and variable coordination numbers to the metal. We chose as starting geometry for the ferric complex that based on the crystal structure: hexacoordinate octahedral involving complexion with 3N and 3O (37) with high-spin Fe(III), $S=5/2$. Starting with yersiniabactin having the protons of the three hydroxyl moieties removed and complexed with ferric ion, we added sequentially protons, optimized, and determined enthalpies to which was added the next proton to that state of the complex and procedure repeated until the singly-charged positive-ion state was achieved. For other metal complexes, we substituted the metal cations for ferric, optimized geometries similarly, and determined optimum molecular-orbital spin state. For the other metals: Cu(II), $S=1/2$; Co(III), $S=0$; Ga(III), $S=0$, Ni(II), $S=1$, Cr(III), $S=3/2$.

Fe(III)-Ybt dependent growth

Following overnight growth in YESCA media, strains were normalized for starting OD600 in YESCA with 2mM EDDHA (Complete Green Company) and grown for 1 hour in 37 degrees while shaking. 1 μ M HPLC-purified Fe(III)-Ybt was added to strains and grown for 9 hours in 37 degrees while shaking. Bacterial growth was measured using OD600 readings as well as viable colony forming unit (CFU) measurements. Fold increase in growth was determined by calculating the ratio of CFU at end point over start point for every strain examined.

Cell-associated metal-Ybt

Following overnight growth in YESCA media, strains were diluted to OD600 of 0.8 in YESCA. HPLC-purified metal-Ybt was added to strains and grown for 30 minutes in 37 degrees while shaking. In case of multiple metal-Ybt complexes, metal-Ybt mixture in a cell-free control was conducted to check for changes in relative metal-Ybt ratios. Bacteria were pelleted at 7500 g for 10 minutes (Eppendorf) and washed with 1X PBS (Sigma). Bacteria were resuspended in 100% ethanol (Sigma) and pelleted at 20000 g for 10 minutes (Eppendorf). Supernatant was collected and dried overnight using a vacuum concentrator. Samples were resuspended in ultrapure water and applied to a conditioned C18 silica column with added ¹³C-labeled Fe(III)-Ybt internal standard. Metal-Ybt quantification was carried out in the multiple reaction monitoring mode using known collision-induced dissociation fragmentations and ¹³C-labeled Fe(III)-Ybt internal standards.

Statistical Analyses

Statistics and graphs were generated using GraphPad Prism 5 (GraphPad software). Student's *t*-test was used to compare growth differences and cell-associated metal-Ybt levels between paired strains.

RESULTS

Mass spectrometric screen for stable metal-Ybt complexes

To identify stable metal-Ybt complexes, we used a previously described mass spectrometric screen (liquid chromatography-constant neutral loss; LC-CNL) to detect metal-Ybt complexes in aqueous solutions containing *apo*-Ybt at pH 7 and metal salts in molar excess (10mM final concentration) (16). We selected transition metal species with known physiologic roles such as zinc(II), manganese(II), nickel(II) and cobalt(II) (2), and chromium(II). The established Ybt ligands iron(III), copper(II), and gallium(III) served as positive controls. LC-CNL ion chromatograms from Ybt solutions containing chromium, cobalt and nickel revealed new peaks with mass spectra and retention times that differ from *apo*-Ybt or other known metal-Ybt complexes. No new peaks were observed from Ybt solutions containing zinc and manganese (Fig 1). When HPLC was performed without acid modifier to avoid possible acidic dissociation of complexes, no new peaks corresponding to zinc or manganese complexes were observed (data not shown). A molar excess of Zn(II) furthermore did not alter 0.1 μ M *apo*-Ybt and Fe(III)-Ybt peaks areas (Supplementary Fig 1). Detection of chromium, cobalt and nickel-Ybt complexes suggest a broader range of Ybt ligands beyond the previously identified Fe(III), Cu(II) and Ga(III) ions. While these results do not rule out the existence of Ybt complexes with zinc or manganese, isolated complexes with these metals may not be sufficiently stable or sensitive to be detected under these conditions.

To obtain more detailed structural information about the new products observed in the LC-CNL screen, we subjected the new peaks from chromium, cobalt and nickel-containing Ybt samples to MS and MS/MS analyses. The chromium-Ybt mass spectrum showed a dominant peak at m/z

531 and prominent M-2 and M+1 peaks at m/z 529 and 532 respectively. These are 49 a.m.u. higher than the Ybt $[M+H]^+$ ion with M-2 and M+1 isotopes, consistent with a singly charged chromium complex of the form $[Ybt-2H + Cr(III)]^+$. The mass spectrum isotope distribution was consistent with the natural abundance of ^{50}Cr , ^{52}Cr and ^{53}Cr isotopes at 4%, 84% and 10% respectively (Fig 2A). MS/MS fragmentation of the monoisotopic peak at m/z 531 revealed a prominent 187 a.m.u. neutral loss alongside other fragments. One such fragment was a 46-a.m.u. neutral loss, which is consistent with a thioformaldehyde loss (Fig 2D), from the thiazoline ring bearing the terminal carboxylic acid. The cobalt-Ybt mass spectrum revealed a base peak at m/z 538 without additional prominent isotope peaks. At 56 a.m.u. higher than the Ybt $[M+H]^+$ ion, this ion was consistent with a singly charged cobalt complex of the form $[Ybt-2H + Co(III)]^+$ (Fig 2B). The lack of a prominent isotope peak was consistent with cobalt, whose only stable isotope is ^{59}Co . MS/MS analysis of the monoisotopic peak at m/z 538 revealed a fragmentation pattern with a 187-a.m.u. neutral loss as well as other fragments, including a 44-a.m.u. neutral loss consistent with loss of CO_2 from the terminal carboxyl group (Fig 2E). Ambient oxidizing conditions together with possible stabilization of the trivalent forms by Ybt likely contributed to trivalent cobalt and chromium complex formation despite their addition as divalent salts. Nickel-Ybt mass spectrum also features a dominant peak at m/z 538 but also exhibits a prominent M+2 peak at m/z 540. At 56 a.m.u. higher than the Ybt $[M+H]^+$ ion with a prominent M+2 isotope, this is consistent with a singly charged nickel complex of the form $[Ybt-H + Ni(II)]^+$. The observed isotope pattern matches the natural ^{58}Ni and ^{60}Ni abundances of 68% and 26% respectively (Fig 2C). The monoisotopic m/z 538 peak MS/MS spectrum was dominated by a 187 a.m.u. neutral loss (Fig 2F).

Additional compositional information was achieved by stable isotope labeling and ICP-MS. ^{13}C -isotope labeling shifted all new products 21 m/z units higher than unlabeled complexes, consistent with yersiniabactin's 21 carbon atoms (16). Subsequent MS/MS analysis revealed a shifted dominant MS/MS neutral loss of 195 mass units, corresponding to loss of a fragment containing eight carbons (Supplementary Fig 2). All metal-Ybt complexes identified above were stable following chromatographic purification on the basis of LC-MS and UV/visible absorption profiles. We further validated metal-Ybt complex identifications using ICP-MS to measure the dominant metal species in HPLC-purified specimens. Through ICP-MS analysis, we found that the metal ion corresponding to the metal-Ybt sample was the dominant metal ion. Together, these data support Ybt's ability to bind and form stable metal complexes with Fe(III), Cu(II), Cr(III), Ga(III), Co(III), and Ni(II).

Theoretical structural modeling supports a distinctive Cu(II)-Ybt structure

To address the physical plausibility of new yersiniabactin complexes we used a quantum-based density function theory (DFT) approach (17) to simulate each complex in both the gas-phase (mass spectrometer) and in solution (H_2O). We validated this approach by comparing the calculated neutral Fe(III)-Ybt complex structure to the experimentally-determined Fe(III)-Ybt X-ray crystal structure (37). Both structures were virtually identical, supporting the validity of the DFT approach (Supplementary Fig 3). We then simulated the stable metal-Ybt complexes observed in the mass spectrometer: Cu(II)-, Co(III)-, Ni(II)-, Fe(III)-, Cr(III)-, and Ga(III)-Ybt. All complexes are predicted to share a common square planar core involving the salicylate oxygen and the three nitrogens of yersiniabactin. Although thioethers have been shown to interact with copper ions in some proteins (through methionine (38)), forcing these interactions

in DFT simulations eliminated the nitrogen interactions and led to markedly less stable isomers. With the notable exception of Cu(II)-Ybt, all other complexes were predicted to share the hexa-coordinate octahedral configuration previously observed for Fe(III)-Ybt (37). Cu(II)-Ybt is distinguished by two elongated axial ligand bonds to the aliphatic alcohol and terminal carboxyl groups. Cu(II)-Ybt has a second energetically competitive form that lacks the axial cupric to carbonyl bond (Fig 3) rendering that form penta-coordinate with an open coordination site.

The MS/MS fragmentation data is consistent with the calculated gas phase structures (relevant to MS experimental conditions) for each complex. Gas phase structures vary for M(III)-Ybt mono-positive complexes, which were calculated to have the charging proton on the terminal carbonyl oxygen of the axial carboxylate ligand rather than the secondary alcohol. Overall, the calculated structures agree with the available experimental data. All the chromatographically isolated metal yersiniabactin complexes observed here are predicted to be stable by DFT simulation. Among these complexes, Cu(II)-Ybt is predicted to be the most structurally and electronically distinctive.

FyuA and YbtPQ are required for Fe(III)-Ybt dependent growth in UPEC

To confirm the role of UPEC-encoded FyuA and YbtPQ in *E. coli* Fe(III)-Ybt utilization, we measured growth of the model UPEC strain UTI89 and the *Yersinia* HPI-null K12 strain MG1655 with purified Fe(III)-Ybt as the sole iron source in otherwise nutrient-rich media. *E. coli* strains were grown in nutrient-rich YESCA (yeast extract-casamino acids) media containing 1 μ M purified Fe(III)-Ybt and the iron chelator EDDHA, which sequesters non-siderophore-bound Fe(III). Wild type UTI89 growth exceeded that of UTI89 Δ *fyuA* and UTI89 Δ *ybtPQ* in the

presence (Fig 4A), but not absence (Fig 4B) of Fe(III)-Ybt. Plasmid-complemented UTI89 Δ *fyuA* and UTI89 Δ *ybtPQ* showed restored growth to wild type UTI89 levels (Supplementary Fig 4). In the *Yersinia* HPI-null MG1655 strain background, which lacks yersiniabactin transport genes, Fe(III)-Ybt-dependent growth required simultaneous ectopic expression of FyuA and YbtPQ (Fig 4C, D). These results show that FyuA and YbtPQ are sufficient for Fe(III)-Ybt-dependent growth in both UPEC and K12 *E. coli*. The inability of FyuA alone to promote Fe(III)-Ybt-dependent growth in MG1655 is consistent with the current model in which FyuA delivers Fe(III)-Ybt to the periplasmic, not cytoplasmic space.

FyuA imports intact Fe(III)-Ybt complexes in a TonB-dependent manner

To determine whether *E. coli* use FyuA to import Fe(III)-Ybt complexes, we used stable isotope dilution mass spectrometry (LC-MS/MS) to directly localize exogenously-supplied metal-yersiniabactin complexes. With this approach, Fe(III)-Ybt could be quantified in UTI89 cell extracts following a 30 minute exposure to 0.1 μ M purified Fe(III)-Ybt (Fig 5A, B). These cell-associated Fe(III)-Ybt levels were nearly eliminated in UTI89 Δ *fyuA* and were restored by genetic complementation in UTI89 Δ *fyuA* *pfyuA*. This complementing plasmid further conferred robust cellular Fe(III)-Ybt localization in MG1655 (Fig 5C). Because Fe(III)-Ybt can form a stable FyuA-bound complex (19), we examined localization in MG1655 Δ *tonB* background, which lacks the energy transduction system required for active transport to the periplasm. Cell-associated Fe(III)-Ybt was significantly lower in MG1655 Δ *tonB* *pfyuA* than in MG1655 *pfyuA*. Furthermore, cell-associated Fe(III)-Ybt in MG1655 Δ *tonB* *pfyuA* lacked the dose-dependent relationship observed in MG1655 *pfyuA* (Fig 5D). Overall, these observations support the model

in which FyuA is sufficient to transport intact Fe(III)-Ybt through the Gram negative outer membrane in a TonB-dependent manner.

FyuA imports Cu(II)-Ybt and other non-ferric complexes in a TonB-dependent manner

To determine whether *E. coli* can use FyuA to import non-iron Ybt complexes, we used LC-MS/MS to directly localize exogenously-supplied yersiniabactin complexes. With this approach, non-iron Ybt complexes could be quantified in bacterial cell extracts following a 30-minute exposure to 0.1 μ M purified metal-Ybt (Fig 6, *left*). These cell-associated metal-Ybt levels were nearly absent in wild type MG1655 while MG1655 *pfyuA* conferred robust cellular metal-Ybt localization at similar molar quantities (Fig 6, *left*). To investigate non-iron Ybt interactions with FyuA, we examined localization in MG1655 Δ *tonB pfyuA*. Cell-associated Ybt complexes were significantly lower in MG1655 Δ *tonB pfyuA* than in MG1655 *pfyuA*. Furthermore, cell-associated metal-Ybt in MG1655 Δ *tonB pfyuA* lacked the dose-dependent relationship observed in MG1655 *pfyuA* (Fig 6, *right*). Interestingly, we found cell-associated Cu(II)-, Ga(III)-, Co(III)- and Ni(II)-Ybt levels rise and then decrease in MG1655 *pfyuA* with increasing metal-Ybt concentrations in the media (Fig 6, *right*). These distinctive transport features at higher concentrations may reflect higher order interactions with FyuA or variable intracellular metal-Ybt instability. Overall, these observations support a model in which FyuA imports non-iron Ybt complexes through TonB-mediated active transport. While this was expected for Ga(III), a classic non-physiologic ferric ion mimic, import of physiologically relevant metals raises the possibility that these are imported by FyuA during infections.

Cu(II)-Ybt does not competitively inhibit Fe(III)-Ybt uptake

The specific molecular sequence of events by which FyuA imports yersiniabactin complexes is incompletely understood. To determine whether ferric and non-ferric-Ybt complexes are imported through a similar pathway and whether Fe(III)-Ybt is a preferred substrate, we measured import by MG1655 *pfyuA* exposed to both complexes under competitive conditions. Ectopic expression in MG1655 allows consistent FyuA expression for all experimental conditions, whereas native FyuA expression in UTI89 is subject to an incompletely understood regulatory network for yersiniabactin genes (12). In this experimental system, increasing Fe(III)-Ybt concentrations in media containing 0.1 μM of each non-ferric-Ybt complex inhibited non-metal Ybt complex import (Fig 7, *left*) in the order Ni(II)~Cr(III) > Cu(II)~Co(III) > Ga(III). This is consistent with competitive inhibition of non-ferric yersiniabactin complex uptake by Fe(III)-Ybt, again suggesting a common uptake mechanism for all metal-yersiniabactin complexes.

When Fe(III)-Ybt was instead held constant at 0.1 μM and non-ferric-Ybt concentrations increased, all non-ferric-Ybt complexes with the notable exception of Cu(II)-Ybt competitively inhibited Fe(III)-Ybt import. Of note, while Ni(II)-Ybt inhibited Fe(III)-Ybt transport, cellular Ni(II)-Ybt levels remained low (Fig 7, *right*). Overall, Cu(II)-Ybt exhibited the most distinctive dose-response relationship, with diminished cell-associated Cu(II)-Ybt at higher concentrations and no discernable ability to inhibit Fe(III)-Ybt uptake. Distinctive transport properties of Cu(II)-Ybt may reflect contributions from differential FyuA binding, transport rate, and/or periplasmic dissociation. While the physiologically relevant Cu(II)-Ybt concentration range is unknown, Cu(II)-Ybt may reach high levels in the intracellular compartments of mammalian cells (18), making FyuA's ability to sustain import of scarce Fe(III)-Ybt a possible adaptation to this

environment. This ability may reflect an interaction between FyuA and the distinctive Cu(II)-Ybt structure predicted above (Fig 3).

DISCUSSION

This study uses direct mass spectrometric detection to show that Ybt is a promiscuous trivalent and divalent metal chelator, forming stable complexes with physiologically relevant metal ions Fe(III), Cu(II), Ni(II), Co(III), and Cr(III). FyuA imports each stable Ybt complex in a TonB-dependent manner in the absence of other *Yersinia* HPI-encoded proteins. Fe(III)-Ybt competitively inhibits non-ferric Ybt uptake, consistent with a shared transport mechanism. Cu(II)-Ybt, however, does not competitively inhibit Fe(III)-Ybt import and exhibits maximal import at low (0.1 μM) extracellular concentrations. Together these findings provide new evidence for metal-selectivity by the yersiniabactin system (Fig 8) while demonstrating a new experimental framework for characterizing siderophore system metal specificity.

Uropathogenic *E. coli* must adapt to numerous physiologic environments during infection pathogenesis. In these environments, the host may deliberately decrease the availability of iron and other transition metals to restrict microbial growth (nutritional immunity) and may increase copper availability as a microbicidal effector (2, 18, 39, 40). Within an intracellular vesicle such as the macrophage phagolysosome, UPEC are confined to a small volume ($\sim 1.2 \times 10^{-15}$ L)(41) where iron is likely to be scarce while copper ions may be abundant. Yersiniabactin secretion within this space would therefore be expected to result in high local Cu(II)-Ybt concentrations. The distinctive ability of FyuA to maintain Fe(III)-Ybt import in the presence of excess Cu(II)-Ybt (Fig 7) suggests that the yersiniabactin import system may have adapted to copper-rich intracellular compartments. Specifically, the yersiniabactin system distinguishes yersiniabactin bound to copper versus iron to avoid the toxic metal (copper) while still importing the nutritionally valuable one (iron). This is in agreement with previous works showing Ybt-

mediated copper resistance in intracellular compartments (17, 18), as well as observations by *Braud et al.*, where expression of the siderophores pyoverdine and pyochelin by *Pseudomonas aeruginosa* increased copper resistance (42). Further investigation is necessary to determine where these compartments might exist during urinary tract pathogenesis.

Cu(II)-Ybt's distinctive ability to be transported at low concentrations without inhibiting Fe(III)-Ybt transport (Fig. 7) suggests a specific molecular interaction with Cu(II)-Ybt. While the nature of this interaction is currently unclear, DFT calculations raise the possibility that the distinctive "open" pentacoordinate form (Fig. 3) of Cu(II)-Ybt could enable protein interactions with the free carboxylic acid, the open axial Cu coordination site, or both. Copper specificity in *E. coli* ectopically expressing FyuA (Fig. 7) suggests that this protein may be the relevant discriminator. This could occur through an unrecognized allosteric site or through an intermediate site occupied during transport. Although TonB-dependent transporters (TBDT) have been the subject of multiple structural analyses, a better mechanistic understanding of their transport will be necessary to discern precisely how Cu(II)-Ybt-specificity is achieved (3, 43).

Outside of endosomal compartments where copper availability and yersiniabactin concentrations are low, the yersiniabactin system may function as a copper scavenging (chalkophore) system (44) (Fig. 6, 7). Yersiniabactin's ability to form stable, FyuA-importable complexes with physiologically relevant copper, nickel, cobalt, and chromium ions may supply trace nutrients for pathogens beyond iron. Because bacterial metalloproteomes are incompletely understood; the full extent of transition metal demands exhibited by pathogenic bacteria at various stages of infection are unclear (45). The lack of stable zinc and manganese Ybt complexes are notable.

Recent work by Bobrov *et al.* linked Ybt to a distinctive, non-TonB-dependent zinc import pathway in *Yersinia pestis* involving the *Yersinia* HPI gene *ybtX* (46). However as MG1655 lacks *ybtX*, our transport results do not implicate this gene in transport of the stable metal-Ybt complexes observed here. As with Bobrov *et al.*, we were unable to observe stable Zn(II)-Ybt and further found that Zn(II) does not interfere with Fe(III)-Ybt formation. The selectivity of Ybt to bind Fe(III) despite excess Zn(II) may be advantageous for UPEC infecting males where it may encounter excess zinc in prostate glands (47–49). Future studies of the UPEC metalloproteome will help fully discern roles for yersiniabactin-delivered metals in UTI pathogenesis.

The results described here suggest an approach to define siderophore-associated metallomes. Prior studies have demonstrated siderophore-mediated uptake of certain non-ferric metals in other siderophore systems using spectrometric and radiolabeling approaches (42, 50–52). The quantitative mass spectrometry approach developed here allows us to directly compare siderophore interactions with a wide range of non-radioactive metals. Although this method is insensitive to transient or unstable Ybt complexes, weak complexes would appear to be of less biological significance unless stabilized by an additional component such as a binding protein.

ACKNOWLEDGEMENTS

J.P.H. holds a Career Award for Medical Scientists from the Burroughs Wellcome Fund and acknowledges National Institute of Diabetes and Digestive and Kidney Diseases grant R01DK099534. Mass spectrometry was supported by United States Public Health Service grants P41-RR00954, P60-DK20579, P30-DK56341 and P30HL101263. ICP-MS was supported by the Nano Research Facility at Washington University in St. Louis. Computations were conducted in collaboration with Dr. Daryl Giblin using the facilities of the Washington University Center for High Performance Computing and by the Washington University Computational Chemistry Facility, supported by NSF grant #CHE-0443501.

CHAPTER TWO: FIGURES

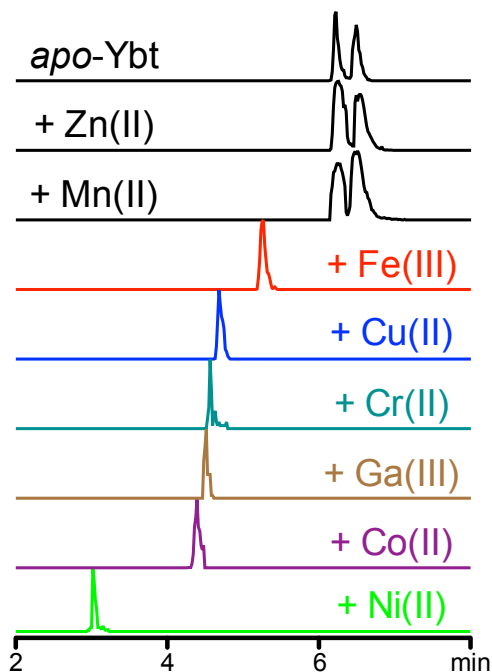


Figure 1. Mass spectrometric neutral loss screen reveals multiple stable metal-Ybt complexes. Liquid chromatography-constant neutral loss (LC-CNL) chromatograms reveal new chromatographic peaks corresponding to different stable metal Ybt complexes in solutions combining *apo*-Ybt (*top*) and different metal ions. The established Ybt ligands iron, copper, and gallium were used as positive controls while Ybt solutions containing chromium, cobalt and nickel revealed new peaks that differ from *apo*-Ybt or other known metal-Ybt complexes. Ybt solutions containing zinc and manganese did not reveal new peaks.

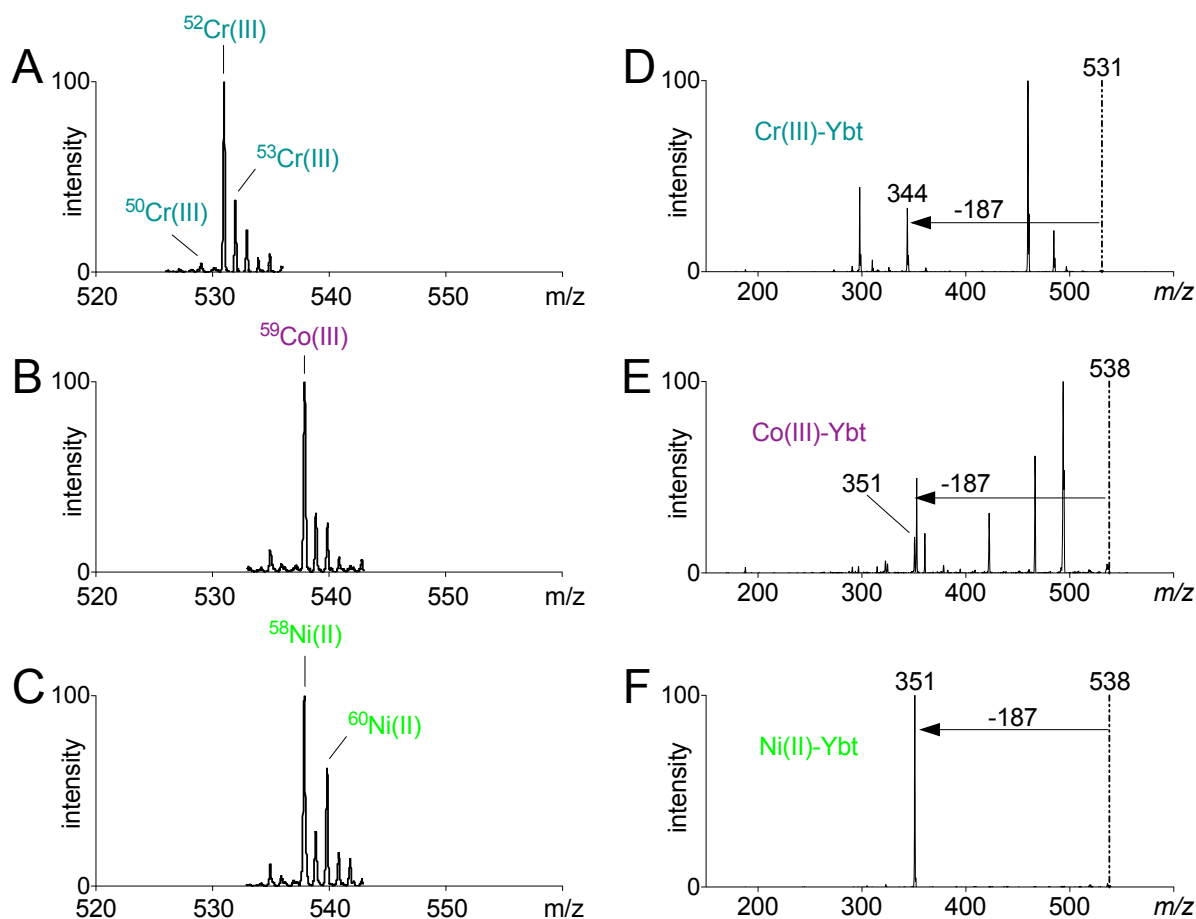


Figure 2. MS and MS/MS spectral analyses reveal non-ferric metal-Ybt complexes. (A) MS spectrum of chromium-Ybt exhibits a base peak at m/z 531 consistent with Cr(III) and its natural abundance ^{50}Cr , ^{52}Cr and ^{53}Cr isotopes. **(B)** MS spectrum of cobalt-Ybt exhibits a base peak at m/z 531 consistent with $^{59}\text{Co(III)}$. **(C)** MS spectrum of nickel-Ybt exhibits a base peak at m/z 538 and a prominent M+2 peak consistent with Ni(II) and its ^{58}Ni and ^{60}Ni isotopes. **(D, E, F)** Tandem MS/MS spectra for each complex confirms the dominant neutral loss of 187 m/z units observed with previously characterized metal-Ybt species.

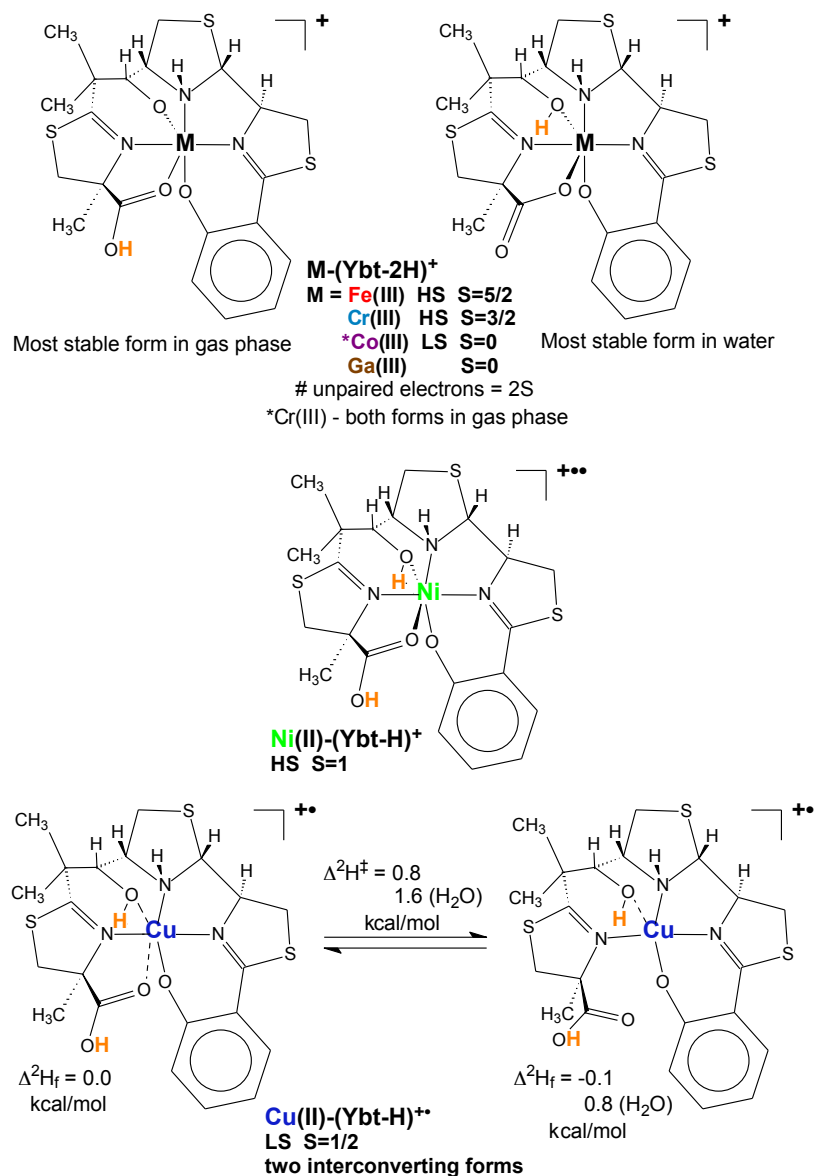


Figure 3. Density function theory (DFT) models structurally differentiate Cu(II)-Ybt complexes. Metal ion bonds predicted by DFT calculations of Ybt complexes with Fe(III), Cr(III), Ga(III), Ni(II), Co(III), and Cu(II). Spin states are indicated (S, total spin; HS, high spin; LS, low spin). In Cu(II)-Ybt, axial Cu-O bonds are relatively stretched (0.15 - 0.20 nm indicated by dashed lines) and interconvert with a competitive penta-coordinate form. Calculated position of charging proton(s) for mono-cationization (ESI in the mass spectrometer) are indicated in bold orange.

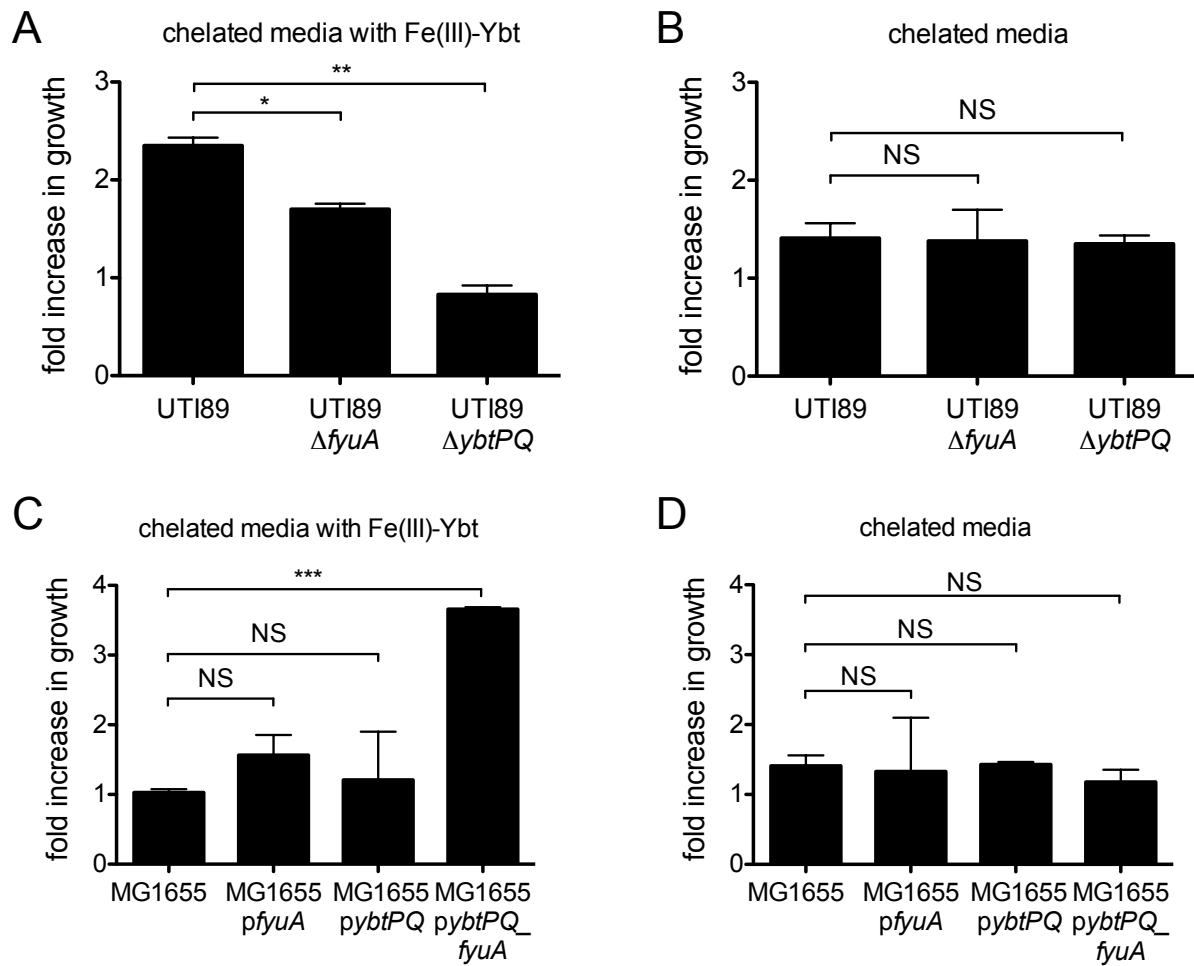


Figure 4. FyuA and YbtPQ are necessary for Fe(III)-Ybt-dependent growth in pathogenic (UTI89) and non-pathogenic (MG1655) *E. coli*. (A) Fe(III)-Ybt-dependent growth is limited in UTI89 mutants lacking FyuA and YbtPQ. In this condition, Fe(III)-Ybt is added to a rich media in which bioavailable ferric ions are chelated with EDDHA. (B) UTI89 strains are indistinguishable in the absence of Fe(III)-Ybt. (C) MG1655 *pybtPQ_fyuA*, which constitutively express both FyuA and YbtPQ, gains Fe(III)-Ybt-dependent growth. (D) MG1655 strains are indistinguishable in the absence of Fe(III)-Ybt. Fold increase in growth represents the ratio of CFU at end point over start point for each strain. Results are shown as mean \pm s.d.; $n=3$; * $P<0.05$, ** $P<0.01$, *** $P<0.001$.

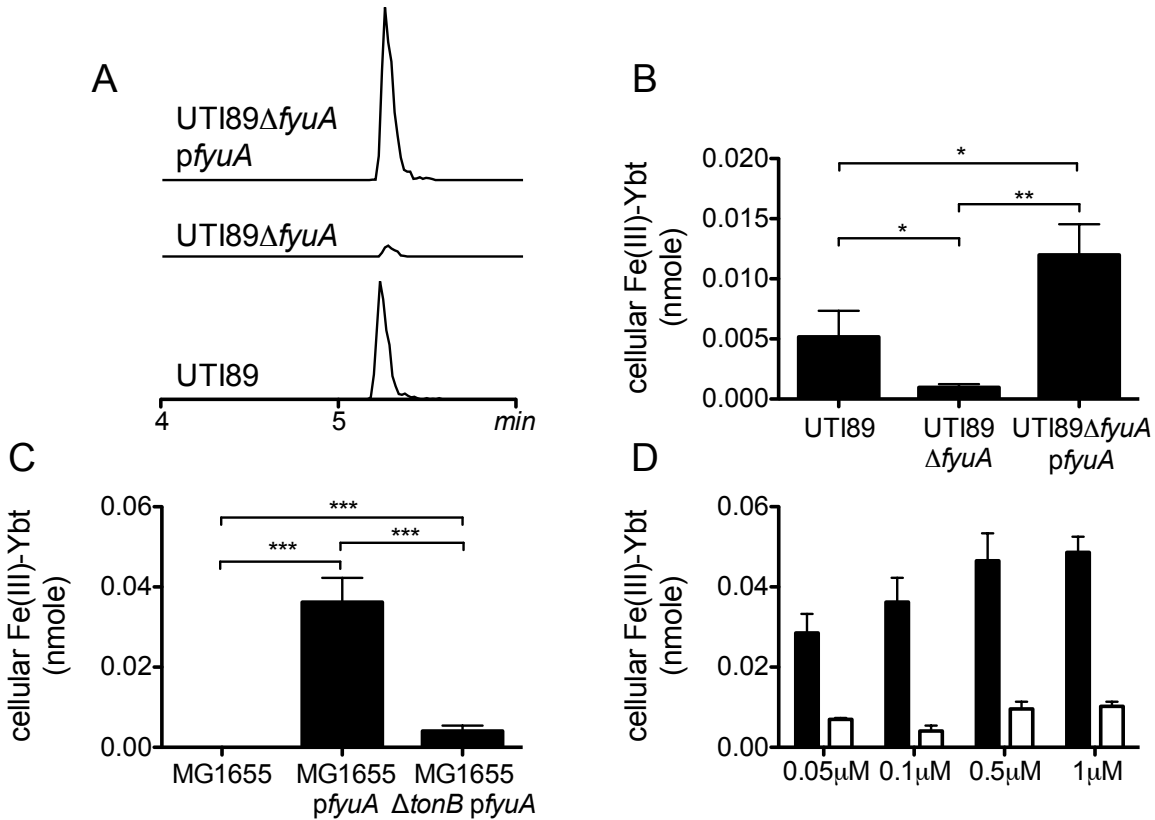


Figure 5. Direct LC-MS/MS detection of cell-associated Fe(III)-Ybt in FyuA-expressing

UTI89 and MG1655. Bacteria grown in Fe(III)-Ybt-containing media were extracted to quantify cell-associated Fe(III)-Ybt using LC-MS/MS with a ^{13}C -labeled Fe(III)-Ybt internal standard.

(A) Representative LC-MS/MS chromatograms of cell-associated Fe(III)-Ybt scaled to internal

standard peaks. **(B)** Cell-associated Fe(III)-Ybt was abolished in an FyuA-deficient mutant and

restored by genetic complementation. **(C)** Exogenous FyuA expression in MG1655 significantly

increased cell-associated Fe(III)-Ybt levels while expression in a MG1655ΔtonB resulted in

lower levels. **(D)** A positive Fe(III)-Ybt dose-response relationship was observed in MG1655

pfyuA (black bars) but not MG1655ΔtonB pfyuA (white bars). Results are shown as nanomoles,

mean \pm s.d.; $n=3$; *** $P<0.001$.

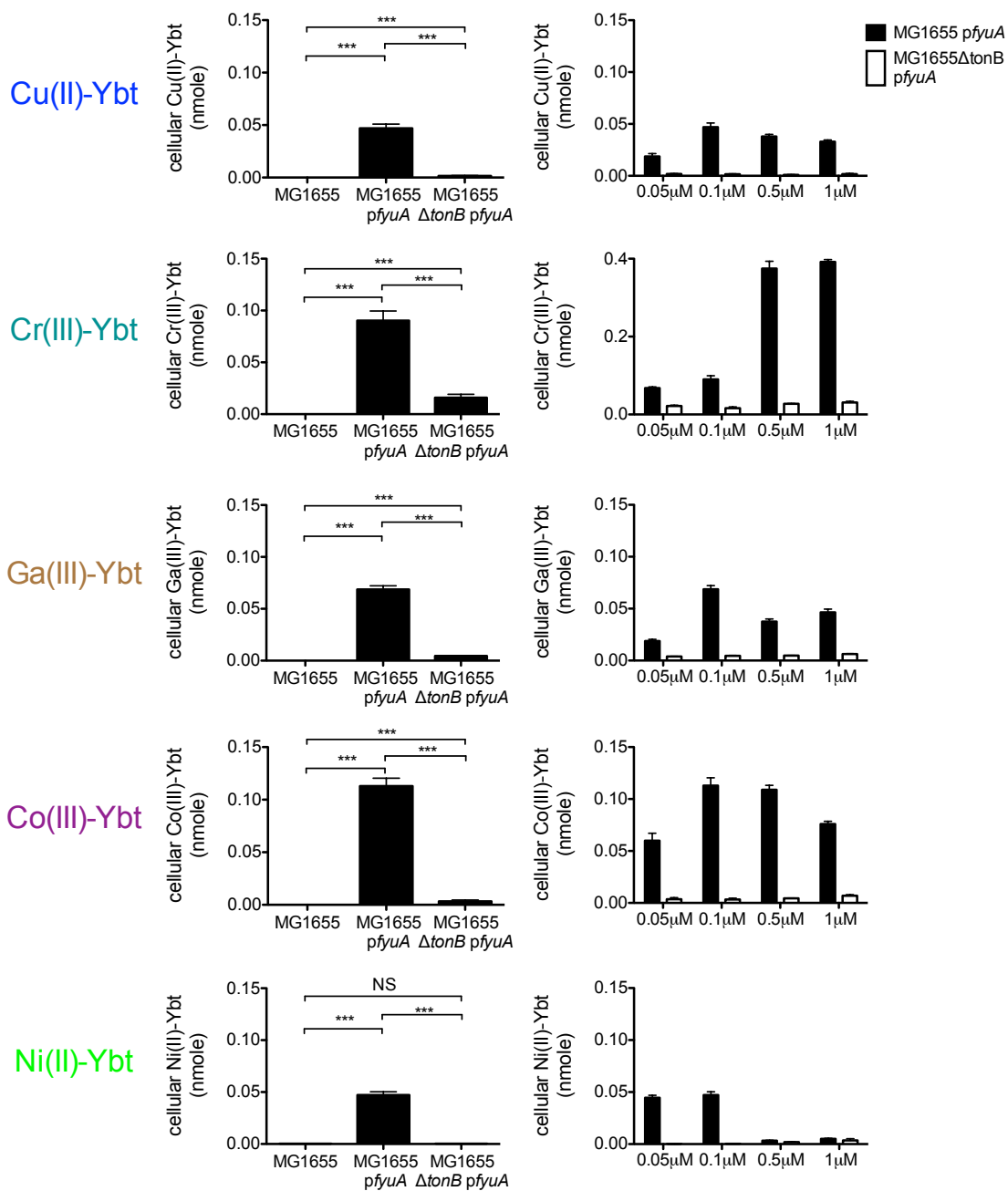


Figure 6. FyuA and TonB-dependent uptake of Cu(II)-Ybt and other non-ferric complexes.

Cell-associated metal-Ybt complexes were measured in *E. coli* MG1655 strains. **(left)** Ectopic FyuA expression significantly increased cell-associated metal-Ybt levels but this increase was significantly lower in a *tonB*-null mutant background. **(right)** *tonB*-null mutants exhibited lower

cell-associated Ybt complexes over a range of applied media concentrations. Black bars indicate MG1655 *pfyuA* while white bars indicate MG1655 Δ *tonB* *pfyuA*. Results are shown as nanomoles, mean \pm s.d.; $n=3$; * $P<0.05$, ** $P<0.01$ and *** $P<0.001$.

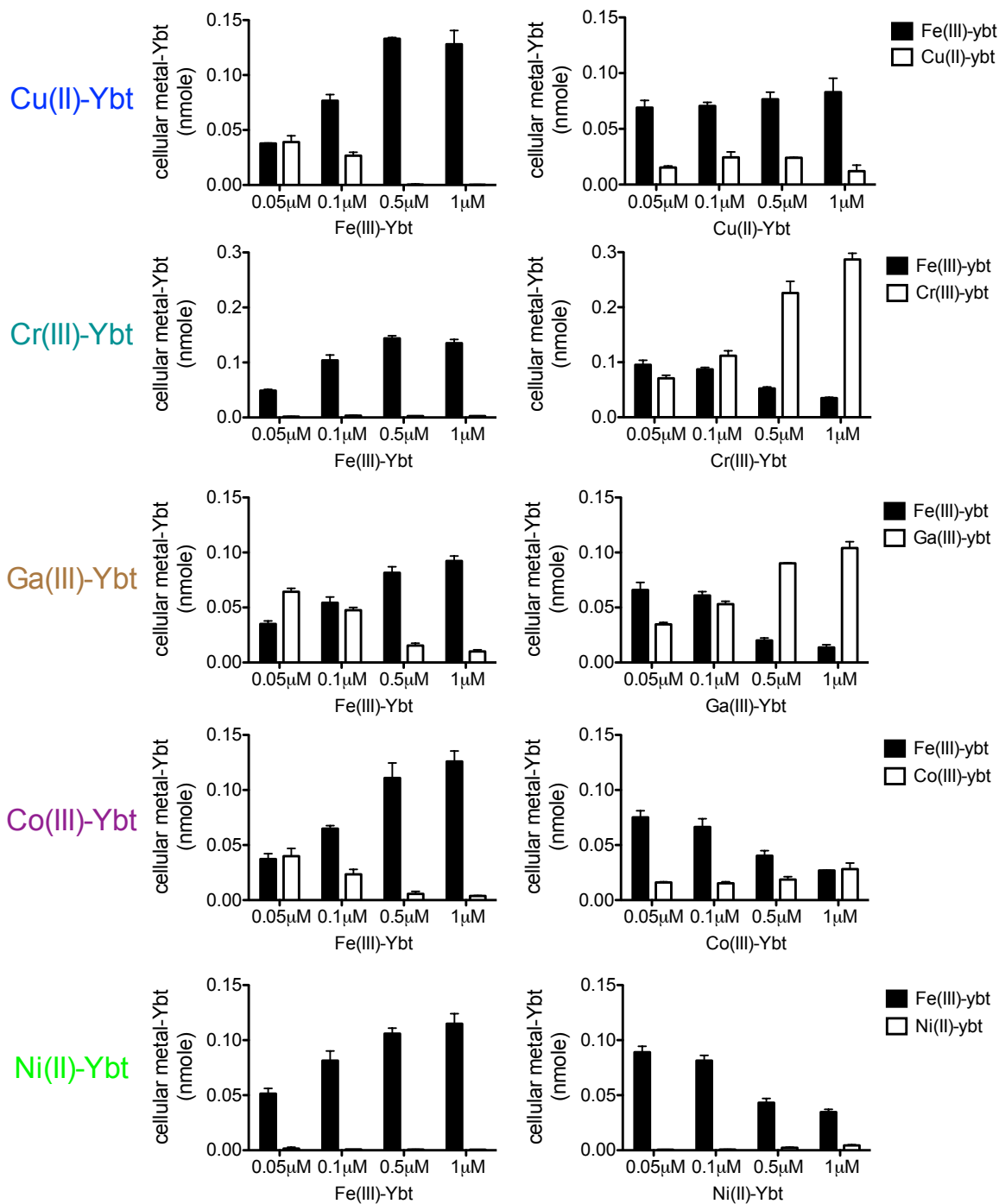


Figure 7. Cu(II)-Ybt does not competitively inhibit Fe(III)-Ybt uptake. MG1655 strains ectopically expressing FyuA were grown in rich media with the indicated concentrations of Fe(III)-Ybt and 0.1 μM non-iron Ybt complexes (*left*) or the indicated concentrations of non-iron

Ybt complexes and 0.1 μ M Fe(III)-Ybt (*right*). Fe(III)-Ybt levels are represented in black with non-ferric Ybt complexes in white. Results are shown as nanomoles, mean \pm s.d.; $n=3$

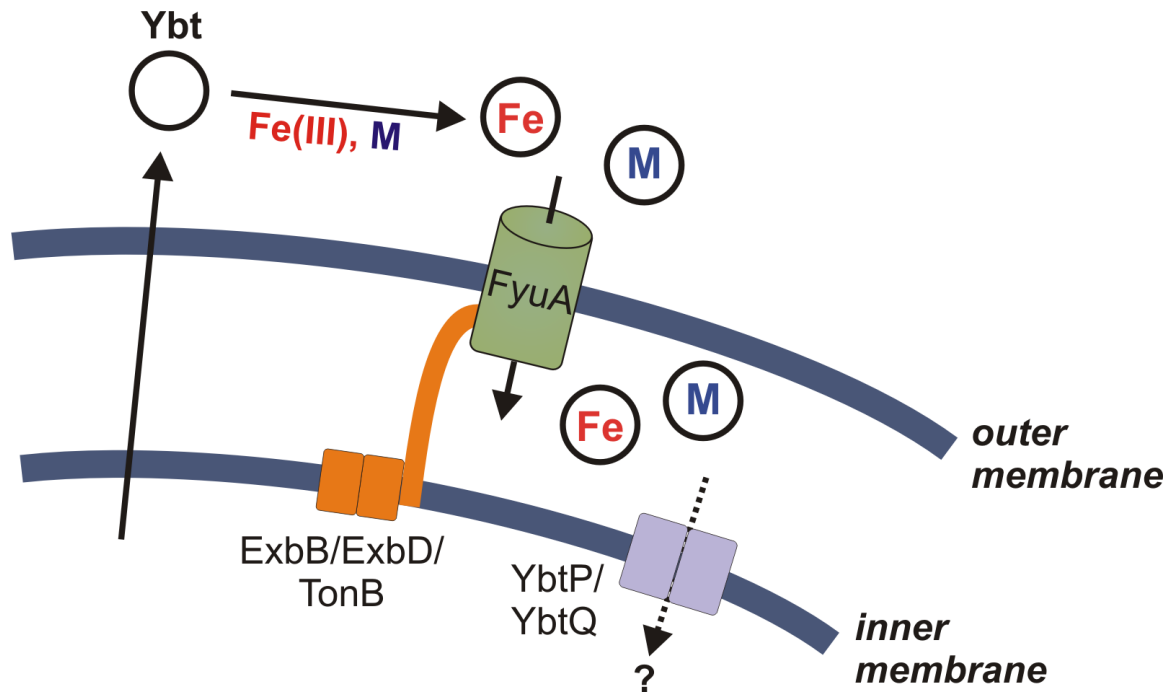
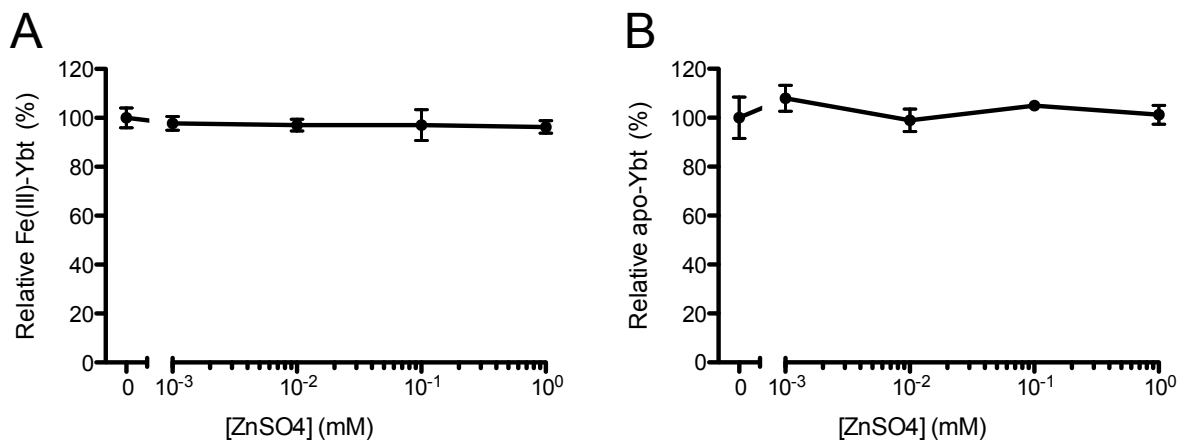
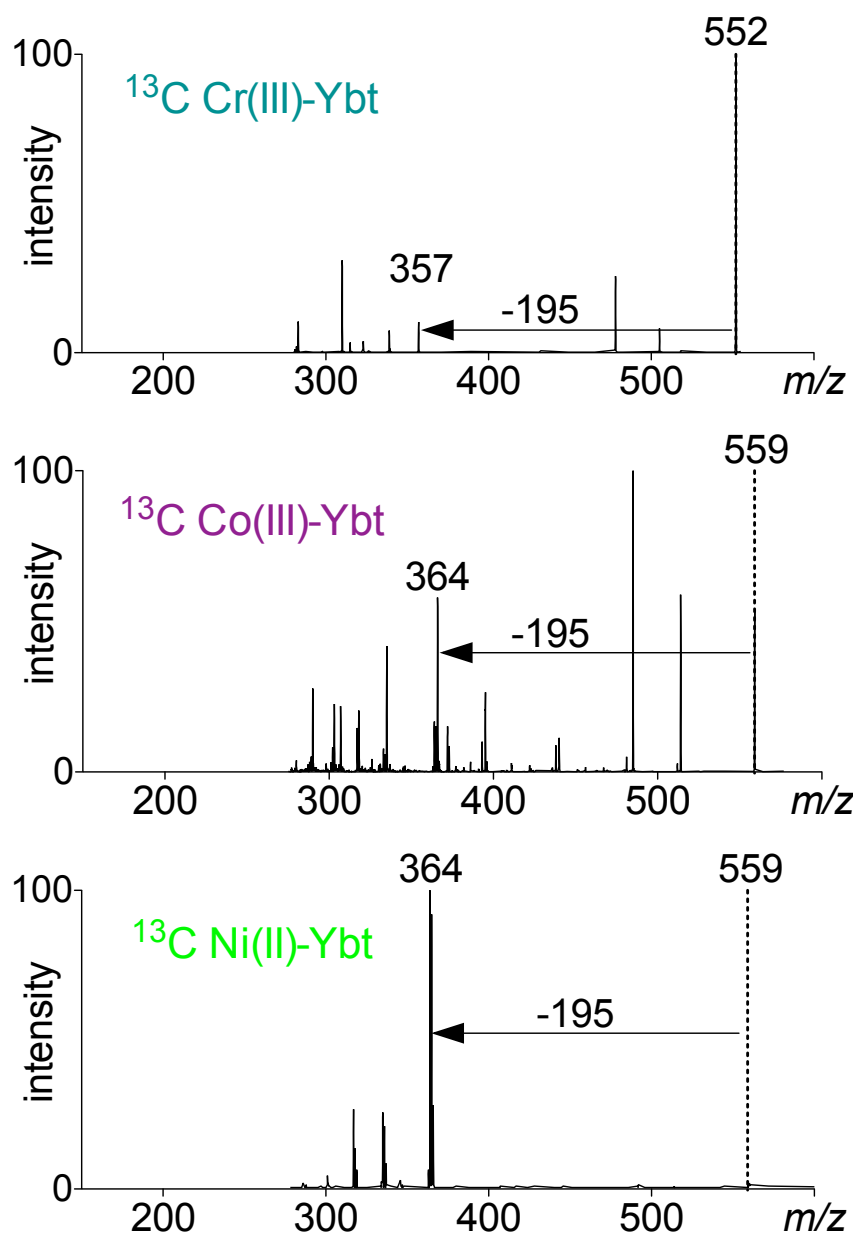


Figure 8. Metal-Ybt transport model. Extracellular *apo*-Ybt interacts with Fe(III) (red) and select transition metals (light blue). Stable metal-Ybt complexes are transported through the outer membrane receptor, FyuA, in a TonB-dependent manner. The precise interactions between metal-Ybt and the inner membrane transporters YbtPQ, is not known.

CHAPTER TWO: SUPPLEMENTARY FIGURES

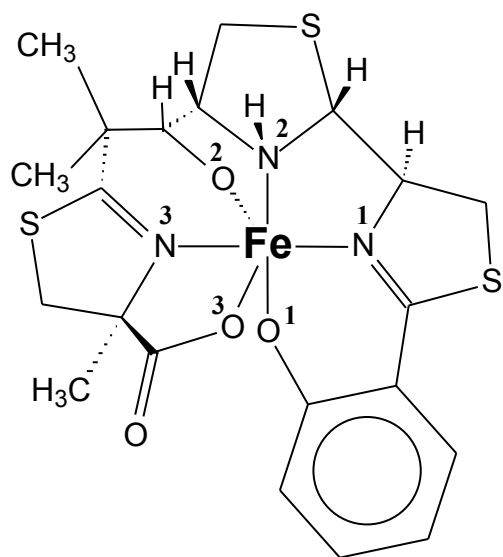


Supplementary Figure 1. Fe(III)-Ybt and *apo*-Ybt levels do not decrease in presence of excess zinc ions. HPLC-purified Fe(III)-Ybt and *apo*-Ybt were separately incubated with excess zinc ions. Samples were eluted on C18 silica columns to remove unbound zinc ions and ¹³C-labeled Fe(III)-Ybt was added just prior to elution to normalize for column retention. Fe(III)-Ybt and *apo*-Ybt levels were measured using MRM detection method. Relative levels were calculated using MRM peak areas normalized with ¹³C-labeled internal standard. **(A)** Fe(III)-Ybt and **(B)** *apo*-Ybt levels did not change despite mixing with zinc ions in molar excess. Results are shown as mean ± s.d.; *n*=3.



Supplementary Figure 2. Structural confirmation of metal-Ybt complexes by stable isotope labeling. MS/MS of new ^{13}C -labeled metal-Ybt complexes revealed a shifted dominant MS/MS neutral loss of 195 mass units, corresponding to loss of a fragment containing eight carbons as previously observed for Fe(III)-Ybt and Cu(II)-Ybt.

Neutral Ferric Yersiniabactin Complex, calculated



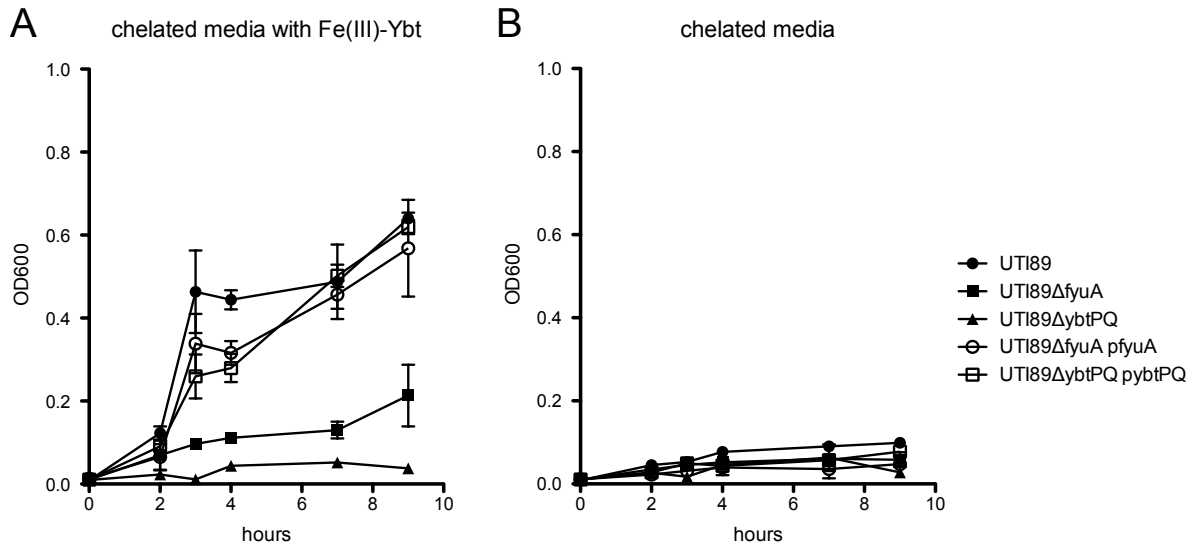
Bond	Bond Lengths	
	Calculated	Crystal Structure(A)
Fe-O(1)	1.913	1.920
Fe-O(2)	1.902	1.899
Fe-O(3)	2.007	2.078
Fe-N(1)	2.084	2.084
Fe-N(2)	2.322	2.255
Fe-N(3)	2.164	2.130

Mean absolute deviation: 0.030

RMS deviation: 0.042

In Angstroms

Supplementary Figure 3. Comparison of neutral Fe(III)-Ybt complexes. Figure and Table show comparison of ligand bond lengths to the ferric ion between as calculated to the published crystal structure (37) (structure A of four in unit cell) of neutral Fe(III)-Ybt.



Supplementary Figure 4. FyuA and YbtPQ are necessary for Fe(III)-Ybt-dependent growth in UPEC. (A) Fe(III)-Ybt-dependent growth is limited in UTI89 mutants lacking FyuA and YbtPQ. In this condition, Fe(III)-Ybt is added to a rich media in which bioavailable ferric ions are chelated with EDDHA. Plasmid-complemented mutants show restored growth with exogenous Fe(III)-Ybt. **(B)** UTI89 strains are indistinguishable in the absence of Fe(III)-Ybt in chelated media.

CHAPTER TWO: TABLES

Table 1. Calculated metal-Ybt extinction coefficient values

metal-Ybt	local maximum (nm)	extinction coefficient
Fe(III)-Ybt	385	5295
Cu(II)-Ybt	350	4578
Cr(III)-Ybt	350	3948
Ga(III)-Ybt	345	6448
Co(III)-Ybt	370	4076
Ni(II)-Ybt	355	5902

CHAPTER TWO: REFERENCES

1. Miethke, M., and Marahiel, M. A. (2007) Siderophore-based iron acquisition and pathogen control. *Microbiol. Mol. Biol. Rev. MMBR.* **71**, 413–51
2. Hood, M. I., and Skaar, E. P. (2012) Nutritional immunity: transition metals at the pathogen–host interface. *Nat. Rev. Microbiol.* **10**, 525–537
3. Noinaj, N., Guillier, M., Barnard, T. J., and Buchanan, S. K. (2010) TonB-Dependent Transporters: Regulation, Structure, and Function. *Annu. Rev. Microbiol.*
4. Perry, R. D., and Fetherston, J. D. (2011) Yersiniabactin iron uptake: mechanisms and role in *Yersinia pestis* pathogenesis. *Microbes Infect. Inst. Pasteur.* **13**, 808–17
5. Chu, B. C., Garcia-Herrero, A., Johanson, T. H., Krewulak, K. D., Lau, C. K., Peacock, R. S., Slavinskaya, Z., and Vogel, H. J. (2010) Siderophore uptake in bacteria and the battle for iron with the host; a bird’s eye view. *Biometals.* **23**, 601–6111
6. Fetherston, J. D., Bertolino, V. J., and Perry, R. D. (1999) YbtP and YbtQ: two ABC transporters required for iron uptake in *Yersinia pestis*. *Mol. Microbiol.* **32**, 289–99
7. Raymond, K. N., Dertz, E. A., and Kim, S. S. (2003) Enterobactin: an archetype for microbial iron transport. *Proc. Natl. Acad. Sci. U. S. A.* **100**, 3584–8
8. Schalk, I. J. (2008) Metal trafficking via siderophores in Gram-negative bacteria: specificities and characteristics of the pyoverdine pathway. *J. Inorg. Biochem.* **102**, 1159–69
9. Brem, D., Pelludat, C., Rakin, A., Jacobi, C. A., and Heesemann, J. (2001) Functional analysis of yersiniabactin transport genes of *Yersinia enterocolitica*. *Microbiology.* **147**, 1115–27

10. Henderson, J. P., Crowley, J. R., Pinkner, J. S., Walker, J. N., Tsukayama, P., Stamm, W. E., Hooton, T. M., and Hultgren, S. J. (2009) Quantitative Metabolomics Reveals an Epigenetic Blueprint for Iron Acquisition in Uropathogenic *Escherichia coli*. *PloS Pathog.*
11. Mabbetta, A. N., Uletta, G. C., Watta, R. E., Treea, J. J., Totsikaa, M., Onga, C. Y., Wooda, J. M., Monaghanb, W., Lookec, D. F., Nimmod, G. R., Svanborge, C., and Schembria, M. A. (2009) Virulence properties of asymptomatic bacteriuria *Escherichia coli*. *Int. J. Med. Microbiol.*
12. Fetherston, J. D., Bearden, S. W., and Perry, R. D. (1996) YbtA, an AraC-type regulator of the *Yersinia pestis* pesticin/yersiniabactin receptor. *Mol. Microbiol.* **22**, 315–25
13. Perry, R. D., Balbo, P. B., Jones, H. A., Fetherston, J. D., and DeMoll, E. (1999) Yersiniabactin from *Yersinia pestis*: biochemical characterization of the siderophore and its role in iron transport and regulation. *Microbiology*
14. Reigstad, C. S., Hultgren, S. J., and Gordon, J. I. (2007) Functional genomic studies of uropathogenic *Escherichia coli* and host urothelial cells when intracellular bacterial communities are assembled. *J. Biol. Chem.* **282**, 21259–67
15. Hagan, E. C., Lloyd, A. L., Rasko, D. A., Faerber, G. J., and Mobley, H. L. T. (2010) *Escherichia coli* Global Gene Expression in Urine from Women with Urinary Tract Infection. *PloS Pathog.*
16. Chaturvedi, K. S., Hung, C. S., Crowley, J. R., Stapleton, A. E., and Henderson, J. P. (2012) The siderophore yersiniabactin binds copper to protect pathogens during infection. *Nat. Chem. Biol.* 10.1038/nchembio.1020

17. Chaturvedi, K. S., Hung, C. S., Giblin, D. E., Urushidani, S., Austin, A. M., Dinauer, M. C., and Henderson, J. P. (2013) Cupric Yersiniabactin Is a Virulence-Associated Superoxide Dismutase Mimic. *ACS Chem. Biol.* **9**, 551–561
18. White, C., Lee, J., Kambe, T., Fritsche, K., and Petris, M. J. (2009) A role for the ATP7A copper-transporting ATPase in macrophage bactericidal activity. *J. Biol. Chem.* **284**, 33949–56
19. Lukacik, P., Barnard, T. J., Keller, P. W., Chaturvedi, K. S., Seddiki, N., Fairman, James W., Noinaj, N., Kirby, T. L., Henderson, J. P., Steven, A. C., Hinnebusch, B. J., and Buchanan, S. K. (2012) Structural engineering of a phage lysin that targets Gram-negative pathogens. *PNAS.* **109**, 9857–9862
20. Chen, S. L., Hung, C. S., Xu, J., Reigstad, C. S., Magrini, V., Sabo, A., Blasiar, D., Bieri, T., Meyer, R. R., Ozersky, P., Armstrong, J. R., Fulton, R. S., Latreille, J. P., Spieth, J., Hooton, T. M., Mardis, E. R., Hultgren, S. J., and Gordon, J. I. (2006) Identification of genes subject to positive selection in uropathogenic strains of *Escherichia coli*: a comparative genomics approach. *Proc. Natl. Acad. Sci. U. S. A.* **103**, 5977–82
21. Mulvey, M. A., Schilling, J. D., and Hultgren, S. J. (2001) Establishment of a persistent *Escherichia coli* reservoir during the acute phase of a bladder infection. *Infect. Immun.* **69**, 4572–9
22. Datsenko, K. A., and Wanner, B. L. (2000) One-step inactivation of chromosomal genes in *Escherichia coli* K-12 using PCR products. *PNAS.* **97**, 6640–6645
23. Amann, E., Ochs, B., and Abel, K. J. (1988) Tightly regulated tac promoter vectors useful for the expression of unfused and fused proteins in *Escherichia coli*. *Gene.* **69**, 301–15

24. Drechsel, H., Stephan, H., Lotz, R., Haag, H., Zähler, H., Hantke, K., and Jung, G. (1995) Structure elucidation of yersiniabactin, a siderophore from highly virulent *Yersinia* strains. *Eur. J. Org. Chem.*
25. Acevedo, O., and Jorgensen, W. L. (2010) Advances in quantum and molecular mechanical (QM/MM) simulations for organic and enzymatic reactions. *Acc. Chem. Res.* **43**, 142–51
26. Ohlinger, W. S., Klunzinger, P. E., Deppmeier, B. J., and Hehre, W. J. (2009) Efficient calculation of heats of formation. *J. Phys. Chem. A.* **113**, 2165–75
27. Fromager, E. (2011) Rigorous formulation of two-parameter double-hybrid density-functionals. *J. Chem. Phys.* **135**, 244106
28. Zawada, A., Kaczmarek-Kedziera, A., and Bartkowiak, W. (2012) On the potential application of DFT methods in predicting the interaction-induced electric properties of molecular complexes. Molecular H-bonded chains as a case of study. *J. Mol. Model.* **18**, 3073–86
29. Morschel, P., Janikowski, J., Hilt, G., and Frenking, G. (2008) Ligand-tuned regioselectivity of a cobalt-catalyzed Diels-Alder reaction. A theoretical study. *J. Am. Chem. Soc.* **130**, 8952–66
30. Bailey, W. C. (1998) B3LYP Calculation of Deuterium Quadrupole Coupling Constants in Molecules. *J. Mol. Spectrosc.* **190**, 318–23
31. Cossi, M., Rega, N., Scalmani, G., and Barone, V. (2003) Energies, structures, and electronic properties of molecules in solution with the C-PCM solvation model. *J. Comput. Chem.* **24**, 669–81
32. Rydberg, P., and Olsen, L. (2009) The accuracy of geometries for iron porphyrin complexes from density functional theory. *J. Phys. Chem. A.* **113**, 11949–53

33. Ansbacher, T., Srivastava, H. K., Martin, J. M., and Shurki, A. (2010) Can DFT methods correctly and efficiently predict the coordination number of copper(I) complexes? A case study. *J. Comput. Chem.* **31**, 75–83
34. Scott, A. P., and R.L. (1996) Harmonic vibrational frequencies: An evaluation of Hartree-Fock, Moller-Plesset, quadratic configuration interaction, density functional theory, and semiempirical scale factors. *J Phys Chem.* **100**, 16502–16513
35. Shephard, M. J., and Paddon-Row, M. N. (1995) Gas phase structure of the bicyclo [2.2.1] heptane (Norbornane) cation radical: A combined ab initio MO and density functional theory. *J Phys Chem.* **99**, 3101–3108
36. Turecek, F. (1998) Proton affinity of dimethyl sulfoxide and relative stabilities of C₂H₆OS molecules and C₂H₇OS⁺ ions. A comparative G2(MP2) ab initio and density functional theory study. *J Phys Chem*
37. Miller, M. C., Parkin, S., Fetherston, J. D., Perry, R. D., and Demoll, E. (2006) Crystal structure of ferric-yersiniabactin, a virulence factor of *Yersinia pestis*. *J. Inorg. Biochem.* **100**, 1495–500
38. Zaitseva, I., Zaitsev, V., Card, G., Moshkov, K., Bax, B., Ralph, A., and Lindley, P. (1996) The X-ray structure of human serum ceruloplasmin at 3.1 Å: nature of the copper centres. *JBIC J. Biol. Inorg. Chem.* **1**, 15–23
39. Fu, Y., Chang, F. M., and Giedroc, D. P. (2014) Copper transport and trafficking at the host-bacterial pathogen interface. *Acc. Chem. Res.* **47**, 3605–13
40. Subashchandrabose, S., Hazen, T. H., Brumbaugh, A. R., Himpsl, S. D., Smith, S. N., Ernst, R. D., Rasko, D. A., and Mobley, H. L. (2014) Host-specific induction of *Escherichia coli*

- fitness genes during human urinary tract infection. *Proc. Natl. Acad. Sci. U. S. A.* **111**, 18327–32
41. Winterbourn, C. C., Hampton, M. B., Livesey, J. H., and Kettle, A. J. (2006) Modeling the reactions of superoxide and myeloperoxidase in the neutrophil phagosome: implications for microbial killing. *J. Biol. Chem.* **281**, 39860–9
 42. Braud, A., Geoffroy, V., Hoegy, F., Mislin, G. L., and Schalk, I. J. (2010) Presence of the siderophores pyoverdine and pyochelin in the extracellular medium reduces toxic metal accumulation in *Pseudomonas aeruginosa* and increases bacterial metal tolerance. *Environ. Microbiol. Rep.* **2**, 419–25
 43. Ma, Z., Jacobsen, F. E., and Giedroc, D. P. (2009) Metal transporters and metal sensors: How coordination chemistry controls bacterial metal homeostasis. *Chem Rev.* **109**, 4644–4681
 44. Kenney, G. E., and Rosenzweig, A. C. (2012) Chemistry and biology of the copper chelator methanobactin. *ACS Chem. Biol.* **7**, 260–8
 45. Cvetkovic, A., Menon, A. L., Thorgersen, M. P., Scott, J. W., Poole, F. L., 2nd, Jenney, F. E., Jr., Lancaster, W. A., Praissman, J. L., Shanmukh, S., Vaccaro, B. J., Trauger, S. A., Kalisiak, E., Apon, J. V., Siuzdak, G., Yannone, S. M., Tainer, J. A., and Adams, M. W. (2010) Microbial metalloproteomes are largely uncharacterized. *Nature.* **466**, 779–82
 46. Bobrov, A. G., Kirillina, O., Fetherston, J. D., Miller, M. C., Burlison, J. A., and Perry, R. D. (2014) The *Yersinia pestis* siderophore, yersiniabactin, and the ZnuABC system both contribute to zinc acquisition and the development of lethal septicaemic plague in mice. *Mol. Microbiol.* **93**, 759–75

47. Zaichick, Vy., Sviridova, T. V., and Zaichick, S. V. (1997) Zinc in the human prostate gland: normal, hyperplastic and cancerous. *Int. Urol. Nephrol.* **29**, 565–74
48. Zhang, D. Y., Azrad, M., Demark-Wahnefried, W., Frederickson, C. J., Lippard, S. J., and Radford, R. J. (2014) Peptide-Based, Two-Fluorophore, Ratiometric Probe for Quantifying Mobile Zinc in Biological Solutions. *ACS Chem. Biol.* 10.1021/cb500617c
49. Kelleher, S. L., McCormick, N. H., Velasquez, V., and Lopez, V. (2011) Zinc in specialized secretory tissues: roles in the pancreas, prostate, and mammary gland. *Adv. Nutr.* **2**, 101–11
50. Braud, A., Hannauer, M., Mislin, G. L., and Schalk, I. J. (2009) The *Pseudomonas aeruginosa* pyochelin-iron uptake pathway and its metal specificity. *J. Bacteriol.* **191**, 3517–25
51. Emery, T. (1971) Role of ferrichrome as a ferric ionophore in *Ustilago sphaerogena*. *Biochemistry (Mosc.)*. **10**, 1483–8
52. Ecker, D. J., and Emery, T. (1983) Iron uptake from ferrichrome A and iron citrate in *Ustilago sphaerogena*. *J. Bacteriol.* **155**, 616–22

CHAPTER THREE

The yersiniabactin-associated ATP binding cassette proteins YbtP and YbtQ enhance *E. coli* fitness during high titer cystitis

ABSTRACT

The *Yersinia* High Pathogenicity Island (HPI) is common to multiple virulence strategies used by *Escherichia coli* strains associated with urinary tract infection (UTI). Among the genes in this island are *ybtP* and *ybtQ*, encoding distinctive ATP binding cassette (ABC) proteins associated with ferric yersiniabactin import in *Yersinia pestis*. In this study, we compared the impact of *ybtPQ* on a model *E. coli* cystitis strain during *in vitro* culture and experimental murine infections. A *ybtPQ*-null mutant exhibited no growth defect in standard culture conditions consistent with non-essentiality in this background. A growth defect phenotype was observed, and genetically complemented *in vitro* during ferric yersiniabactin-dependent growth. Following bladder inoculation in C3H/HEN and C3H/HeOuJ mice, this strain exhibited a profound, million-fold competitive infection defect in the subgroup of mice that progress to high titer bladder infections. These results identify a virulence role for YbtPQ during the highly inflammatory microenvironment characteristic of high titer cystitis. The profound competitive defect may relate to the apparent selection of *Yersinia* HPI-positive *E. coli* in uncomplicated clinical UTIs.

INTRODUCTION

Urinary tract infection (UTI) is one of most common bacterial infections, affecting nearly 9 million individuals every year (1). Uropathogenic *Escherichia coli* (UPEC) are responsible for over 80% of all community-acquired UTI cases and in some patients progresses from a localized bladder infection to infect the kidneys and bloodstream (2, 3). Over 50% of women acquire a UTI over their lifetime, with 30% suffering from recurrent UTI (4, 5). Uncomplicated UTIs appear to follow an ascending route of infection in which the bladder is exposed to a polymicrobial inoculum of intestinal bacteria that colonize the vaginal vestibule and urethra (6–10). This early colonization event may precede patients' visits to physicians by several days. Our understanding of the molecular mechanisms UPEC use to emerge from this early inoculum and dominate the urinary microbiome at the time of clinical UTI diagnosis remains incomplete.

When an uncomplicated UTI patient's rectal and urinary *E. coli* strains are compared, the urinary strain is more likely to carry the 30 kilobase *Yersinia* High Pathogenicity Island (HPI) (11). The *Yersinia* HPI is nearly ubiquitous among model uropathogenic *E. coli* strains, is associated with fluoroquinolone resistance when present in combination with the aerobactin siderophore system, and is typically present in over 70% of clinical urinary isolates (3, 11, 12). The *Yersinia* HPI encodes the yersiniabactin siderophore system including yersiniabactin biosynthetic enzymes in addition to outer and inner membrane transporters associated with metal-yersiniabactin complex import (13–16). Yersiniabactin is one of three genetically non-conserved *E. coli* siderophore types (yersiniabactin, salmochelin and aerobactin) that may be expressed in addition to enterobactin, the conserved *E. coli* siderophore (3, 11, 12). The *Yersinia* HPI is central to multiple *E. coli* urovirulence strategies, raising the possibility that it is functionally distinct from

other siderophore systems (12). In uropathogenic *E. coli*, the yersiniabactin system has been appreciated to facilitate importer-independent copper and reactive oxygen species resistance (17, 18). Furthermore in *Y. pestis*, the yersiniabactin system is linked to zinc import (19). *E. coli* virulence may be enhanced in strains that use multiple siderophore types, including yersiniabactin, to overcome metal ion limitation characteristic of “nutritional immunity” (20, 21). These observations raise the question of whether importer-dependent functions associated with the *Yersinia* HPI such as metal ion acquisition are pathophysiologically important during UTI (14, 16).

Seminal studies in *Yersinia pestis* identified several proteins that are specifically necessary for ferric yersiniabactin-dependent growth (14, 15). Within the *Yersinia* HPI, the inner membrane transporter genes (*ybtP* and *ybtQ*) are present in an operon that is separate from the outer membrane transporter gene (denoted as *psn* in *Y. pestis*, and *fyuA* in other bacteria) operon. Both operons are regulated in part by the AraC-like transcription factor YbtA (Fig 1) (13, 14, 22, 23). Typical of most outer membrane siderophore transporters, FyuA uses the TonB complex to import its cognate iron(III)-siderophore complex (Fe(III)-yersiniabactin) into the periplasmic space (15, 16, 24). Unlike most siderophore-associated inner membrane transporters, *ybtP* and *ybtQ* are overlapping genes (by 40 nucleotides) that each encode half of an inner membrane ATP-binding cassette (ABC) transporter, each with unusual amino-terminal membrane-spanning domains and carboxy-terminal ATPases (14). It is unclear whether these unusual structural features correspond to atypical or complex functionality. While siderophore-associated ABC transporters are typically implicated in ferric siderophore transport, some members of this family

possess additional signaling roles (25). Metabolomic comparisons also raise the possibility that YbtP and Q may exert functions distinct from ferric yersiniabactin utilization in UPEC (26).

Overall expression of the yersiniabactin system can be inferred by evidence of yersiniabactin biosynthesis as well as serological and transcriptional evidence of *ybtP*, *ybtQ* and *fyuA* expression during mouse and human cystitis (17, 27–29). Beyond UTI, *ybtPQ* mutants in *Yersinia pestis* and *Klebsiella pneumoniae* exhibit diminished virulence in mouse models of bubonic plague and pneumonia, respectively (14, 30). *ybtP* and *ybtQ* homologues in *Pseudomonas aeruginosa* and *Mycobacterium tuberculosis* also affected virulence in a burned mouse model of sepsis and mouse aerosol infection model (31, 32). The broad spectrum of pathogens associated with these distinctive bacterial proteins makes their associated functions an intriguing target for future virulence-associated therapies.

In this study, we sought to determine whether YbtP and YbtQ affect urinary tract infection pathogenesis. Using a combined bacteriologic and liquid chromatography-mass spectrometry approach, we found that YbtPQ is necessary for ferric-Ybt dependent growth but not Ybt synthesis in a UPEC strain. We next compared isogenic wild type and *ybtPQ* mutant strains in an experimental murine cystitis model using C3H/HeN and C3H/HeOuJ mice, which are known to develop distinctive high titer, persistent infections with UPEC. Uropathogenic *E. coli* lacking *ybtPQ* exhibited a profound competitive fitness defect during high titer infections but not during low iron liquid culture conditions. These results are consistent with an important role for YbtP and Q in inflamed bladder microenvironments during UTI infection pathogenesis.

EXPERIMENTAL PROCEDURES

Bacterial strains, plasmids and culture conditions

Uropathogenic *E. coli* isolate UTI89, which encodes the enterobactin, salmochelin and yersiniabactin siderophore systems, was used in this study (33, 34). Strains were grown in LB agar (Becton, Dickson and Company) or M63 minimal medium supplemented with 0.2% glycerol (v/v) and 10 mg ml⁻¹ niacin (Sigma) with antibiotics as appropriate (11). Ampicillin (100 µg ml⁻¹, Goldbio) and kanamycin (50 µg ml⁻¹, Goldbio) were used for strain selection. UTI89 mutant strains used in this study are listed in Table 1. In-frame deletions in UTI89 were made using the lambda Red recombinase method with pKD4 or pKD13 as templates (35). PCR with flanking primers were used to confirm deletions. Antibiotic resistance insertions were removed by transforming strains with pCP20 expressing FLP recombinase. YbtPQ-expressing plasmid was constructed with the pTrc99a vector (36) and using standard PCR and recombination techniques.

Yersiniabactin and ¹³C-yersiniabactin preparation

Apo-Ybt was generated from UTI89 Δ entB grown in M63 minimal medium supplemented with 0.2% glycerol (v/v) and 10 mg ml⁻¹ niacin (Sigma) as previously described (17). ¹³C-Ybt was generated by growing UTI89 Δ fur in medium supplemented ¹³C-labeled glycerol as previously described (17). Ferric-Ybt complexes were produced by adding iron(III) chloride (Sigma) to apo-Ybt. Ferric-Ybt was applied to a methanol conditioned C18 silica column (Sigma) and eluted with 80% methanol as previously described (16). Eluates were lyophilized overnight. Dried samples were resuspended in deionized water and purified through high-performance liquid chromatography using C18 silica column (Whatman Partisil). Ferric-Ybt containing

fractions were collected, dried down using a lyophilizer and resuspended in deionized water. Stock ferric-Ybt quantification was carried out using previously described extinction coefficient (16). Sample ferric-Ybt levels were quantified in multiple reaction monitoring mode using known collision-induced dissociation fragmentations and ¹³C-labeled Fe(III)-Ybt internal standards.

Fe(III)-Ybt dependent growth

After overnight growth in M63 minimal medium, strains were normalized for starting OD₆₀₀ in M63 with 2 mM EDDHA (Complete Green Company). 1 μM HPLC-purified Fe(III)-Ybt was added to strains and grown for 18 hours in 37 °C with shaking, as previously described (16). Bacterial growth was measured using OD₆₀₀ readings.

Mouse infections

Bacteria for infection were prepared as previously described (37). Six to seven week old female C3H/HeN (Harlan) and C3H/HeOuj (JAX) were transurethrally infected with a 50 μL suspension containing 1 x 10⁷ CFU of UTI89 or UTI89Δ*ybtPQ* in PBS while anesthetized under 4% isoflurane (37, 38). For competitive infections, mice were infected with a 50 μL combined suspension containing 5 x 10⁶ CFU each of UTI89 and UTI89Δ*ybtPQ*::Kan^R in PBS while anesthetized under 4% isoflurane. At indicated time points, mice were sacrificed by cervical dislocation under isoflurane anesthesia and bladders and kidneys aseptically removed. Organs were homogenized in PBS and were then serially diluted and 50 μL total of each dilution was spotted onto LB agar plates and LB agar plates with 50 μg/mL kanamycin where appropriate.

Competitive indices (CI) were calculated by using UTI89 as the reference strain, as follows: $CI = (UTI89_{CFU\ out} / UTI89_{CFU\ in}) / (UTI89\Delta ybtPQ::Kan^R_{CFU\ out} / UTI89\Delta ybtPQ::Kan^R_{CFU\ in})$ (39).

Bladder intracellular bacterial communities

Bladders were aseptically removed at 6 hours post infection to count the number of IBCs.

Harvested bladders were bisected, splayed on silicone plates, and fixed in 2% paraformaldehyde.

IBC counts were quantified by LacZ staining of whole bladders as previously described (40).

In vitro co-growth experiments

Bacteria for co-growth experiments were prepared the same as mice infections described above.

5 μ L combined suspension containing 5×10^6 CFU each of UTI89 and UTI89 $\Delta ybtPQ::Kan^R$ in PBS were inoculated to 5 mL M63 minimal medium and grown in 37 °C statically or shaking as indicated. At indicated time points, cultures were removed and serially diluted with 50 μ L total of each dilution spotted onto LB agar plates and LB agar plates with 50 μ g/mL kanamycin where appropriate.

Statistical analysis

Student's *t*-test was used to compare yersiniabactin biosynthesis levels between paired strains.

Two-tailed Mann-Whitney U test was used to compare bladder and kidney colonization levels and IBC counts between UTI89 and UTI89 $\Delta ybtPQ$. Wilcoxon signed rank test was used to compare the log of competitive indices to a theoretical median of 0. Statistics and graphs were generated using GraphPad Prism 5 (GraphPad software).

RESULTS

ybtPQ deletion does not affect growth in ferric-Ybt independent conditions

To investigate the role of YbtPQ in uropathogenic *E. coli* growth, we first measured growth of the model UPEC strain UTI89 in nutrient-rich LB medium as well as M63 minimal medium. UTI89 Δ *ybtPQ* growth was indistinguishable from wild type UTI89 in both media conditions (Fig 2A, B). Addition of the ferric ion chelator EDDHA (2mM), which sequesters Fe(III) and renders it poorly accessible to siderophores, to M63 minimal medium prior to inoculation diminished growth of both strains to a similar degree. Addition of 1 μ M purified Fe(III)-Ybt reversed EDDHA-mediated inhibition of wild type UTI89 but not UTI89 Δ *ybtPQ*. Genetic complementation with plasmid-encoded *ybtPQ* restored UTI89 Δ *ybtPQ* growth to wild type levels in this EDDHA/Fe(III)-Ybt condition (Fig 2C, D). Insertion of empty vector did not restore UTI89 Δ *ybtPQ* growth to wild type levels in this EDDHA/Fe(III)-Ybt condition (Data not shown). These results are consistent with YbtPQ as non-essential genes that permit Fe(III)-Ybt to be used as an iron source in UPEC.

ybtPQ is not required for yersiniabactin synthesis in UPEC

ybtPQ shares an operon with the yersiniabactin biosynthetic gene *ybtS* (Fig 1). To determine whether *ybtPQ* deletion exerts pleiotropic effects upon Ybt synthesis in UPEC, we compared Ybt secretion between wild type UTI89, UTI89 Δ *ybtPQ*::Kan^R (Fig 3A) and UTI89 Δ *ybtPQ* (Fig 3B) in M63 minimal medium. Yersiniabactin production by UTI89 Δ *ybtS* was undetectable while UTI89 Δ *ybtPQ*::Kan^R was comparable to that of wild type UTI89. Plasmid-complemented UTI89 Δ *ybtPQ*::Kan^R showed a small but significant increase in Ybt synthesis compared to UTI89. UTI89 Δ *ybtPQ* also showed no difference in Ybt biosynthesis compared to wild type

UTI89. These results show that yersiniabactin biosynthesis is preserved in UTI89 *ybtPQ* deletion mutants, similar to previous results seen in *Y. pestis* and *Y. enterocolitica* (14, 23). These results also support a function for *ybtPQ* in UPEC that is distinct from yersiniabactin biosynthesis.

Individual infections by wild type and ybtPQ mutants in C3H/HeN mice

We hypothesized that loss of *ybtPQ* would affect *in vivo* fitness during urinary tract infection. We tested this in C3H/HeN mice (homozygous for the retinal degeneration allele *Pde6b^{rd1}*), where a 10^7 CFU *E. coli* transurethral inoculum causes an infection involving epithelial cell invasion followed by a bifurcation to high and low CFU values that are evident as soon as 3 days post infection (38). The high CFU mice exhibit high titer ($>10^4$ CFU per organ) bladder colonization by 4 weeks post infection that is characterized by urothelial hyperplasia and high levels of inflammation (37, 38, 41). We first conducted single strain inoculations with UTI89 or UTI89 Δ *ybtPQ*. Bladder and kidneys were harvested at 7 and 14 days post infection, and CFU were determined for both strains (Fig 4). As previously observed, mice infected with wild type UTI89 exhibited a bimodal distribution of bladder CFU at 7 and 14 days post-infection (dpi) with one group greater than 10^5 CFU/bladder and the other less than 10^4 CFU/bladder. Mice infected with UTI89 Δ *ybtPQ* showed no statistically significant differences in CFU for both bladder and kidneys compared to wild type UTI89 (Fig 4A, B). These results indicate that *YbtPQ* is not required for the development of acute and persistent high titer colonization in single strain infections.

Bladder intracellular bacterial community assessment

To further assess the role of YbtPQ in acute cystitis, we quantified the formation of bladder intracellular bacterial communities (IBC). IBCs are biofilm-like aggregation of UPEC that have invaded and subsequently replicated in the cytoplasm of bladder superficial umbrella cells (42, 43). IBCs have been observed during acute bladder infection, up to 24 hours post-inoculation (27, 43). C3H/HeN mice were infected with 10^7 CFU of UTI89 Δ ybtPQ or wild type UTI89. Bladders were harvested at 6 hours post infection with IBC quantification by LacZ staining (Fig 5). IBCs were observed during UTI89 Δ ybtPQ infections and the number of IBCs per bladder were not significantly different from those observed during wild type UTI89 infections. These results indicate that YbtPQ is not required for IBC development.

Competitive infections and in vitro co-growth with wild type and ybtPQ mutant

Previous observations suggest that uncomplicated UTI originate with polymicrobial inoculation of the urinary tract and that patient rectal *E. coli* strains with the *Yersinia* High Pathogenicity Island are preferentially recovered from patient urine once the infections become symptomatic (10, 11). To determine if loss of ybtPQ function would affect fitness during mixed inoculation with a wild type strain with intact ybtPQ, we measured wild type UTI89 and UTI89 Δ ybtPQ::Kan^R in competitive infections. We infected C3H/HeN mice with a 10^7 total CFU inoculum consisting of a 1:1 ratio of wild type and mutant UTI89. In both bladder and kidneys, we saw a significant ($p < 0.05$) increase in mean competitive index (CI) values over time, demonstrating that wild type UTI89 outcompetes the mutant strain (Fig 6A, B). By 3-days post infection, a markedly bimodal CI distribution became apparent in bladders, with one group demonstrating CI greater than 10^4 (10,000-fold increase in wild type selection) and the other with CI less than 10^1 (10-fold increase in wild type selection). This separation was widened by 7

and 14-days post infection. Similar progression toward a bimodal CI distribution was observed in kidneys. Neither a high CI nor a bimodal distribution was observed in competitive inoculation of wild type UTI89 and UTI89 Δ ybtPQ::Kan^R into M63 minimal medium under shaking or static conditions at 37 °C (Fig 6C, D). UTI89 Δ ybtPQ::Kan^R showed only a small competitive defect against the wild type strain in both static and shaking conditions near 7-days post inoculation. Together, these results suggest that UPEC lacking YbtPQ are at a marked competitive disadvantage in the distinctive host environment of the mouse cystitis model.

The unusual bimodal CI distribution observed here resembles the bimodal distribution of bladder CFU values in this C3H/HeN mouse cystitis model (38) (Fig 4). To determine whether the CI distribution is related to infection severity, we compared CI values with total CFU (Fig 7A, B). In the bladder, the high CI group corresponded to high titer mice while the low CI group corresponded to low titer mice. CI values within the high titer group progressively increased over the course of 3, 7 and 14-day infections until nearing the maximum resolvable CI limit (based on CFU). A similar relationship was observed in kidneys, although CFUs were more evenly distributed and CI values appeared to approach the maximum resolvable limit for all CFU values. Together, these results suggest that the persistent high titer, but not low titer, bladder infection environment strongly favors UPEC with an intact yersiniabactin import system. This may relate to the apparent selection of *E. coli* strains with the *Yersinia* HPI in UTI patients (11).

Competitive infections by wild type and ybtPQ mutants in C3H/HeOuJ mice

To determine whether loss of YbtPQ has similar effects during infection in other mouse backgrounds, we competitively inoculated C3H/HeOuJ mice (homozygous for the retinal

degeneration allele *Pde6b^{rd1}*) with wild type UTI89 and UTI89 Δ *ybtPQ*::Kan^R as described previously for C3H/HeN mice. C3H/HeOuJ mice have been shown previously to be highly susceptible to persistent bladder and kidney infections from UPEC (38, 44). Similar to results seen in C3H/HeN mice, we saw significant increase ($p < 0.05$) in mean competitive index (CI) values over time in both bladder (Fig 8A) and kidneys (Fig 8C). When we compared CI values with total CFU, we again observed high CI group corresponding to high titer mice and the low CI group corresponding to low titer mice in both bladder (Fig 8B) and kidneys (Fig 8D), similar to C3H/HeN mice.

We also conducted single strain inoculations with UTI89 or UTI89 Δ *ybtPQ*. Similar to results seen in C3H/HeN mice, mice infected with wild type UTI89 exhibited a bimodal distribution of bladder CFU. In mice infected with UTI89 Δ *ybtPQ*, there was a significant decrease by 14 days in mean CFU/bladder when compared to wild type UTI89 (Fig 9A). Despite observing significantly lower CFU in the kidneys at 3-days post infection with UTI89 Δ *ybtPQ*, there were no statistically significant differences in CFU/kidney at later time points (Fig 9B). These results suggest that UPEC with an intact yersiniabactin import system have greater fitness during persistent high titer bladder infections.

DISCUSSION

In this study, we show that the UPEC-encoded ATP-binding cassette transporters YbtP and Q promote bacterial fitness during urinary tract infections. YbtPQ most profoundly affected fitness in the highly inflammatory infection environment of high titer mouse cystitis. While wild type UPEC exhibited up to one million-fold greater survival than co-inoculated *ybtPQ* deletion mutants in murine infections, no such competitive defect was noted during *in vitro* cultures. This is the first report of a role for YbtPQ during *E. coli* urinary tract infection and is among the highest competitive defects reported for a non-conserved, non-essential gene during experimental cystitis. It is notable that this phenotype is evident in UTI89, where *in vitro* iron uptake by yersiniabactin is redundant with the enterobactin and salmochelin siderophore systems. Together, these data suggest that YbtPQ contributes distinctive functions that facilitate the urovirulence of *E. coli* carrying the *Yersinia* High Pathogenicity Island.

Previous work has found that in patients with intestinal colonization by multiple *E. coli* strains, strains possessing the *Yersinia* HPI are preferentially isolated from patient urine at the time of UTI diagnosis (11). Here, the profound competitive disadvantage for YbtPQ-null UPEC during high titer infections – but not *in vitro* culture – suggests a similar advantage for *Yersinia* HPI-expressing *E. coli* in the polymicrobial inoculum preceding uncomplicated UTIs in humans. Features of the high titer infection state in C3H/HeN and C3H/HeOuJ suggest aspects of the host response that may select against YbtPQ-null UPEC. In these infections, up to 20% of bladder UPEC are intracellular within urothelial cells, macrophages and neutrophils. The high titer infection state is also characterized by a robust inflammatory response, which was shown to be required for the development of chronic cystitis (38, 45). If so, a virulence defect during single

strain infections may be more difficult to resolve if the mutant strain elicits a less vigorous inflammatory response than what is present during a mixed infection with wild type UPEC. As such, a potentially greater inflammatory response during a mixed infection may favor wild type UPEC survival. These inflammatory responses may resemble those present during the 2-3 days of “pre-clinical UTI” that pre-date patients’ decisions to seek treatment for UTI symptoms (5). The current study thus raises the possibility that the yersiniabactin import pathway equips UPEC to better overcome barriers to growth imposed by inflammatory microenvironments in the infected host.

With the notable exception of *Y. pestis* YbtP and *Salmonella enterica* serovar Typhimurium IroC (14, 46), experimental infection studies have tended to focus upon the TonB-dependent outer membrane siderophore transporters, rather than siderophore-associated inner membrane ABC protein components. A recent study using a *fyuA*-deficient UPEC strain found a lower competitive defect in the bladder than was observed for *ybtPQ*-deficient UPEC in the present study. In contrast, the single strain infection defect was somewhat more pronounced for *fyuA* than *ybtPQ* mutants (29, 47–50). A previous study using a *tonB*-deficient UPEC strain yielded similar results to the *fyuA* mutant (51). The notable differences between *fyuA* and *ybtPQ* mutants are interesting and may derive from different strain backgrounds or distinctive features of the C3H background mice used in this study. It is possible that robust inflammation in C3H mice increases UPEC outer membrane permeability (through antimicrobial peptides), making outer membrane transporters relatively less critical for metal-yersiniabactin import (52–54). Lastly, the marked competitive advantage observed with YbtPQ may derive from additional virulence functions that are not directly related to yersiniabactin import. For example, *Lv* et al. have shown

that a UTI89 *ybtP* mutant exhibits a significant change in cellular cysteine compared an isogenic *fyuA* mutant (26). More direct experimental functional comparisons between outer or inner membrane siderophore import proteins will be necessary to understand how functionally distinct these proteins may be.

Structurally diverse ABC cassette transporters such as YbtPQ have been the subject of extensive pharmacologic study in both eukaryotes and prokaryotes, making this an appealing class of targets for next generation anti-infectives (55, 56). Structural differences in ABC transporters between humans and bacteria may enable antibiotics with specificity to be identified. Numerous functions have been described for the bacterial ATP-binding cassette transporter superfamily in both Gram positive and Gram negative pathogens (25, 55–57). Further investigation on the mechanisms of ABC transporters will provide insight to their role during pathogenesis as well as allow development of countermeasures targeting these transporters.

ACKNOWLEDGEMENTS

J.P.H. holds a Career Award for Medical Scientists from the Burroughs Wellcome Fund and acknowledges National Institute of Diabetes and Digestive and Kidney Diseases grants R01DK099534 and P50DK064540. The funders had no role in study design, data collection and interpretation, or the decision to submit the work for publication. We thank Dr. Scott Hultgren for reagents and helpful discussion, and Dr. Jennifer Walker and Samara Levine for technical assistance.

CHAPTER THREE: FIGURES

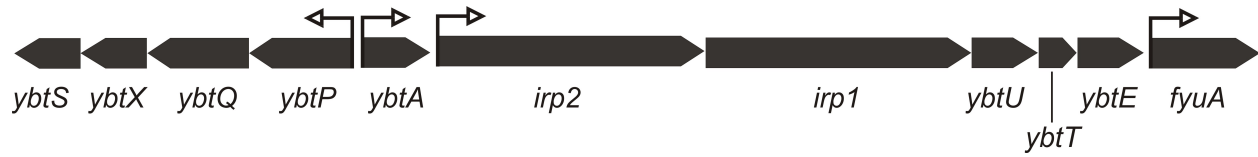


Figure 1. Genetic organization of UTI89 *Yersinia* High Pathogenicity Island (HPI). The non-conserved ~30 kb UTI89 *Yersinia* HPI encodes 11 genes in 4 operons. Promoters are designated by white arrows. Direction of arrow represents direction of transcription/translation for respective operon.

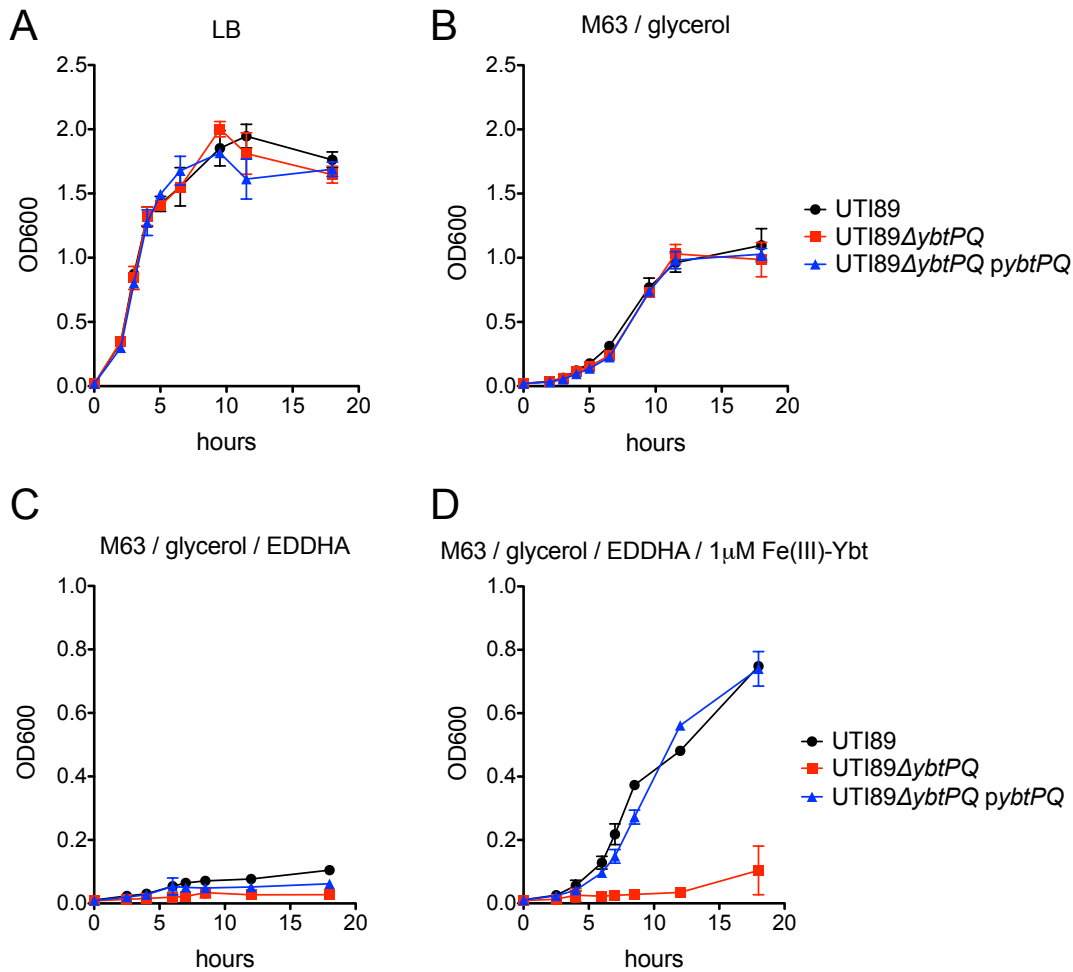


Figure 2. YbtPQ is required for Fe(III)-Ybt-dependent growth in UPEC. Growth of UTI89 (black circle), UTI89ΔybtPQ (red square), and UTI89ΔybtPQ pybtPQ (blue triangle) were indistinguishable in nutrient-rich Lysogeny broth (LB) medium (A) and nutrient-limiting M63 minimal medium supplemented with 0.2% glycerol (v/v) and 10 mg ml⁻¹ niacin (B). In M63 minimal medium chelated with 2 mM EDDHA, all strains show decreased growth (C). This growth defect was rescued for UTI89 and UTI89ΔybtPQ pybtPQ upon addition of exogenous 1 μM Fe(III)-Ybt to the chelated media (D). Results are shown as mean ± s.d.; n=3.

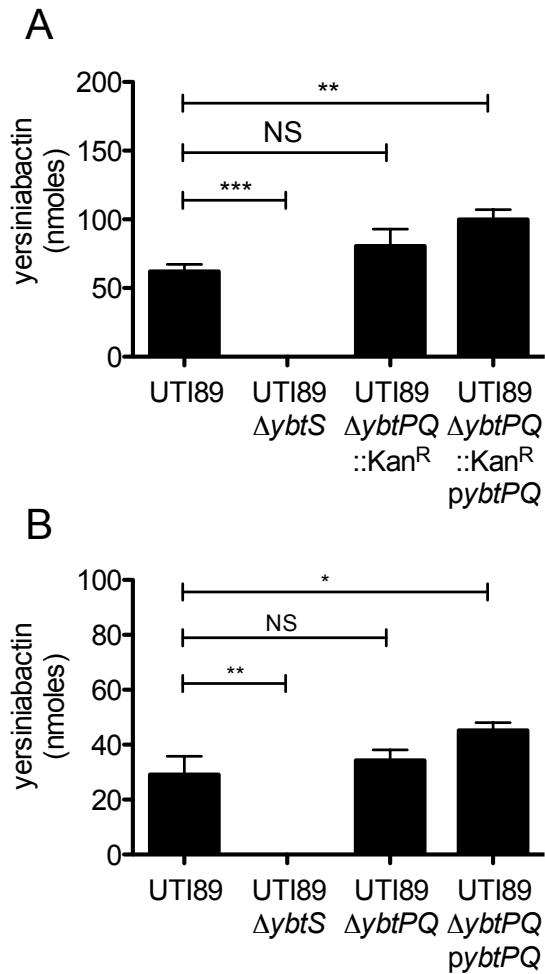


Figure 3. YbtPQ is not required for Ybt synthesis in UPEC. Yersiniabactin production was determined from culture supernatants of UTI89 strains using quantitative LC-MS/MS methods. While salicylate synthesis-deficient UTI89 $\Delta ybtS$ showed decreased Ybt production, UTI89 $\Delta ybtPQ::Kan^R$ (**A**) and UTI89 $\Delta ybtPQ$ (**B**) showed no difference compared to wild type. Plasmid-complemented UTI89 $\Delta ybtPQ::Kan^R$ *pybtPQ* (**A**) and UTI89 $\Delta ybtPQ$ *pybtPQ* (**B**) showed increased Ybt synthesis compared to wild type. Results are shown as mean \pm s.d.; $n=3$. * $p < 0.05$ ** $p < 0.005$, *** $p < 0.0005$.

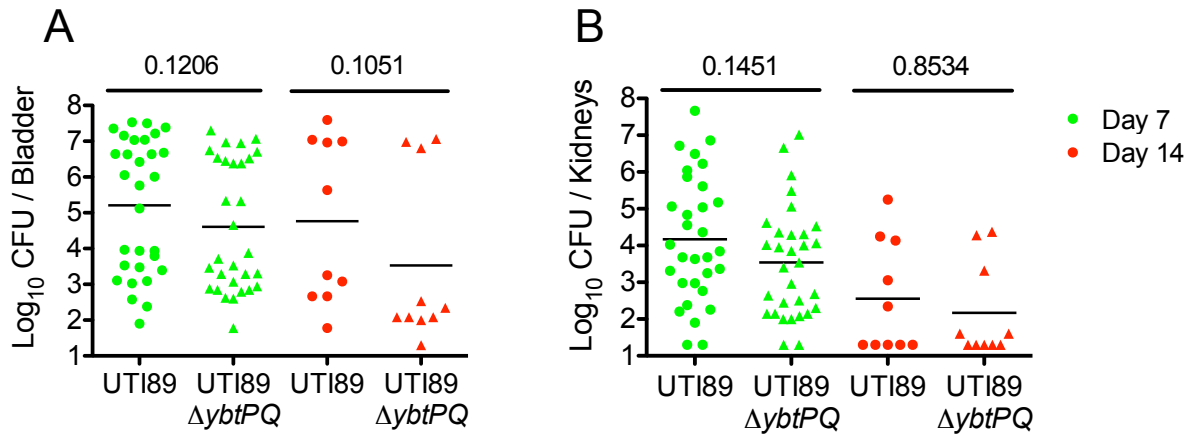


Figure 4. *In vivo* single strain infections in C3H/HeN mice background. Bacterial titers at the 7 days (green) and 14 days (red) following inoculation with 10^7 CFU UTI89 (●) or UTI89 $\Delta ybtPQ$ (▲) in (A) bladder and (B) kidneys from C3H/HeN mice are shown. Statistical significance was assessed using the two-tailed Mann-Whitney U test. Bars indicate mean values.

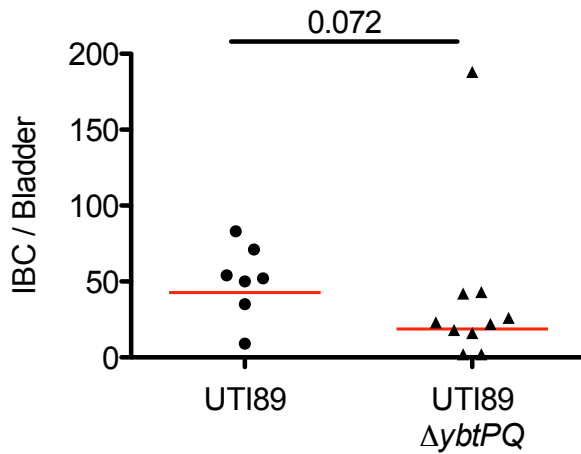


Figure 5. Bladder intracellular bacterial communities at 6 hours post infection in C3H/HeN mice. Intracellular bacterial communities (IBC) were quantified by LacZ staining at 6 hours post infection from 10^7 CFU UTI89 or UTI89 $\Delta ybtPQ$ in C3H/HeN mice. Statistical significance was assessed using the two-tailed Mann-Whitney U test. Bars indicate mean values.

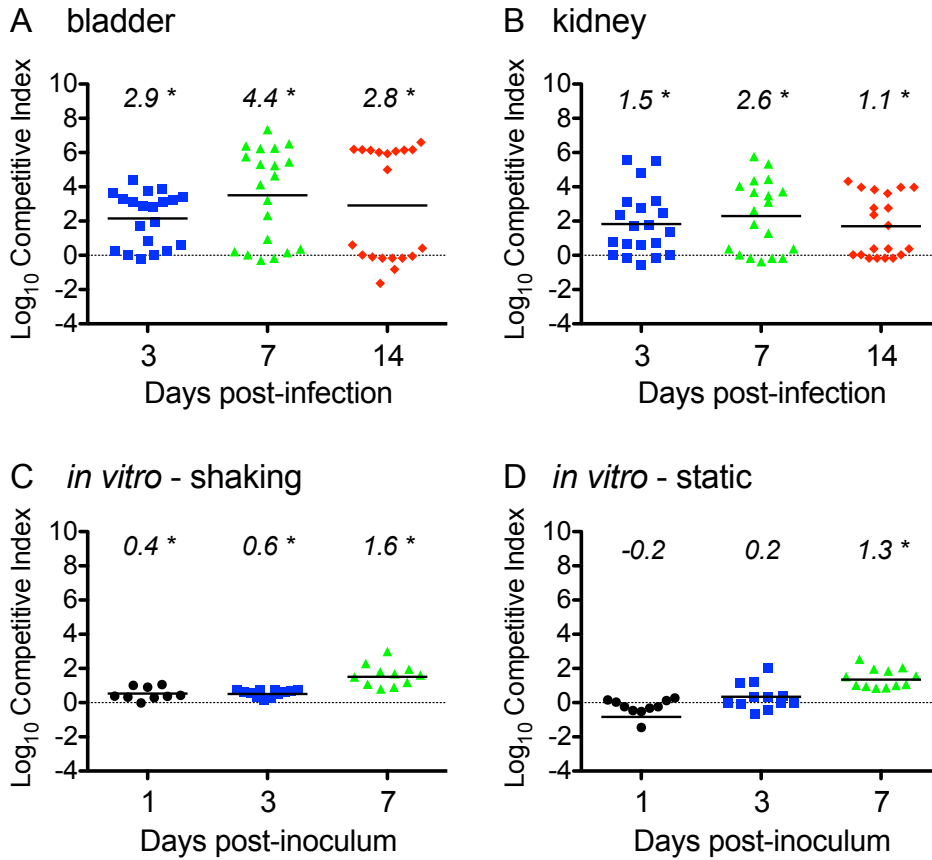


Figure 6. *In vivo* competitive infection in C3H/HeN mice and *in vitro* co-culture growth.

UTI89 showed significant competitive advantage against UTI89 Δ ybtPQ::Kan^R during *in vivo* competitive infections compared to *in vitro* co-culture growth. UTI89 and UTI89 Δ ybtPQ::Kan^R were mixed 1:1 to 10⁷ total CFU prior to co-infection and co-culture. Competitive infections were performed in C3H/HeN mice and bacterial titers in (A) bladders and (B) kidneys were determined. UTI89 strains were co-cultured in M63 minimal medium under shaking (C) and static (D) conditions. Each symbol represents a datum from an individual mouse or culture. Statistical significance was assessed using the Wilcoxon signed rank test with log₁₀ of CI of 0 as the theoretical median (dotted line). Numbers indicate median values with * denoting those with $p < 0.05$. Bars indicate mean values.

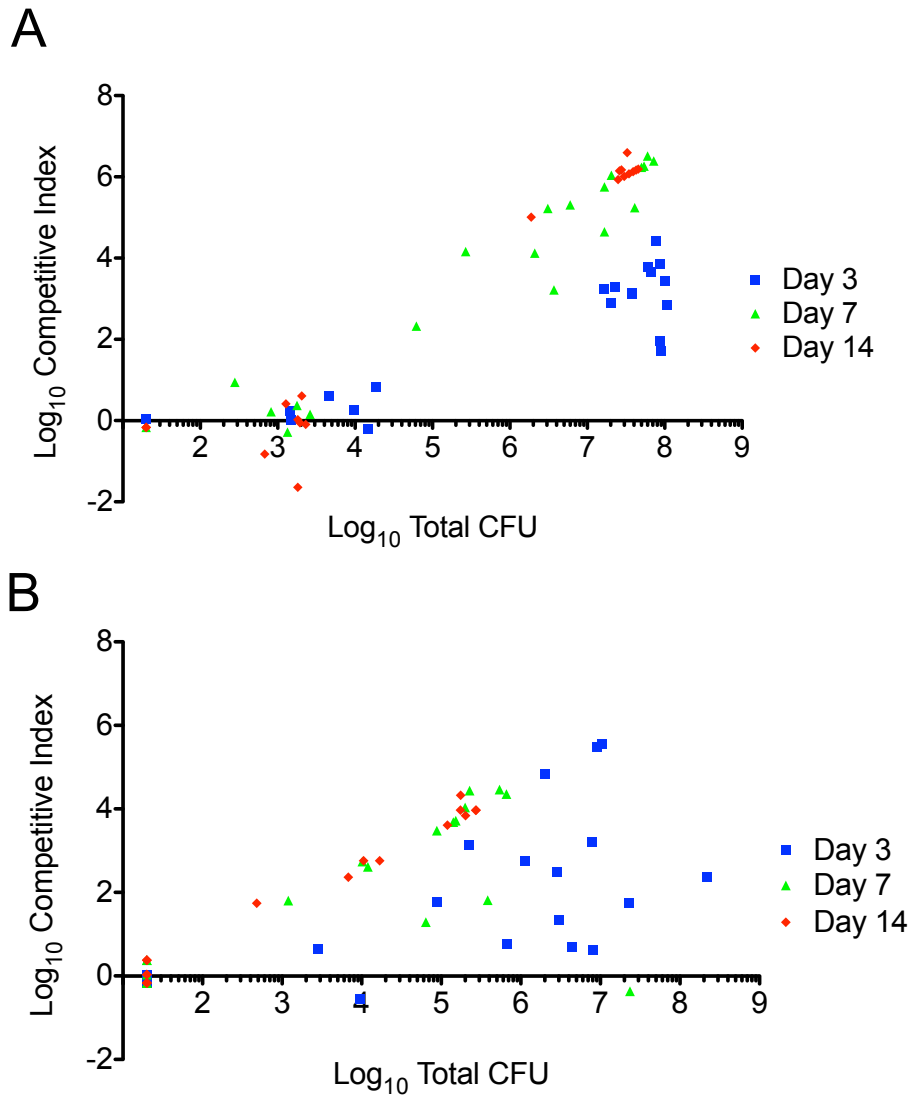


Figure 7. *In vivo* competitive infections in C3H/HeN mice show correlation with bacterial levels. Presenting competitive index values against total bacterial titers from (A) bladder and (B) kidneys of C3H/HeN mice revealed mice with large competitive indices had high bacterial titer while mice with low competitive indices presented low bacterial burden in each organ.

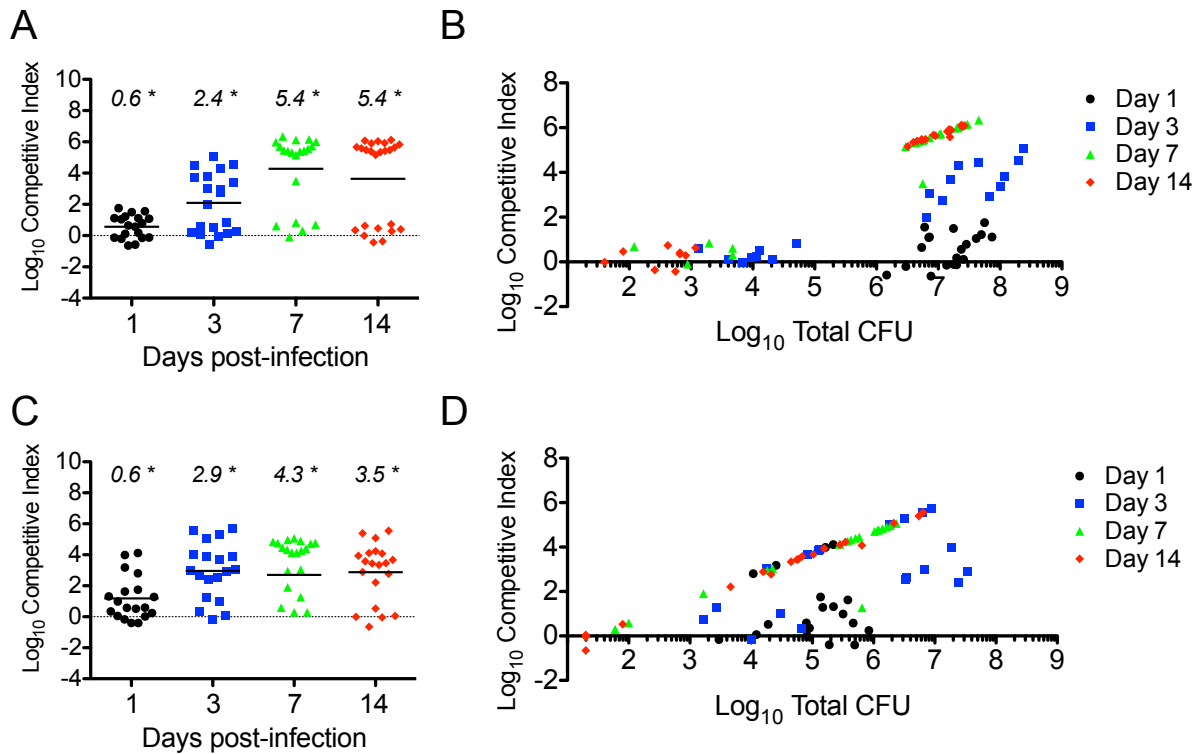


Figure 8. *In vivo* competitive infection with C3H/HeOuJ mice. UTI89 showed significant competitive advantage against UTI89 $\Delta ybtPQ::Kan^R$ during *in vivo* competitive infections with C3H/HeOuJ mice. UTI89 and UTI89 $\Delta ybtPQ::Kan^R$ were mixed 1:1 to 10^7 total CFU prior to co-infection. Competitive indices were calculated from bacterial titers collected from (A) bladder and (C) kidneys. Competitive index values are presented against total bacterial titers from (B) bladder and (D) kidneys. Each symbol represents a datum from an individual mouse. Statistical significance was assessed using the Wilcoxon signed rank test with log_{10} of CI of 0 as the theoretical mean (dotted line). * $p < 0.05$. Bars indicate mean values.

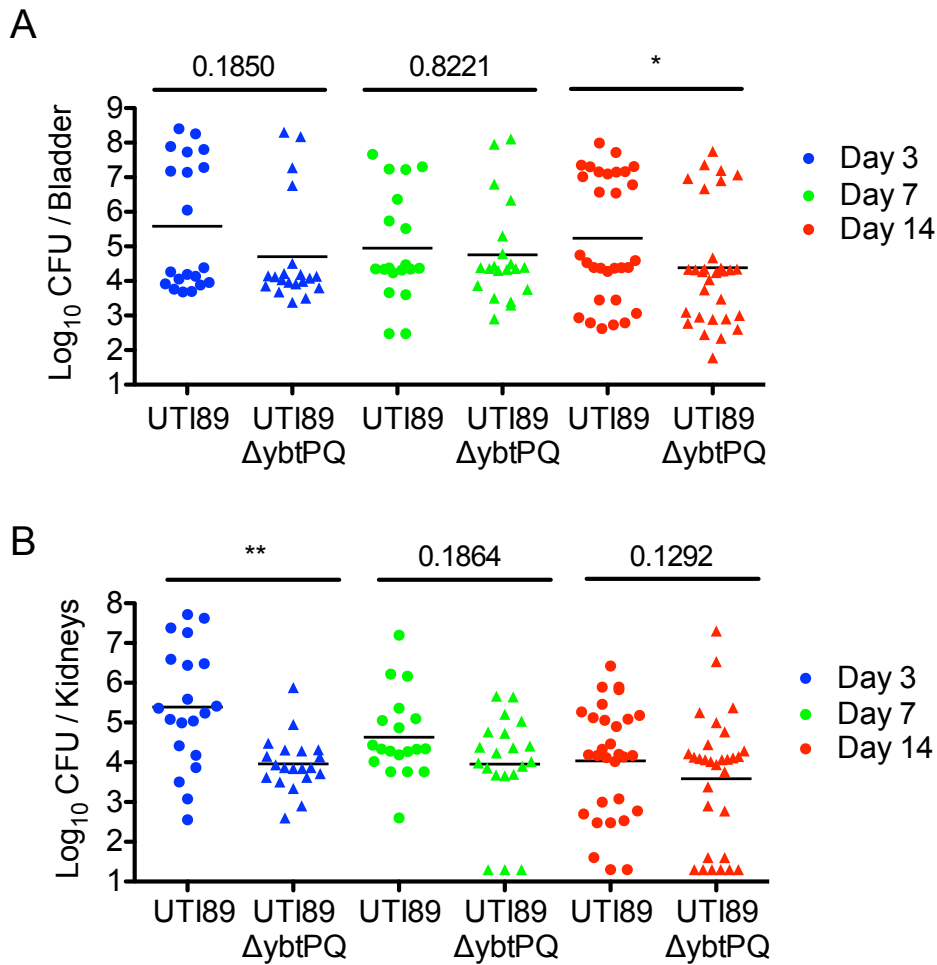


Figure 9. *In vivo* single strain infections in C3H/HeOuJ mice backgrounds. Bacterial titers at day 3 (blue), day 7 (green) and day 14 (red) following inoculation with 10^7 CFU UTI89 (●) or UTI89 Δ ybtPQ (▲) in (A) bladder and (B) kidneys from C3H/HeOuJ mice. Statistical significance was assessed using the two-tailed Mann-Whitney U test with $*p < 0.05$, $**p < 0.01$. Bars indicate mean values.

CHAPTER THREE: TABLES

Table 1. UTI89 mutants strains used in this study

strain	relevant properties	reference
UTI89 Δ <i>ybtS</i>	salicylate synthase deletion, yersiniabactin biosynthesis mutant	(11)
UTI89 Δ <i>ybtPQ</i>	ATP-binding cassette transporter deletion, yersiniabactin transport mutant	(26)
UTI89 Δ <i>ybtPQ</i> ::Kan ^R	Kanamycin resistant insert in place of ATP-binding cassette transporter, yersiniabactin transport mutant	(26), this study

CHAPTER THREE: REFERENCES

1. Foxman, B. (2002) Epidemiology of Urinary Tract Infections: Incidence, Morbidity, and Economic Costs. *Am. J. Med.*
2. Foxman, B. (2010) The epidemiology of urinary tract infection. *Nat. Rev.* **7**, 653–660
3. Marschall, J., Zhang, L., Foxman, B., Warren, D. K., and Henderson, J. P. (2012) Both Host and Pathogen Factors Predispose to Escherichia coli Urinary-Source Bacteremia in Hospitalized Patients. *Clin. Infect. Dis. Off. Publ. Infect. Dis. Soc. Am.* **54**, 1692–1698
4. Foxman, B., Gillespie, B., Koopman, J., Zhang, L., Palin, K., Tallman, P., Marsh, J. V., Spear, S., Sobel, J. D., Marty, M. J., and Marrs, C. F. (2000) Risk Factors for Second Urinary Tract Infection among College Women. *Am. J. Epidemiol.* **151**, 1194–1205
5. Czaja, C. A., Stamm, W. E., Stapleton, A. E., Roberts, P. L., Hawn, T. R., Scholes, D., Samadpour, M., Hultgren, S. J., and Hooton, T. M. (2009) Prospective Cohort Study of Microbial and Inflammatory Events Immediately Preceding Escherichia coli Recurrent Urinary Tract Infection in Women. *J. Infect. Dis.* **200**, 528–536
6. Stamey, T. A., Timothy, M., Millar, M., and Mihara, G. (1971) Recurrent urinary infections in adult women. The role of introital enterobacteria. *Calif. Med.* **115**, 1–19
7. Ta, S. (1973) The role of introital enterobacteria in recurrent urinary infections. *J. Urol.* **109**, 467–472
8. Ta, S., and Cc, S. (1975) The role of vaginal colonization with enterobacteriaceae in recurrent urinary infections. *J. Urol.* **113**, 214–217
9. Marsh, F. P., Murray, M., and Panchamia, P. (1972) The Relationship Between Bacterial Cultures of the Vaginal Introitus and Urinary Infection. *Br. J. Urol.* **44**, 368–375

10. Buckley, R. M., McGuckin, M., and MacGregor, R. R. (1978) Urine bacterial counts after sexual intercourse. *N. Engl. J. Med.* **298**, 321–324
11. Henderson, J. P., Crowley, J. R., Pinkner, J. S., Walker, J. N., Tsukayama, P., Stamm, W. E., Hooton, T. M., and Hultgren, S. J. (2009) Quantitative Metabolomics Reveals an Epigenetic Blueprint for Iron Acquisition in Uropathogenic *Escherichia coli*. *PLoS Pathog.*
12. Parker, K. S., Wilson, J. D., Marschall, J., Mucha, P. J., and Henderson, J. P. (2015) Network Analysis Reveals Sex- and Antibiotic Resistance-Associated Antivirulence Targets in Clinical Uropathogens. *ACS Infect. Dis.* 10.1021/acsinfecdis.5b00022
13. Fetherston, J. D., Bearden, S. W., and Perry, R. D. (1996) YbtA, an AraC-type regulator of the *Yersinia pestis* pesticin/yersiniabactin receptor. *Mol. Microbiol.* **22**, 315–25
14. Fetherston, J. D., Bertolino, V. J., and Perry, R. D. (1999) YbtP and YbtQ: two ABC transporters required for iron uptake in *Yersinia pestis*. *Mol. Microbiol.* **32**, 289–99
15. Perry, R. D., and Fetherston, J. D. (2011) Yersiniabactin iron uptake: mechanisms and role in *Yersinia pestis* pathogenesis. *Microbes Infect. Inst. Pasteur.* **13**, 808–17
16. Koh, E.-I., Hung, C. S., Parker, K. S., Crowley, J. R., Giblin, D. E., and Henderson, J. P. (2015) Metal selectivity by the virulence-associated yersiniabactin metallophore system. *Metallomics.* **7**, 1011–1022
17. Chaturvedi, K. S., Hung, C. S., Crowley, J. R., Stapleton, A. E., and Henderson, J. P. (2012) The siderophore yersiniabactin binds copper to protect pathogens during infection. *Nat. Chem. Biol.* 10.1038/nchembio.1020
18. Chaturvedi, K. S., Hung, C. S., Giblin, D. E., Urushidani, S., Austin, A. M., Dinauer, M. C., and Henderson, J. P. (2013) Cupric Yersiniabactin Is a Virulence-Associated Superoxide Dismutase Mimic. *ACS Chem. Biol.* **9**, 551–561

19. Bobrov, A. G., Kirillina, O., Fetherston, J. D., Miller, M. C., Burlison, J. A., and Perry, R. D. (2014) The *Yersinia pestis* siderophore, yersiniabactin, and the ZnuABC system both contribute to zinc acquisition and the development of lethal septicaemic plague in mice. *Mol. Microbiol.* **93**, 759–75
20. Hood, M. I., and Skaar, E. P. (2012) Nutritional immunity: transition metals at the pathogen–host interface. *Nat. Rev. Microbiol.* **10**, 525–537
21. Subashchandrabose, S., Hazen, T. H., Brumbaugh, A. R., Himpsl, S. D., Smith, S. N., Ernst, R. D., Rasko, D. A., and Mobley, H. L. (2014) Host-specific induction of *Escherichia coli* fitness genes during human urinary tract infection. *Proc. Natl. Acad. Sci. U. S. A.* **111**, 18327–32
22. Perry, R. D., Balbo, P. B., Jones, H. A., Fetherston, J. D., and DeMoll, E. (1999) Yersiniabactin from *Yersinia pestis*: biochemical characterization of the siderophore and its role in iron transport and regulation. *Microbiology*
23. Brem, D., Pelludat, C., Rakin, A., Jacobi, C. A., and Heesemann, J. (2001) Functional analysis of yersiniabactin transport genes of *Yersinia enterocolitica*. *Microbiology.* **147**, 1115–27
24. Lukacik, P., Barnard, T. J., Keller, P. W., Chaturvedi, K. S., Seddiki, N., Fairman, James W., Noinaj, N., Kirby, T. L., Henderson, J. P., Steven, A. C., Hinnebusch, B. J., and Buchanan, S. K. (2012) Structural engineering of a phage lysin that targets Gram-negative pathogens. *PNAS.* **109**, 9857–9862
25. Ma, Z., Jacobsen, F. E., and Giedroc, D. P. (2009) Metal transporters and metal sensors: How coordination chemistry controls bacterial metal homeostasis. *Chem Rev.* **109**, 4644–4681

26. Lv, H., and Henderson, J. P. (2011) Yersinia High Pathogenicity Island Genes Modify the Escherichia coli Primary Metabolome Independently of Siderophore Production. *J. Proteome Res.* **10**, 5547–5554
27. Reigstad, C. S., Hultgren, S. J., and Gordon, J. I. (2007) Functional genomic studies of uropathogenic Escherichia coli and host urothelial cells when intracellular bacterial communities are assembled. *J. Biol. Chem.* **282**, 21259–67
28. Hagan, E. C., Lloyd, A. L., Rasko, D. A., Faerber, G. J., and Mobley, H. L. T. (2010) Escherichia coli Global Gene Expression in Urine from Women with Urinary Tract Infection. *PloS Pathog.*
29. Brumbaugh, A. R., Smith, S. N., Subashchandrabose, S., Himpfl, S. D., Hazen, T. H., Rasko, D. A., and Mobley, H. L. T. (2015) Blocking Yersiniabactin Import Attenuates Extraintestinal Pathogenic Escherichia coli in Cystitis and Pyelonephritis and Represents a Novel Target To Prevent Urinary Tract Infection. *Infect. Immun.* **83**, 1443–1450
30. Lawlor, M. S., Hsu, J., Rick, P. D., and Miller, V. L. (2005) Identification of Klebsiella pneumoniae virulence determinants using an intranasal infection model. *Mol. Microbiol.* **58**, 1054–1073
31. Choi, J. Y., Sifri, C. D., Goumnerov, B. C., Rahme, L. G., Ausubel, F. M., and Calderwood, S. B. (2002) Identification of virulence genes in a pathogenic strain of Pseudomonas aeruginosa by representational difference analysis. *J. Bacteriol.* **184**, 952–61
32. Rodriguez, G. M., and Smith, I. (2006) Identification of an ABC transporter required for iron acquisition and virulence in Mycobacterium tuberculosis. *J. Bacteriol.* **188**, 424–30
33. Chen, S. L., Hung, C. S., Xu, J., Reigstad, C. S., Magrini, V., Sabo, A., Blasiar, D., Bieri, T., Meyer, R. R., Ozersky, P., Armstrong, J. R., Fulton, R. S., Latreille, J. P., Spieth, J., Hooton,

- T. M., Mardis, E. R., Hultgren, S. J., and Gordon, J. I. (2006) Identification of genes subject to positive selection in uropathogenic strains of *Escherichia coli*: a comparative genomics approach. *Proc. Natl. Acad. Sci. U. S. A.* **103**, 5977–82
34. Mulvey, M. A., Schilling, J. D., and Hultgren, S. J. (2001) Establishment of a persistent *Escherichia coli* reservoir during the acute phase of a bladder infection. *Infect. Immun.* **69**, 4572–9
35. Datsenko, K. A., and Wanner, B. L. (2000) One-step inactivation of chromosomal genes in *Escherichia coli* K-12 using PCR products. *PNAS.* **97**, 6640–6645
36. Amann, E., Ochs, B., and Abel, K. J. (1988) Tightly regulated tac promoter vectors useful for the expression of unfused and fused proteins in *Escherichia coli*. *Gene.* **69**, 301–15
37. Hung, C.-S., Dodson, K. W., and Hultgren, S. J. (2009) A murine model of urinary tract infection. *Nat Protoc.* **4**, 1230–1243
38. Hannan, T. J., Mysorekar, I. U., Hung, C. S., Isaacson-Schmid, M. L., and Hultgren, S. J. (2010) Early Severe Inflammatory Responses to Uropathogenic *E. coli* Predispose to Chronic and Recurrent Urinary Tract Infection. *PLoS Pathog.*
39. Freter, R., Allweiss, B., O'Brien, P. C., Halstead, S. A., and Macsai, M. S. (1981) Role of chemotaxis in the association of motile bacteria with intestinal mucosa: in vitro studies. *Infect. Immun.* **34**, 241–249
40. Justice, S. S., Lauer, S. R., Hultgren, S. J., and Hunstad, D. A. (2006) Maturation of Intracellular *Escherichia coli* Communities Requires SurA. *Infect. Immun.* **74**, 4793–4800
41. Hannan, T. J., Totsika, M., Mansfield, K. J., Moore, K. H., Schembri, M. A., and Hultgren, S. J. (2012) Host–pathogen checkpoints and population bottlenecks in persistent and

- intracellular uropathogenic *Escherichia coli* bladder infection. *FEMS Microbiol. Rev.* **36**, 616–648
42. Anderson, G. G., Palermo, J. J., Schilling, J. D., Roth, R., Heuser, J., and Hultgren, S. J. (2003) Intracellular Bacterial Biofilm-Like Pods in Urinary Tract Infections. *Science*. **301**, 105–107
43. Justice, S. S., Hung, C., Theriot, J. A., Fletcher, D. A., Anderson, G. G., Footer, M. J., and Hultgren, S. J. (2004) Differentiation and development pathways of uropathogenic *Escherichia coli* in urinary tract pathogenesis. *PNAS*. **101**, 1333–1338
44. Hopkins, W. J., Gendron-Fitzpatrick, A., Balish, E., and Uehling, D. T. (1998) Time Course and Host Responses to *Escherichia coli* Urinary Tract Infection in Genetically Distinct Mouse Strains. *Infect. Immun.* **66**, 2798–2802
45. Schwartz, D. J., Chen, S. L., Hultgren, S. J., and Seed, P. C. (2011) Population dynamics and niche distribution of uropathogenic *Escherichia coli* during acute and chronic urinary tract infection. *Infect. Immun.* **79**, 4250–9
46. Crouch, M.-L. V., Castor, M., Karlinsey, J. E., Kalhorn, T., and Fang, F. C. (2008) Biosynthesis and IroC-dependent export of the siderophore salmochelin are essential for virulence of *Salmonella enterica* serovar Typhimurium. *Mol. Microbiol.* **67**, 971–983
47. Hancock, V., Ferrieres, L., and Klemm, P. (2008) The ferric yersiniabactin uptake receptor FyuA is required for efficient biofilm formation by urinary tract infectious *Escherichia coli* in human urine. *Microbiology*. **154**, 167–75
48. Brumbaugh, A. R., Smith, S. N., and Mobley, H. L. T. (2013) Immunization with the Yersiniabactin Receptor, FyuA, Protects against Pyelonephritis in a Murine Model of Urinary Tract Infection. *Infect. Immun.* **81**, 3309–3316

49. Garcia, E. C., Brumbaugh, A. R., and Mobley, H. L. T. (2011) Redundancy and specificity of Escherichia coli iron acquisition systems during urinary tract infection. *Infect. Immun.* **79**, 1225–1235
50. Spurbeck, R. R., Dinh, P. C., Walk, S. T., Stapleton, A. E., Hooton, T. M., Nolan, L. K., Kim, K. S., Johnson, J. R., and Mobley, H. L. T. (2012) Escherichia coli Isolates That Carry *vat*, *fyuA*, *chuA*, and *yfcV* Efficiently Colonize the Urinary Tract. *Infect. Immun.* **80**, 4115–4122
51. Torres, A. G., Redford, P., Welch, R. A., and Payne, S. M. (2001) TonB-Dependent Systems of Uropathogenic Escherichia coli: Aerobactin and Heme Transport and TonB Are Required for Virulence in the Mouse. *Infect. Immun.* **69**, 6179–6185
52. Canny, G., Levy, O., Furuta, G. T., Narravula-Alipati, S., Sisson, R. B., Serhan, C. N., and Colgan, S. P. (2002) Lipid mediator-induced expression of bactericidal/ permeability-increasing protein (BPI) in human mucosal epithelia. *Proc. Natl. Acad. Sci.* **99**, 3902–3907
53. Elsbach, P., and Weiss, J. (1998) Role of the bactericidal/permeability-increasing protein in host defence. *Curr. Opin. Immunol.* **10**, 45–49
54. Kim, B., Richards, S. M., Gunn, J. S., and Slauch, J. M. (2010) Protecting against antimicrobial effectors in the phagosome allows SodCII to contribute to virulence in Salmonella enterica serovar Typhimurium. *J. Bacteriol.* **192**, 2140–9
55. Higgins, C. F. (1992) ABC Transporters: From Microorganisms to Man. *Annu. Rev. Cell Biol.* **8**, 67–113
56. Davidson, A. L., and Chen, J. (2004) Atp-Binding Cassette Transporters in Bacteria. *Annu. Rev. Biochem.* **73**, 241–268

57. Noinaj, N., and Buchanan, S. K. (2014) Structural insights into the transport of small molecules across membranes. *Curr. Opin. Struct. Biol.* **27**, 8–15

CHAPTER FOUR

Metal acquisition by the virulence-associated yersiniabactin metallophore system

ABSTRACT

Uropathogenic *Escherichia coli* express several distinct siderophore systems during human infections. Of these, the virulence-associated siderophore yersiniabactin binds divalent copper ions during infections, with copper(II) yersiniabactin a transport substrate of the yersiniabactin outer membrane importer FyuA. Here, we use a mass spectrometric approach to investigate the interactions of yersiniabactin with its ATP-binding cassette inner membrane transporters YbtP and YbtQ, and the intracellular fate of metal yersiniabactin complexes. In *fyuA* and *ybtPQ*-expressing *E. coli*, iron, copper and nickel are released from their respective intracellular metal yersiniabactin complexes, with *apo*-yersiniabactin recycled to the extracellular medium. Intracellular gallium(III) yersiniabactin, however, remained stable with no detectable *apo*-yersiniabactin recycling, while physiologic reducing agents facilitated the release of iron from yersiniabactin. These results are consistent with yersiniabactin as part of a metallophore system able to deliver select transition metals to uropathogenic *E. coli*.

INTRODUCTION

Many bacterial pathogens synthesize and secrete chemically diverse specialized metabolites called siderophores to scavenge for ferric iron (Fe(III)) (1). Uropathogenic *E. coli* (UPEC) isolates can express multiple siderophore systems consisting of enterobactin (which is genetically conserved in all *E. coli*) in combination with salmochelin, aerobactin and/or yersiniabactin, even though only a single siderophore system is required for iron-dependent growth in iron-chelated culture conditions (2). Of these, the yersiniabactin (Ybt) system is the most frequently-carried, non-conserved siderophore system in UPEC (2, 3). The multi-operon *Yersinia* High Pathogenicity Island (HPI) consists of genes encoding Ybt biosynthesis proteins, a transcription factor (*ybtA*), an outer membrane import protein (*fyuA*), and putative inner membrane transporters (*ybtP*, *Q*) (4–6). *Yersinia* HPI genes are highly upregulated during experimental mouse cystitis with Ybt inner membrane proteins enhancing UPEC fitness during competitive high titer mouse cystitis (7, 8). Furthermore Ybt has been directly detected in the urine of UTI patients infected with Ybt-expressing pathogens (9). These findings combined are consistent with a pathogenic gain-of-function role attributed to the yersiniabactin system.

Recent works have shown both copper and iron complexes with Ybt during human and experimental mouse cystitis, suggesting a potential gain-of-function by the Ybt system through interactions with non-iron metal ions (9, 10). Copper homeostasis is critical for microbes as copper is used as a potent antimicrobial agent by the host at elevated concentrations, but it is also an essential micronutrient acting as a cofactor for several microbial enzymes including NADH dehydrogenase, cytochrome oxidase, and copper/zinc superoxide dismutase (11–14). Therefore in an intracellular compartment where UPEC are exposed to high copper concentrations, Ybt

may protect UPEC by sequestering host copper ions and catalyzing superoxide dismutation (9, 10, 15). However in copper-deficient environments, Ybt may be used to import copper ions to UPEC. The Ybt outer membrane importer (FyuA) was recently found to be a promiscuous transporter of metal-Ybt complexes, including Cu(II)-Ybt (16), but it has been unclear whether non-iron metal-Ybt complexes share similar intracellular fates as Fe(III)-Ybt. Methanobactin, a siderophore-like molecule secreted by methanotrophic Gram-negative bacteria, is notable in its delivery of copper but it is unclear whether pathogenic bacteria share this strategy (17, 18). If Ybt delivers physiologic metal ions in addition to iron, Ybt may function as a metallophore system beyond its classic iron scavenging pathway to overcome the effects of nutritional immunity by the host (19).

For numerous Gram-negative bacteria, ferric-siderophore complexes must first be actively transported to the periplasm through dedicated outer membrane transporters powered by the TonB complex (16, 20–22). These ferric-siderophore complexes or the iron released from them, are then subsequently transported to the cytoplasm through inner membrane ATP-binding cassette transporters (6, 23–25). In Gram-negative bacteria, two mechanisms of iron release from ferric-siderophore complexes have been described previously. One mechanism involves siderophore complex hydrolysis, seen with ferric-enterobactin in *E. coli* where an esterase hydrolyzes the cyclic triester (26–28). Another pathway involves reduction of the coordinated Fe(III) to Fe(II), in which Fe(II) has significantly lower binding affinity for the siderophore. Following iron release through reduction, the siderophore is recycled into the extracellular matrix. This mechanism has been shown in siderophore systems in *E. coli* including ferrichrome and ferrioxamine B, as well as for other virulence-associated siderophores pyoverdine and

mycobactin in *Pseudomonas aeruginosa* and *Mycobacterium tuberculosis* respectively (25, 29–32). To date, the molecular sequence of events by which iron or other physiologic metals are released from Ybt complexes is incompletely understood, as enzymes associated with this role have yet to be identified on the *Yersinia* HPI (6, 21). Siderophore biosynthesis requires energy and cellular building blocks, both of which may be scarce during an infection (33, 34). Siderophore recycling may therefore decrease the cellular metabolic burden by providing an alternative option to siderophore de novo synthesis.

In this study, we sought to investigate the intracellular fate of metal-Ybt complexes. Using a combined bacterial genetics and quantitative mass spectrometric approach, we showed that in *fyuA* and *ybtPQ*-expressing *E. coli*, intracellular Fe(III)-Ybt is dissociated with *apo*-Ybt subsequently recycled, while intracellular Ga(III)-Ybt remains intact. Consistent with these findings, physiologic reducing agents facilitated iron release from Ybt. Furthermore in *fyuA* and *ybtPQ*-expressing *E. coli*, intracellular Cu(II)- and Ni(II)-Ybt complexes are dissociated with *apo*-Ybt subsequently recycled. A radiolabeling approach showed copper remains intracellular upon delivery through Cu(II)-Ybt. Together these results are consistent with Ybt as a metallophore that delivers physiologic metal ions to UPEC.

EXPERIMENTAL PROCEDURES

Bacterial strains, plasmids and culture conditions

Uropathogenic *E. coli* isolates UTI89 and CFT073, and the non-uropathogenic K-12 *E. coli* isolate MG1655 were used in this study (1–3). Strains were grown in LB agar (Becton, Dickson and Company), LB broth (Becton, Dickson and Company or M63 minimal salts media (4) with antibiotics as appropriate. Ampicillin ($100\mu\text{g ml}^{-1}$, Goldbio), chloramphenicol ($25\mu\text{g ml}^{-1}$, Goldbio) were used for plasmid selection. Arabinose (0.2% v/v) was used for plasmid induction. In-frame deletions in UTI89 were made using the standard red recombinase method, using pKD4 or pKD13 as a template (5). Antibiotic resistance insertions were removed by transforming the strains with pCP20 expressing the FLP recombinase. Plasmids were made using the pTrc99a vector (6) or a modified pBAD33 vector (7), with genes cloned in using standard PCR and recombination techniques.

Yersiniabactin preparation

Apo-Ybt was generated from UTI89 Δ *entB* grown in M63 minimal salts medium supplemented with 0.2% glycerol (v/v) and 10mg ml^{-1} niacin (Sigma) as previously described (8). ^{13}C -salicylate labeled *apo-Ybt* was produced from UTI89 Δ *entB* Δ *ybtS* grown in M63 minimal salts medium supplemented with 0.2% glycerol (v/v), ^{13}C -labeled salicylic acid and 10mg ml^{-1} niacin (Sigma). ^{13}C -Ybt was produced by growing UTI89 Δ *fur* strain in media supplemented with ^{13}C -labeled glycerol as previously described (8). Metal-Ybt complexes were produced by adding iron(III) chloride, copper(II) sulfide, gallium(III) nitrate or nickel(II) nitrate (Sigma) to *apo-Ybt*. Metal-Ybt was applied to a methanol conditioned C18 silica column (Sigma) and eluted with 80% methanol as previously described (9). Lyophilizer was used to concentrate the eluate

overnight. Dried samples were resuspended in deionized water and purified through high-performance liquid chromatography using C18 silica column (Whatman Partisil). Metal-Ybt containing fractions were collected, dried down using a lyophilizer and resuspended in deionized water. Stock metal-Ybt quantification was carried out using previously described extinction coefficient (9). Sample metal-Ybt levels were quantified in multiple reaction monitoring mode using known collision-induced dissociation fragmentations and ^{13}C -labeled Fe(III)-Ybt internal standards.

Fe(III)-Ybt dependent growth

After overnight growth in M63 media, strains were normalized for starting OD_{600} in M63 with 2 mM EDDHA (Complete Green Company). 1 μM HPLC-purified Fe(III)-Ybt was added to strains and grown for 18 hours in 37 °C with shaking, as previously described (9). Bacterial growth was measured using OD_{600} readings.

Liquid chromatography-mass spectrometry

LC-MS analyses were conducted using a Shimadzu UFLC-equipped AB-Sciex 4000 QTrap operated in positive ion mode using a Turbo V ESI ion source and a Thermo LCQ Deca as previously described (8). The samples were injected onto a Fused-core phenylhexyl column (Ascentis Express, Supelco) with a flow rate of 0.4ml min^{-1} and following solvents: solvent A (0.1% (v/v) formic acid) and solvent B (90% (v/v) acetonitrile in 0.1% formic acid (v/v)). The ion spray voltage was set to 5kV and heater temperature was 500°C. The declustering potential, nebulizer gas (G1), auxiliary gas (G2) and collision energy were set at 110V, 40V, 35V and 35V, respectively.

Cell-associated metal-Ybt

Strains were grown overnight in M63 minimal salts media with supplements as described above. Strains were diluted OD600 of 0.8 in M63 with supplements described above. HPLC-purified 0.1 μ M metal-Ybt was added to strains and grown for 2 hours in 37 degrees while shaking. Bacteria were pelleted at 7500 g for 10 minutes (Eppendorf) and washed with 1X PBS (Sigma). Supernatant was collected and applied to a conditioned C18 silica column with added ^{13}C -labeled Fe(III)-Ybt internal standard. Bacteria were resuspended in 100% ethanol (Sigma) and pelleted at 20,000 g for 10 minutes. Supernatant was collected and dried for 3 hours using a vacuum concentrator. Samples were resuspended in ultrapure water and applied to a conditioned C18 silica column with added ^{13}C -labeled Fe(III)-Ybt internal standard. Metal-Ybt quantification was carried out in the multiple reaction monitoring mode using known collision-induced dissociation fragmentations and ^{13}C -labeled Fe(III)-Ybt internal standards as done previously (9).

Fe(III)-Ybt reduction

Bathophenanthrolinedisulfonic acid disodium salt hydrate (BPDS, Sigma), glutathione reduced (Sigma), L-ascorbic acid (Sigma) were prepared in phosphate buffered saline pH 7.4 (PBS, Sigma). Samples were appropriately mixed in a 96 well plate and incubated for 2 hours at room temperature. Spectrophotometrical changes were monitored at 535nm using standard UV/Vis spectrometer. Samples were applied to conditioned C18 silica columns and Ybt quantification was carried out in the multiple reaction monitoring mode using known collision-induced dissociation fragmentations as done previously (9).

⁶⁴Cu(II)-Ybt Radiolabeling

⁶⁴Cu ($t_{1/2}$ = 12.7 h, β^+ = 17%, β^- = 39%, EC = 43%, E_{\max} = 0.656 MeV) produced by a (p,n) reaction on enriched ⁶⁴Ni on a CS-15 biomedical cyclotron (Cyclotron Corporation, Berkeley, CA) at Mallinckrodt Institute of Radiology, Washington University School of Medicine and purified an automated system using standard procedures (10, 11). All radioactive procedures were conducted in the Department of Radiation Oncology premises under the guidance and authorization of Drs. Buck E. Rogers and Nilantha Bandara. A stock solution of ⁶⁴Cu in 0.05 M HCl received from the production team was diluted in 0.1 M ammonium acetate (NH₄OAc) buffer solution (pH 7) for radiolabeling purposes. Apo-Ybt sample with a known concentration (250 μ M) was used. A typical reaction involves using 74 – 111 MBq of ⁶⁴Cu was added to 20 μ L of Apo-Ybt (5 nmol) and 0.1 M NH₄OAc buffer added to bring the reaction volume to 100 μ L. The reaction mixture was incubated on a mixer with 800 rpm agitation at 37 °C for 1 hour. Labeling efficiency and radiochemical purity were determined using radio-high performance liquid chromatography (Agilent 1200 system with a Flow-RAM radio-HPLC detector) on a C18 column (Kinetex, Phenomenex). The mobile phase consisted of water (A) and acetonitrile (B) with a gradient of 0 – 100 % B over 10 min using a flow rate of 1 mL/min. The retention time of ⁶⁴Cu-Ybt was 6.1 min and a radiochemical yield of greater than 99 % was achieved and used without further purification.

Cell-associated ⁶⁴Cu(II)-Ybt

Strains were grown overnight in M63 minimal salts media with supplements as described above. Strains were diluted OD₆₀₀ of 0.8 in M63 with supplements described above. HPLC-purified

0.1 μ M Cu(II)-Ybt and 64 Cu(II)-Ybt were added to strains and grown for 2 hours while shaking. Bacteria were pelleted at 7500 g for 10 minutes (Eppendorf) and washed with 1X PBS (Sigma) multiple times. Cell-associated 64 Cu levels were measured from pelleted bacteria using a gamma counter (Packard II, Perkin Elmer).

Statistical analyses

Statistics and graphs were generated using GraphPad Prism 5 (GraphPad software). Student's *t*-test was used to compare growth differences and cell-associated metal-Ybt levels between paired strains.

RESULTS

FyuA and YbtPQ are necessary and sufficient for Fe(III)-Ybt dependent growth in UPEC

To confirm UPEC-encoded FyuA and YbtPQ are sufficient for UPEC growth under Fe(III)-Ybt dependent conditions, we used the *ybtA*-deletion mutant background in the model UPEC strain UTI89, which has lower expression of genes associated with Ybt biosynthesis and transport on the *Yersinia* HPI (1, 2). FyuA and YbtPQ were ectopically expressed to assess Ybt transport and utilization. We measured growth of UTI89 Δ *ybtA* in M63 minimal salts media containing 1 μ M purified Fe(III)-Ybt and the iron chelator EDDHA. UTI89 Δ *ybtA* *pfyuA* *pybtPQ* growth exceeded that of UTI89 Δ *ybtA* and UTI89 Δ *ybtA* *pfyuA* in the presence but not absence of Fe(III)-Ybt (Fig 1). The ability of only UTI89 Δ *ybtA* *pfyuA* *pybtPQ* to promote Fe(III)-Ybt dependent growth is consistent with the current model that FyuA and YbtPQ are required and sufficient for Fe(III)-Ybt dependent growth (16).

YbtPQ-dependent Fe(III)-Ybt transport and recycling

To determine whether UPEC use FyuA and YbtPQ to import Fe(III)-Ybt complexes, we used stable isotope dilution mass spectrometry (LC-MS/MS) to directly measure exogenously-supplied metal-yersiniabactin complexes (16). In this approach, Fe(III)- and *apo*-Ybt were quantified in culture supernatants and cell extracts following a 2 hour exposure to 0.1 μ M purified Fe(III)-Ybt. Using the *ybtA*-deletion background ensured no native Ybt synthesis with Ybt complexes detected only from those exogenously supplied. Supernatant Fe(III)-Ybt levels were nearly eliminated in UTI89 Δ *ybtA* *pfyuA* and UTI89 Δ *ybtA* *pfyuA* *pybtPQ* suggesting intracellular localization of Fe(III)-Ybt (Fig 2A). Consistent with FyuA-mediated transport of Fe(III)-Ybt to the periplasm (16), cell-associated Fe(III)-Ybt levels were significantly increased in UTI89 Δ *ybtA*

pfyuA compared to UTI89 Δ *ybtA*. Interestingly, in presence of both FyuA and YbtPQ, cellular Fe(III)-Ybt were significantly decreased compared to UTI89 Δ *ybtA* *pfyuA* (Fig 2B). As FyuA and YbtPQ are sufficient for Fe(III)-Ybt dependent growth, we hypothesized that intracellular Fe(III)-Ybt complex is dissociated to iron and *apo*-Ybt in UTI89 Δ *ybtA* *pfyuA* *pybtPQ*, with *apo*-Ybt subsequently secreted back to the supernatant. When we examined the culture supernatants for *apo*-Ybt, *apo*-Ybt levels were significantly increased in UTI89 Δ *ybtA* *pfyuA* *pybtPQ* compared to UTI89 Δ *ybtA* and UTI89 Δ *ybtA* *pfyuA* (Fig 2C). These observations support a model in which FyuA and YbtPQ are required for Fe(III)-Ybt transport, and YbtPQ-dependent transport subsequently leads to iron release from the Fe(III)-Ybt complex with the resulting *apo*-Ybt recycled to the supernatant.

Fe(III)-Ybt transport and utilization by pathogenic E. coli

To determine if wild type pathogenic *E. coli* isolates can utilize Fe(III)-Ybt, we examined a model UPEC strain, CFT073, which encodes genes on the *Yersinia* HPI including FyuA and YbtPQ, but does not synthesize Ybt due to mutations in the biosynthetic machinery (4–6). We compared growths of wild type pathogenic *E. coli* strains UTI89 and CFT073 with non-pathogenic strain MG1655 in M63 minimal salts media containing 1 μ M purified Fe(III)-Ybt and the iron chelator EDDHA. Both UTI89 and CFT073 growth exceeded that of MG1655 in the presence but no absence of Fe(III)-Ybt (Fig 3). UTI89 did show increased growth in EDDHA-chelated media with and without Fe(III)-Ybt compared to CFT073, which may be attributed to UTI89's native Ybt biosynthesis. To examine whether CFT073 can recycle *apo*-Ybt from exogenous-supplied Fe(III)-Ybt, we used LC-MS/MS methods as above to measure supernatant Fe(III)- and *apo*-Ybt levels following a 2 hour exposure to 0.1 μ M purified ¹³C-salicylate-labeled

Fe(III)-Ybt-¹³C₆. Supernatant Fe(III)-Ybt-¹³C₆ levels were nearly eliminated in UTI89 and CFT073 compared to MG1655 (Fig 4A, B), while *apo*-Ybt-¹³C₆ levels were significantly increased in UTI89 and CFT073 (Fig 4C, D). *Apo*-Ybt-¹³C₆ levels were significantly greater in UTI89 compared to CFT073, which may be due to a carrier effect from native Ybt synthesis by UTI89. These findings show that wild type pathogenic *E. coli* strains can transport Fe(III)-Ybt and recycle the resulting *apo*-Ybt, and is also consistent with previous findings that Ybt transport and recycling are independent of Ybt biosynthesis.

Mechanisms of metal-Ybt dissociation

The molecular sequence of events by which iron is released from intracellular Fe(III)-Ybt complex is incompletely understood, as enzymes associated with Fe(III)-Ybt dissociation have yet to be identified on the *Yersinia* HPI (6, 21). Previously identified mechanisms of iron release in other siderophore systems include siderophore degradation as well as reduction of the coordinated iron(III) to iron(II), which has significantly lower binding affinity for the siderophore (8–11). We have shown above that *apo*-Ybt is detected in the culture supernatant from exogenously supplied Fe(III)-Ybt, suggesting intact Ybt recycling upon iron release. Therefore we hypothesized that reduction of Fe(III) to Fe(II) may be the mechanism of iron release from Fe(III)-Ybt.

To investigate this, we used physiological reducing agents, ascorbic acid and glutathione (12, 13), and Bathophenanthroline (BPDS), a strong Fe(II) chelator, to examine iron release from Fe(III)-Ybt (14). We mixed 5μM HPLC-purified Fe(III)-Ybt with 2.5mM BPDS and 50mM reducing agents for 2 hours at room temperature in pH 7 and measured Fe(II)-BPDS complex

formation ($\lambda_{\max} = 533\text{nm}$). Fe(II)-BPDS formation was significantly increased with both ascorbic acid and glutathione, compared to Fe(III)-Ybt and BPDS control (Fig 5A). To determine changes in *apo*-Ybt levels, the reaction was stopped by eluting over a C18 column and changes in *apo*- and Fe(III)-Ybt levels were measured using LC-MS/MS. Consistent with increased Fe(II)-BPDS complex formation, we found significant increase in *apo*-Ybt to Fe(III)-Ybt ratios in presence of both ascorbic acid and glutathione (Fig 5B). Interestingly, ascorbic acid led to significantly greater *apo*-Ybt formation compared to glutathione, which is consistent with previous studies that showed ascorbic acid to be more efficient compared to glutathione (14–16).

To further examine the mechanism of iron release from Fe(III)-Ybt, we examined the intracellular fate of Ga(III)-Ybt. Gallium(III) has similar properties to Fe(III) including atomic radius, coordination chemistry and charge, which allows Ga(III) to substitute for Fe(III) and disrupt many biomolecular processes (17–19). However, unlike Fe(III), Ga(III) cannot be reduced to Ga(II) under physiological conditions (20, 21). We quantified Ga(III)- and *apo*-Ybt from culture supernatants and cell extracts following a 2 hours exposure to 0.1 μM purified Ga(III)-Ybt. Supernatant Ga(III)-Ybt levels were nearly eliminated in UTI89 Δ *ybtA* *pfyuA* and UTI89 Δ *ybtA* *pfyuA* *pybtPQ* demonstrating Ga(III)-Ybt transport (Fig 6A). Consistent with FyuA-mediated transport of Ga(III)-Ybt to the periplasm, cell-associated Ga(III)-Ybt levels were significantly increased in UTI89 Δ *ybtA* *pfyuA* compared to UTI89 Δ *ybtA*. However unlike Fe(III)-Ybt, no significant differences in cellular Ga(II)-Ybt levels were detected between UTI89 Δ *ybtA* *pfyuA* and UTI89 Δ *ybtA* *pfyuA* *pybtPQ* (Fig 6B). Consequently, *apo*-Ybt was also not detected in the supernatant of all the strains tested (Fig 6C). These findings suggest that gallium is not released from the intracellular Ga(III)-Ybt complex unlike Fe(III)-Ybt, and combined with

results from *in vitro* reduction of Fe(III)-Ybt, support a model in which iron is released from intracellular Fe(III)-Ybt through reduction of Fe(III) to Fe(II).

YbtPQ-dependent Cu(II)- and Ni(II)-Ybt transport and recycling

To determine whether UPEC can transport and dissociate non-iron metal-Ybt complexes, we used stable isotope dilution mass spectrometry (LC-MS/MS) to directly measure exogenously-supplied metal-yersiniabactin complexes. In this approach, Cu(II)-, Ni(II)- and *apo*-Ybt could be quantified in culture supernatants and cell extracts following a 2 hour exposure to 0.1 μM purified Cu(II)- or Ni(II)-Ybt. Supernatant Cu(II)- and Ni(II)-Ybt levels were nearly eliminated in UTI89Δ*ybtA* *pfyuA* and UTI89Δ*ybtA* *pfyuA* *pybtPQ* suggesting intracellular localization of Cu(II)- and Ni(II)-Ybt (Fig 7AB). Consistent with FyuA-mediated transport of Cu(II)- and Ni(II)-Ybt to the periplasm shown previously, cell-associated Cu(II)- and Ni(II)-Ybt levels were significantly increased in UTI89Δ*ybtA* *pfyuA* compared to UTI89Δ*ybtA*. In presence of both FyuA and YbtPQ, cellular Cu(II)- and Ni(II)-Ybt levels were significantly decreased compared to UTI89Δ*ybtA* *pfyuA* (Fig 7CD). When we examined the culture supernatants for *apo*-Ybt, *apo*-Ybt levels were significantly increased in UTI89Δ*ybtA* *pfyuA* *pybtPQ* from both from exogenously supplied Cu(II)- and Ni(II)-Ybt (Fig 7EF). These observations support a model in which similar to the fate of Fe(III)-Ybt, YbtPQ-dependent transport of Cu(II)- and Ni(II)-Ybt complexes subsequently leads to metal release from the metal-Ybt complex with the resulting *apo*-Ybt recycled to the supernatant. These findings also raise the possibility that Ybt may act as a metallophore to import and utilize select metal-Ybt complexes during infections.

Copper from Cu(II)-Ybt remains intracellular

The fate of copper released from intracellular Cu(II)-Ybt upon YbtPQ-dependent transport remains unclear. *E. coli* has several known enzymes that require copper for their function (55–60). However there are also copper resistance mechanisms that are sensitive to changes in intracellular copper levels, including efflux mechanisms to export excess copper (24, 28–30). To determine whether the released copper remains intracellular, we used radiolabeled $^{64}\text{Cu(II)-Ybt}$ to directly localize ^{64}Cu from exogenously supplied $^{64}\text{Cu(II)-Ybt}$. In this approach, ^{64}Cu levels were measured in cell pellets following a 2 hour exposure to $0.1\mu\text{M}$ purified Cu(II)-Ybt and $^{64}\text{Cu(II)-Ybt}$. ^{64}Cu levels were significantly increased in UTI89 $\Delta ybtA$ *pfyuA* compared to UTI89 $\Delta ybtA$, consistent with FyuA-mediated transport of Cu(II)-Ybt. Interestingly, no significant differences in ^{64}Cu levels were observed between UTI89 $\Delta ybtA$ *pfyuA* and UTI89 $\Delta ybtA$ *pfyuA* *pybtPQ* (Fig 8). This was in contrast to intact Cu(II)-Ybt levels between these two strains (Fig 7C). These findings combined show that in the presence of both FyuA and YbtPQ, copper is released from transported Cu(II)-Ybt and remains intracellular. Copper ions delivered from Cu(II)-Ybt may then act as cofactors to *E. coli* cuproenzymes during infections.

DISCUSSION

In this study, we use direct mass spectrometric detection to show that in presence of Ybt importers FyuA and YbtPQ, Ybt delivers physiologically relevant metal ions Fe(III), Cu(II) and Ni(II). Iron is released from Ybt through reduction of bound Fe(III) to Fe(II), resulting in intact *apo*-Ybt dissociation and recycling. This however is not seen for Ga(III)-Ybt complex, in which gallium ion is not released from Ybt and is consistent with reduction as the mechanism of metal release from Ybt. We also show Ybt import and recycling in wild type pathogenic *E. coli* isolates that do not synthesize Ybt but express transport genes on the *Yersinia* HPI, suggesting Ybt cheater strains may benefit during polymicrobial infections with Ybt synthesizing strains. Together these findings provide new evidence for a metallophore function by the yersiniabactin system that delivers physiologic metal ions to UPEC.

Within an intracellular vesicle, such as the macrophage phagolysosome, UPEC are confined in an environment where copper ions may be in excess while iron is limiting (1). In such environments where copper is abundant, Ybt has been shown to protect UPEC in a transport-independent manner (2, 3). Recent work has also shown preference for Fe(III)-Ybt in high local Cu(II)-Ybt concentrations by FyuA, suggesting that the yersiniabactin import system may be adapted to a range of copper concentrations (4). As such, our observations showing copper release from intracellular Cu(II)-Ybt at relatively low copper concentrations suggest in environments where copper may be limiting, Ybt may deliver copper to UPEC. Although it is unclear whether the host deliberately limits copper levels to limit microbial growth, *Cryptococcus neoformans* has been shown to encounter copper limitation during brain-stage of infection, resulting in increased expression of fungal copper transporters (64, 65). Further

investigation is necessary to determine whether similar environments are encountered during urinary tract pathogenesis.

The ability of Cu(II) and Ni(II)-Ybt complexes to be transported and dissociated through the same pathway as Fe(III)-Ybt suggests promiscuous interactions with Ybt transporters as well as with potential reductases. Furthermore the intracellular release of reactive Cu(I) and Ni(I) ions from Ybt may require chaperones that interact with these ions and prevent any unwanted consequences of labile ions. Small molecule chelators such as glutathione have been shown to be critical for *E. coli* copper homeostasis in the absence of cytoplasmic copper efflux mechanisms (7). Furthermore metallothioneins have been shown to sequester intracellular copper in fungal pathogens and recent work describing a novel metallothionein in *Mycobacterium tuberculosis* suggest bacterial pathogens may also possess cytoplasmic copper chaperones that are yet to be identified (6, 8, 9). Thus far all known copper-dependent enzymes in *E. coli* are periplasmic or embedded in the cytoplasmic membrane (10). The cytoplasmic requirement for copper may be unclear, but recent work by *Osman et al.*, has shown inner membrane copper efflux ATPases to be required for Salmonella Cu, Zn-superoxide dismutase activity (11). A requirement for copper to first be transported to the cytoplasm prior to being loaded on cuproenzymes may uncover novel interactions among bacterial copper homeostatic machinery and copper-dependent proteins.

Microbial pathogens encounter numerous physiologic environments during infection pathogenesis where the host changes the availability of transition metals to limit microbial growth (12). Ybt provides a gain-of-function through its interactions with iron, copper and

possibly with other physiologic metal ions (2). In addition, recycling of *apo*-Ybt may allow pathogens to effectively conserve scarce resources during an infection without constant *de novo* siderophore synthesis (13, 14). These properties may benefit a polymicrobial UPEC infection community as a whole, including cheater strains, by synthesizing and maintaining physiologic Ybt concentrations with relatively minor costs for the population.

ACKNOWLEDGEMENTS

J.P.H. holds a Career Award for Medical Scientists from the Burroughs Wellcome Fund and acknowledges National Institute of Diabetes and Digestive and Kidney Diseases grants R01DK099534 and P50DK064540. The funders had no role in study design, data collection and interpretation, or the decision to submit the work for publication. The authors thank Dr. Jennifer Walker, Dr. Lloyd Robinson and Stephanie Krieger for technical assistance. The authors have no conflicts of interest to declare.

CHAPTER FOUR: FIGURES

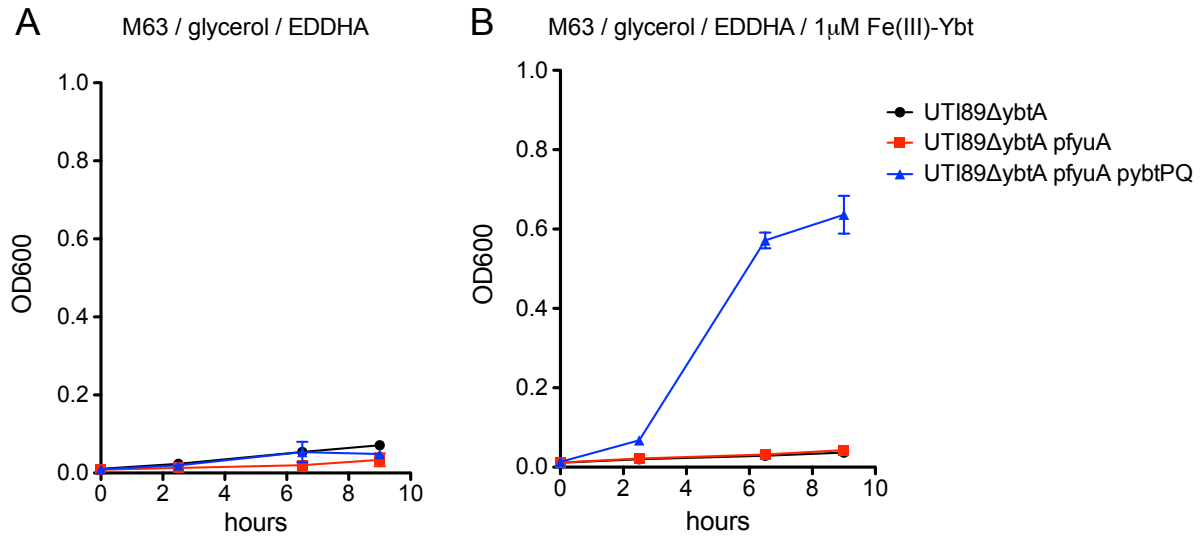


Figure 1. FyuA and YbtPQ are required and sufficient for Fe(III)-Ybt-dependent growth in UPEC. Growth of UTI89ΔybtA (black circle), UTI89ΔybtA pfyuA (red square), and UTI89ΔybtA pfyuA pybtPQ (blue triangle) all show decreased growth in EDDHA-chelated M63 minimal salts media (A), while growth is rescued for UTI89ΔybtA pfyuA pybtPQ upon addition of 1μM Fe(III)-Ybt to chelated media (B). Results are shown as mean ± s.d.; n=3.

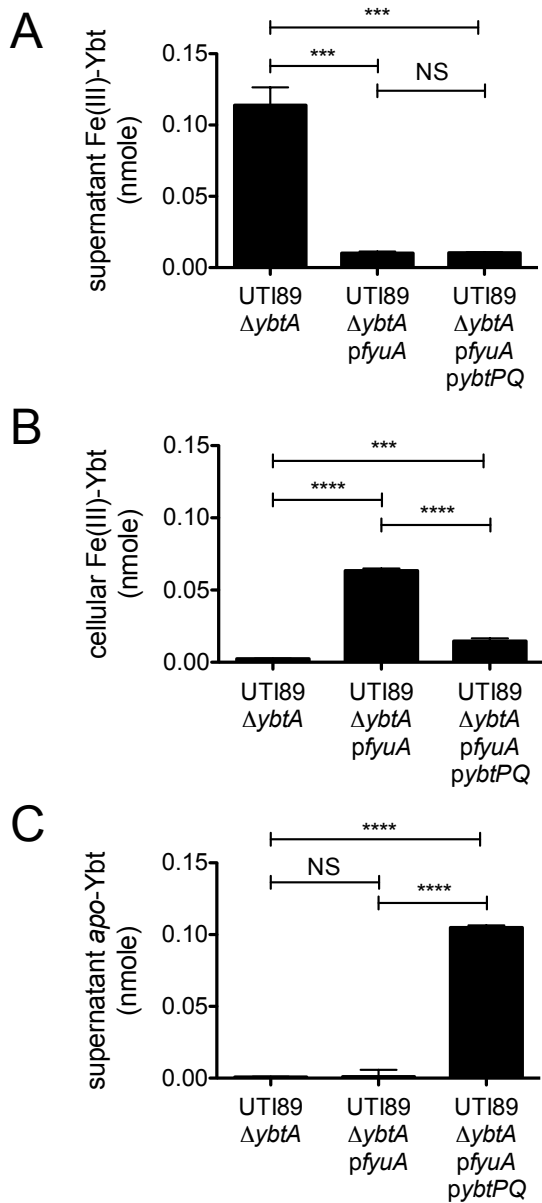


Figure 2. Direct LC-MS/MS detection of supernatant and cell-associated Fe(III)- and *apo*-Ybt in FyuA and YbtPQ-expressing UTI89. Bacteria grown in media containing 0.1 μ M Fe(III)-Ybt were extracted to quantify supernatant and cellular Fe(III)- and *apo*-Ybt levels using LC-MS/MS with a 13 C-labeled Fe(III)-Ybt internal standard. **(A)** Supernatant Fe(III)-Ybt remained extracellular in transport-deficient UTI89 $\Delta ybtA$. **(B)** Exogenous FyuA expression in UTI89 $\Delta ybtA$ significantly increased cell-associated Fe(III)-Ybt levels, but expression of both

FyuA and YbtPQ resulted in decreased cellular Fe(III)-Ybt levels. (C) Apo-Ybt was recycled to the supernatant in UTI89 Δ *ybtA* *pfyuA* *pybtPQ*. Results are shown as nanomoles, mean \pm s.d.; $n=3$; **** $P < 0.0001$.

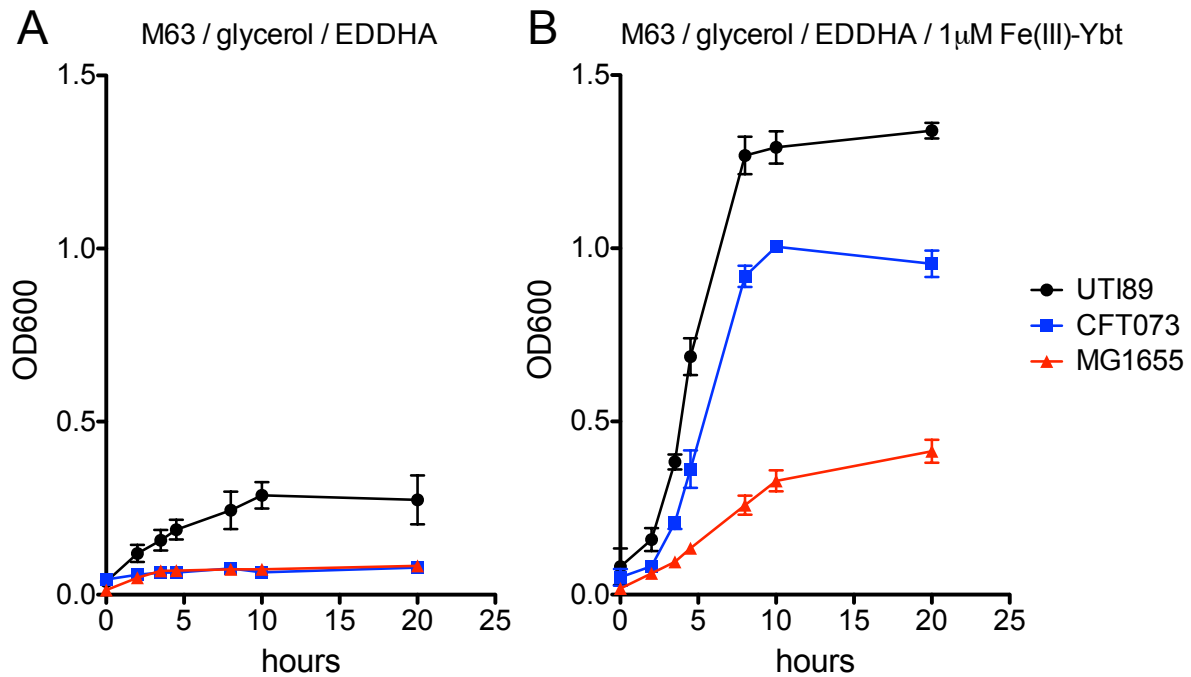


Figure 3. Growth of pathogenic *E. coli* strains under Fe(III)-Ybt-dependent conditions.

Pathogenic strains, UTI89 (*black circle*) and CFT073 (*blue square*), and non-pathogenic MG1655 (*red triangle*) all show limited growth in EDDHA-chelated M63 minimal salts media (**A**). Growth is rescued for both UTI89 and CFT073 upon addition of 1µM Fe(III)-Ybt to chelated media (**B**). Results are shown as mean \pm s.d.; $n=3$.

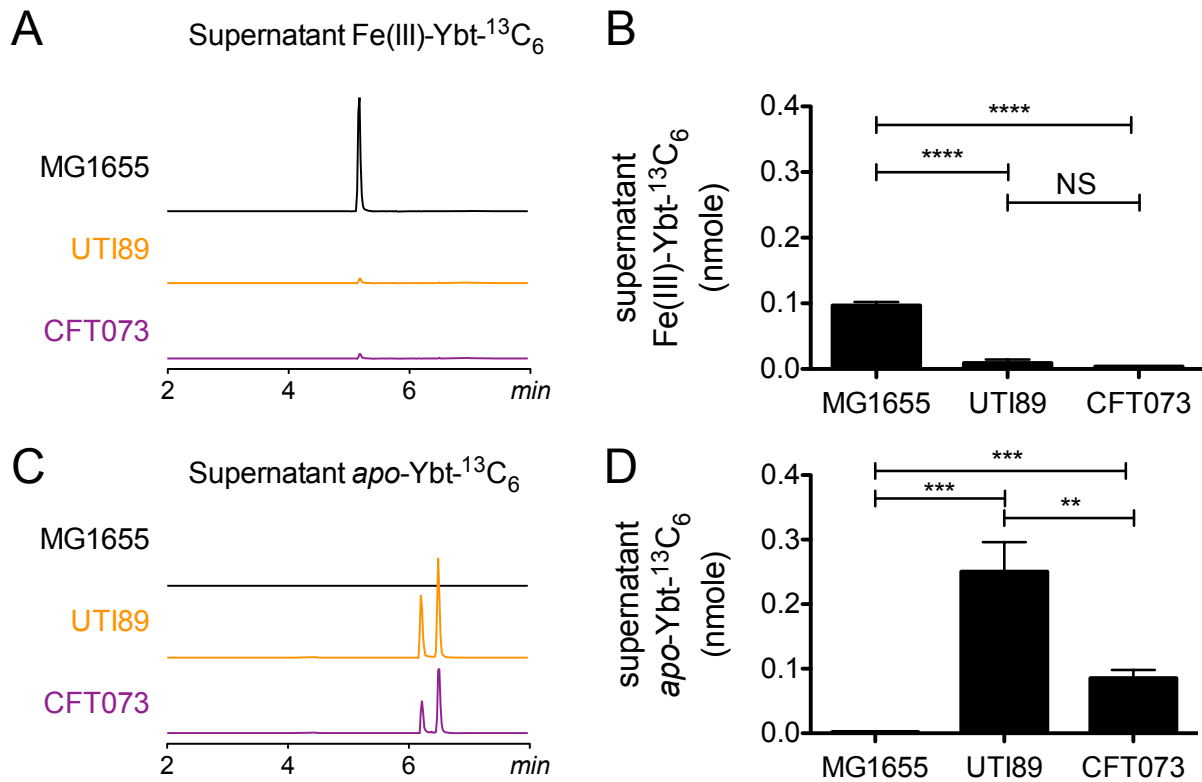


Figure 4. Direct LC-MS/MS detection of Fe(III)- and apo-Ybt from pathogenic *E. coli* culture supernatant. Supernatant from strains grown in $0.1\mu\text{M}$ ^{13}C -salicylate-labeled Fe(III)-Ybt- $^{13}\text{C}_6$ were extracted to quantify Fe(III)-Ybt- $^{13}\text{C}_6$ and apo-Ybt- $^{13}\text{C}_6$ levels. **(A)** Representative LC-MS/MS chromatogram of supernatant Fe(III)-Ybt- $^{13}\text{C}_6$ scaled to internal standard peaks. **(B)** Supernatant Fe(III)-Ybt- $^{13}\text{C}_6$ levels were significantly decreased in UTI89 and CFT073. **(C)** Representative LC-MS/MS chromatogram of supernatant apo-Ybt- $^{13}\text{C}_6$ scaled to internal standard peaks. **(D)** Supernatant apo-Ybt- $^{13}\text{C}_6$ levels were significantly increased in UTI89 and CFT073. Results are shown as nanomoles, mean \pm s.d.; $n=3$; **** $P < 0.0001$.

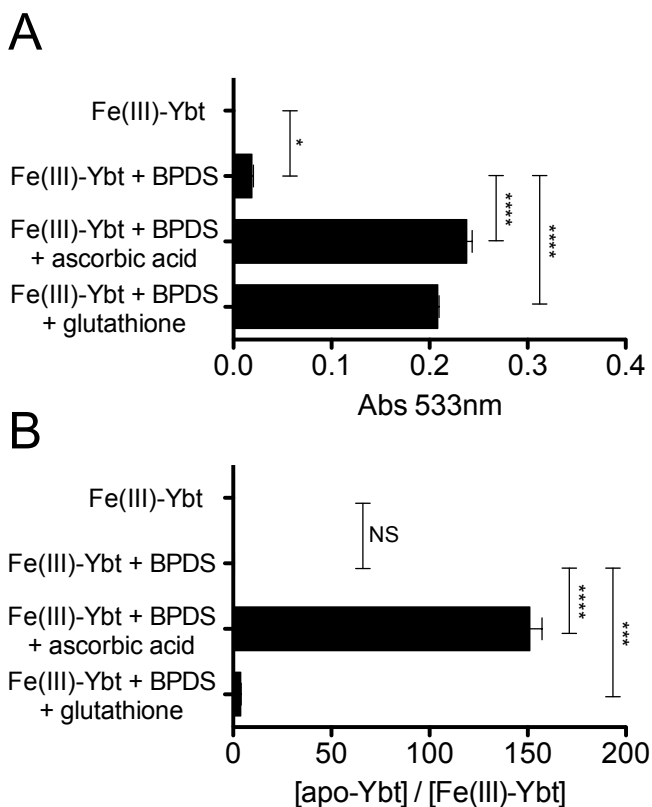


Figure 5. *In vitro* iron release from Fe(III)-Ybt complexes. HPLC-purified Fe(III)-Ybt (5 μ M) were mixed with BPDS (Bathophenanthrolinedisulfonic acid, 2.5mM) and excess reducing agents (50mM) in PBS buffer pH7.0 for 2 hours. Addition of reducing agents, ascorbic acid and glutathione, showed significant increase in **(A)** Fe(II)-BPDS complex formation ($\lambda_{\text{max}} = 533\text{nm}$), as well as **(B)** apo-Ybt determined through apo- and Fe(III)-Ybt ion chromatogram peak ratios using LC-MS/MS. Results are shown as mean \pm s.d.; $n=3$; **** $P < 0.0001$.

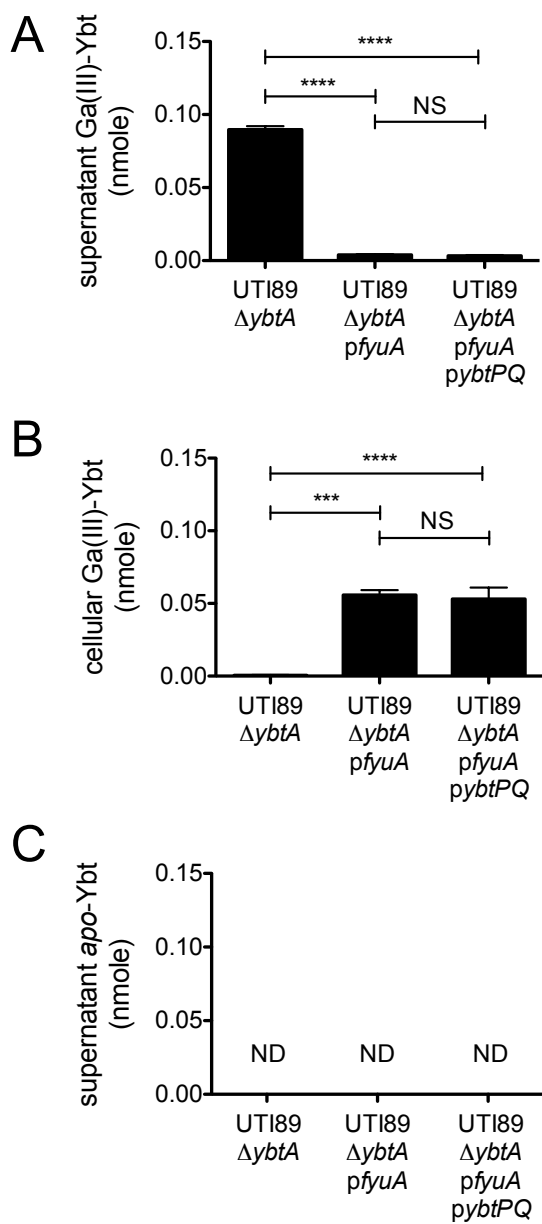


Figure 6. Direct LC-MS/MS detection of supernatant and cell-associated Ga(III)- and apo-Ybt in FyuA and YbtPQ-expressing UTI89. Bacteria grown in media containing 0.1 μ M Ga(III)-Ybt were extracted to quantify supernatant and cellular Ga(III)- and apo-Ybt levels using LC-MS/MS with a 13 C-labeled Fe(III)-Ybt internal standard. **(A)** Supernatant Ga(III)-Ybt remained extracellular in transport-deficient UTI89 $\Delta ybtA$. **(B)** Cellular Ga(III)-Ybt levels were

not significantly different in UTI89 Δ *ybtA* *pfyuA* and UTI89 Δ *ybtA* *pfyuA* *pybtPQ*. (C) Apo-Ybt was not detected (ND) in the supernatants of strains tested. Results are shown as nanomoles, mean \pm s.d.; $n=3$; **** $P < 0.0001$.

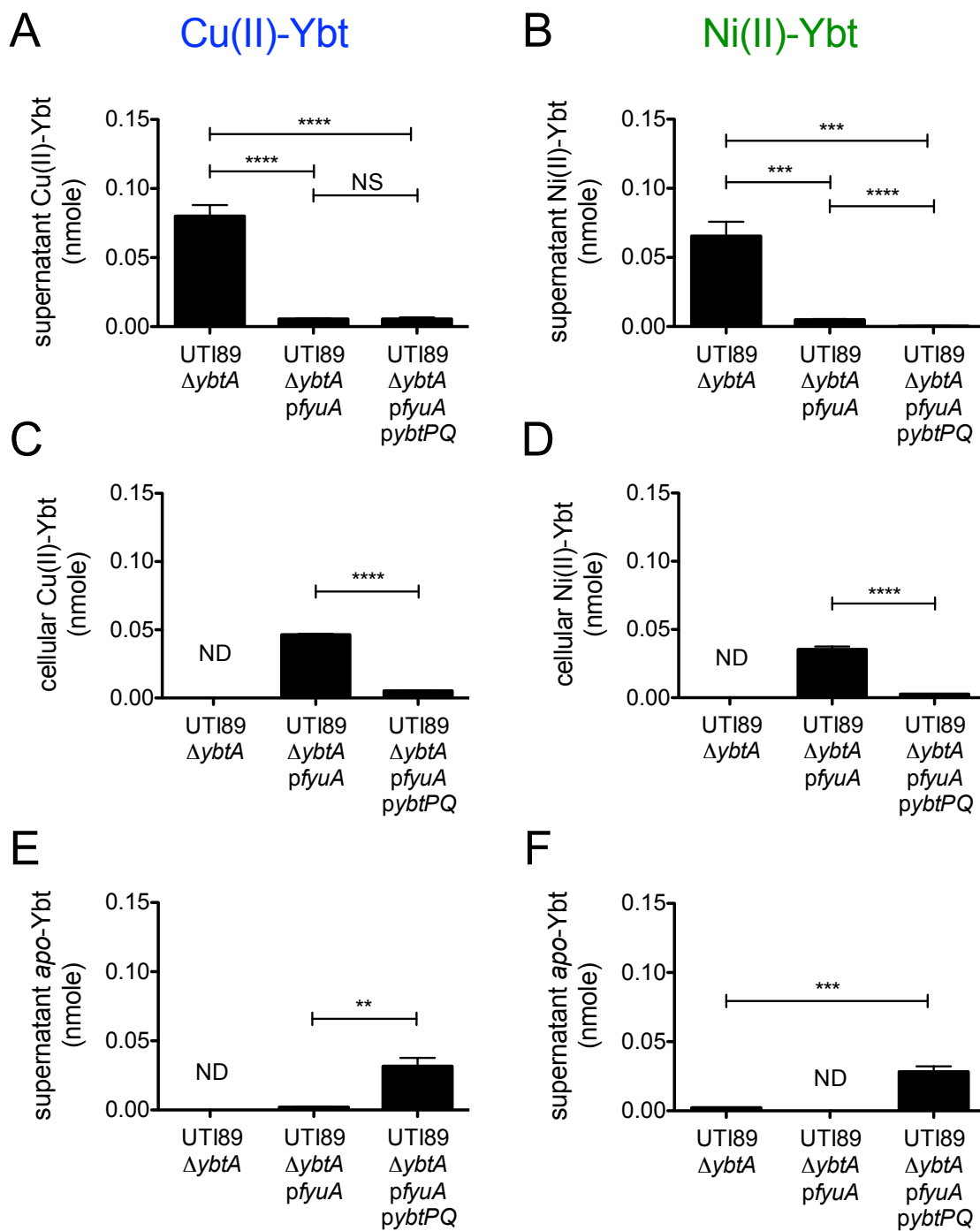


Figure 7. Direct LC-MS/MS detection of supernatant and cell-associated Cu(II)-, Ni(II)- and apo-Ybt in FyuA and YbtPQ-expressing UTI89. Bacteria grown in media containing 0.1 μ M Cu(II)- (*left*) or Ni(II)-Ybt (*right*) were extracted to quantify supernatant and cellular

Cu(II)-, Ni(II)- and *apo*-Ybt levels using LC-MS/MS with a ¹³C-labeled Fe(III)-Ybt internal standard. **(A, B)** Supernatant Cu(II)- and Ni(II)-Ybt remained extracellular in transport-deficient UTI89Δ*ybtA*. **(C, D)** Exogenous FyuA expression in UTI89Δ*ybtA* significantly increased cell-associated Cu(II)- and Ni(II)-Ybt levels, but expression of both FyuA and YbtPQ resulted in decreased cellular Cu(II)- and Ni(II)-Ybt levels. **(E, F)** *Apo*-Ybt was recycled to the supernatant in UTI89Δ*ybtA* *pfyuA* *pybtPQ*. Results are shown as nanomoles, mean ± s.d.; *n*=3; *****P* < 0.0001.

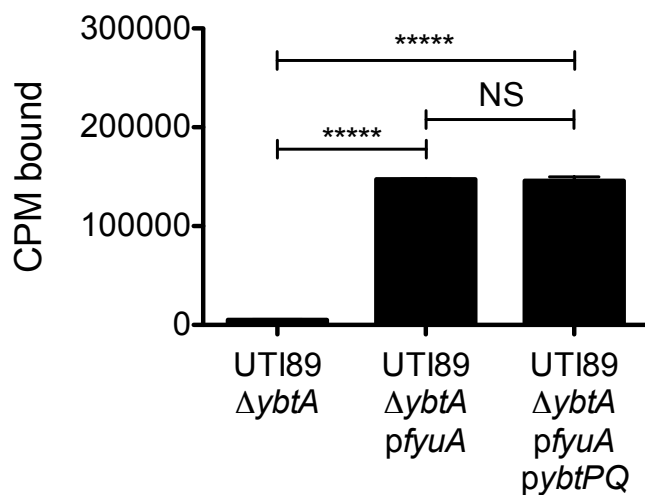


Figure 8. Direct detection of ^{64}Cu from cellular $^{64}\text{Cu(II)-Ybt}$. Bacteria grown in media containing $0.1\mu\text{M}$ Cu(II)-Ybt and $^{64}\text{Cu(II)-Ybt}$ were extracted to quantify cellular ^{64}Cu levels. Cellular ^{64}Cu levels were not significantly different in UTI89 $\Delta ybtA$ *pfyuA* and UTI89 $\Delta ybtA$ *pfyuA* *pybtPQ*. Results are shown as counts per minute, mean \pm s.d.; $n=3$; *****($P < 0.00001$).

CHAPTER FOUR: REFERENCES

1. Miethke, M., and Marahiel, M. A. (2007) Siderophore-based iron acquisition and pathogen control. *Microbiol. Mol. Biol. Rev. MMBR.* **71**, 413–51
2. Henderson, J. P., Crowley, J. R., Pinkner, J. S., Walker, J. N., Tsukayama, P., Stamm, W. E., Hooton, T. M., and Hultgren, S. J. (2009) Quantitative Metabolomics Reveals an Epigenetic Blueprint for Iron Acquisition in Uropathogenic *Escherichia coli*. *PloS Pathog.*
3. Mabbetta, A. N., Uletta, G. C., Watta, R. E., Treea, J. J., Totsikaa, M., Onga, C. Y., Wooda, J. M., Monaghanb, W., Lookec, D. F., Nimmod, G. R., Svanborge, C., and Schembria, M. A. (2009) Virulence properties of asymptomatic bacteriuria *Escherichia coli*. *Int. J. Med. Microbiol.*
4. Perry, R. D., Balbo, P. B., Jones, H. A., Fetherston, J. D., and DeMoll, E. (1999) Yersiniabactin from *Yersinia pestis*: biochemical characterization of the siderophore and its role in iron transport and regulation. *Microbiology*
5. Fetherston, J. D., Bearden, S. W., and Perry, R. D. (1996) YbtA, an AraC-type regulator of the *Yersinia pestis* pesticin/yersiniabactin receptor. *Mol. Microbiol.* **22**, 315–25
6. Fetherston, J. D., Bertolino, V. J., and Perry, R. D. (1999) YbtP and YbtQ: two ABC transporters required for iron uptake in *Yersinia pestis*. *Mol. Microbiol.* **32**, 289–99
7. Reigstad, C. S., Hultgren, S. J., and Gordon, J. I. (2007) Functional genomic studies of uropathogenic *Escherichia coli* and host urothelial cells when intracellular bacterial communities are assembled. *J. Biol. Chem.* **282**, 21259–67
8. Hagan, E. C., Lloyd, A. L., Rasko, D. A., Faerber, G. J., and Mobley, H. L. T. (2010) *Escherichia coli* Global Gene Expression in Urine from Women with Urinary Tract Infection. *PloS Pathog.*

9. Chaturvedi, K. S., Hung, C. S., Crowley, J. R., Stapleton, A. E., and Henderson, J. P. (2012) The siderophore yersiniabactin binds copper to protect pathogens during infection. *Nat. Chem. Biol.* 10.1038/nchembio.1020
10. Chaturvedi, K. S., Hung, C. S., Giblin, D. E., Urushidani, S., Austin, A. M., Dinauer, M. C., and Henderson, J. P. (2013) Cupric Yersiniabactin Is a Virulence-Associated Superoxide Dismutase Mimic. *ACS Chem. Biol.* **9**, 551–561
11. García-Santamarina, S., and Thiele, D. J. (2015) Copper at the Fungal Pathogen-Host Axis. *J. Biol. Chem.* **290**, 18945–18953
12. Koh, E.-I., and Henderson, J. P. (2015) Microbial Copper-binding Siderophores at the Host-Pathogen Interface. *J. Biol. Chem.* **290**, 18967–18974
13. Hodgkinson, V., and Petris, M. J. (2012) Copper homeostasis at the host-pathogen interface. *J. Biol. Chem.* **287**, 13549–55
14. Ridge, P. G., Zhang, Y., and Gladyshev, V. N. (2008) Comparative genomic analyses of copper transporters and cuproproteomes reveal evolutionary dynamics of copper utilization and its link to oxygen. *PloS One.* **3**, e1378
15. White, C., Lee, J., Kambe, T., Fritsche, K., and Petris, M. J. (2009) A role for the ATP7A copper-transporting ATPase in macrophage bactericidal activity. *J. Biol. Chem.* **284**, 33949–56
16. Koh, E.-I., Hung, C. S., Parker, K. S., Crowley, J. R., Giblin, D. E., and Henderson, J. P. (2015) Metal selectivity by the virulence-associated yersiniabactin metallophore system. *Metallomics.* **7**, 1011–1022

17. Knapp, C. W., Fowle, D. A., Kulczycki, E., Roberts, J. A., and Graham, D. W. (2007) Methane monooxygenase gene expression mediated by methanobactin in the presence of mineral copper sources. *Proc. Natl. Acad. Sci. U. S. A.* **104**, 12040–5
18. Balasubramanian, R., Kenney, G. E., and Rosenzweig, A. C. (2011) Dual pathways for copper uptake by methanotrophic bacteria. *J. Biol. Chem.* **286**, 37313–9
19. Hood, M. I., and Skaar, E. P. (2012) Nutritional immunity: transition metals at the pathogen–host interface. *Nat. Rev. Microbiol.* **10**, 525–537
20. Noinaj, N., Guillier, M., Barnard, T. J., and Buchanan, S. K. (2010) TonB-Dependent Transporters: Regulation, Structure, and Function. *Annu. Rev. Microbiol.*
21. Perry, R. D., and Fetherston, J. D. (2011) Yersiniabactin iron uptake: mechanisms and role in *Yersinia pestis* pathogenesis. *Microbes Infect. Inst. Pasteur.* **13**, 808–17
22. Chu, B. C., Garcia-Herrero, A., Johanson, T. H., Krewulak, K. D., Lau, C. K., Peacock, R. S., Slavinskaya, Z., and Vogel, H. J. (2010) Siderophore uptake in bacteria and the battle for iron with the host; a bird’s eye view. *Biometals.* **23**, 601–6111
23. Raymond, K. N., Dertz, E. A., and Kim, S. S. (2003) Enterobactin: an archetype for microbial iron transport. *Proc. Natl. Acad. Sci. U. S. A.* **100**, 3584–8
24. Brem, D., Pelludat, C., Rakin, A., Jacobi, C. A., and Heesemann, J. (2001) Functional analysis of yersiniabactin transport genes of *Yersinia enterocolitica*. *Microbiology.* **147**, 1115–27
25. Schalk, I. J. (2008) Metal trafficking via siderophores in Gram-negative bacteria: specificities and characteristics of the pyoverdine pathway. *J. Inorg. Biochem.* **102**, 1159–69

26. Cooper, S. R., McArdle, J. V., and Raymond, K. N. (1978) Siderophore electrochemistry: relation to intracellular iron release mechanism. *Proc. Natl. Acad. Sci. U. S. A.* **75**, 3551–4
27. Harris, W. R., Carrano, C. J., Cooper, S. R., Sofen, S. R., Avdeef, A. E., McArdle, J. V., and Raymond, K. N. (1979) Coordination chemistry of microbial iron transport compounds. 19. Stability constants and electrochemical behavior of ferric enterobactin and model complexes. *J. Am. Chem. Soc.*
28. Abergel, R. J., Warner, J. A., Shuh, D. K., and Raymond, K. N. (2006) Enterobactin protonation and iron release: structural characterization of the salicylate coordination shift in ferric enterobactin. *J. Am. Chem. Soc.* **128**, 8920–31
29. Matzanke, B. F., Anemüller, S., Schünemann, V., Trautwein, A. X., and Hantke, K. (2004) FhuF, Part of a Siderophore–Reductase System†. *Biochemistry (Mosc.)*. **43**, 1386–1392
30. Mies, K. A., Wirgau, J. I., and Crumbliss, A. L. (2006) Ternary complex formation facilitates a redox mechanism for iron release from a siderophore. *Biometals Int. J. Role Met. Ions Biol. Biochem. Med.* **19**, 115–26
31. Harrington, J. M., and Crumbliss, A. L. (2009) The redox hypothesis in siderophore-mediated iron uptake. *Biometals*. **22**, 679–689
32. Miethke, M., Hou, J., and Marahiel, M. A. (2011) The siderophore-interacting protein YqjH acts as a ferric reductase in different iron assimilation pathways of *Escherichia coli*. *Biochemistry (Mosc.)*. **50**, 10951–64
33. Crosa, J. H., and Walsh, C. T. (2002) Genetics and assembly line enzymology of siderophore biosynthesis in bacteria. *Microbiol. Mol. Biol. Rev.* **66**, 223–249

34. Lv, H., Hung, C. S., and Henderson, J. P. (2014) Metabolomic analysis of siderophore cheater mutants reveals metabolic costs of expression in uropathogenic *Escherichia coli*. *J. Proteome Res.* **13**, 1397–404
35. Chen, S. L., Hung, C. S., Xu, J., Reigstad, C. S., Magrini, V., Sabo, A., Blasiar, D., Bieri, T., Meyer, R. R., Ozersky, P., Armstrong, J. R., Fulton, R. S., Latreille, J. P., Spieth, J., Hooton, T. M., Mardis, E. R., Hultgren, S. J., and Gordon, J. I. (2006) Identification of genes subject to positive selection in uropathogenic strains of *Escherichia coli*: a comparative genomics approach. *Proc. Natl. Acad. Sci. U. S. A.* **103**, 5977–82
36. Blattner, F. R., Plunkett, G., Bloch, C. A., Perna, N. T., Burland, V., Riley, M., Collado-Vides, J., Glasner, J. D., Rode, C. K., Mayhew, G. F., Gregor, J., Davis, N. W., Kirkpatrick, H. A., Goeden, M. A., Rose, D. J., Mau, B., and Shao, Y. (1997) The Complete Genome Sequence of *Escherichia coli* K-12. *Science.* **277**, 1453–1462
37. Welch, R. A., Burland, V., Plunkett, G., Redford, P., Roesch, P., Rasko, D., Buckles, E. L., Liou, S.-R., Boutin, A., Hackett, J., Stroud, D., Mayhew, G. F., Rose, D. J., Zhou, S., Schwartz, D. C., Perna, N. T., Mobley, H. L. T., Donnenberg, M. S., and Blattner, F. R. (2002) Extensive mosaic structure revealed by the complete genome sequence of uropathogenic *Escherichia coli*. *Proc. Natl. Acad. Sci.* **99**, 17020–17024
38. Datsenko, K. A., and Wanner, B. L. (2000) One-step inactivation of chromosomal genes in *Escherichia coli* K-12 using PCR products. *PNAS.* **97**, 6640–6645
39. Amann, E., Ochs, B., and Abel, K. J. (1988) Tightly regulated *tac* promoter vectors useful for the expression of unfused and fused proteins in *Escherichia coli*. *Gene.* **69**, 301–15

40. Guzman, L. M., Belin, D., Carson, M. J., and Beckwith, J. (1995) Tight regulation, modulation, and high-level expression by vectors containing the arabinose PBAD promoter. *J. Bacteriol.* **177**, 4121–4130
41. McCarthy, D. W., Shefer, R. E., Klinkowstein, R. E., Bass, L. A., Margeneau, W. H., Cutler, C. S., Anderson, C. J., and Welch, M. J. (1997) Efficient production of high specific activity ^{64}Cu using a biomedical cyclotron. *Nucl. Med. Biol.* **24**, 35–43
42. Kume, M., Carey, P. C., Gaehle, G., Madrid, E., Voller, T., Margenau, W., Welch, M. J., and Lapi, S. E. (2012) A semi-automated system for the routine production of copper-64. *Appl. Radiat. Isot.* **70**, 1803–1806
43. Bultreys, A., Gheysen, I., and Hoffmann, E. de (2006) Yersiniabactin Production by *Pseudomonas syringae* and *Escherichia coli*, and Description of a Second Yersiniabactin Locus Evolutionary Group. *Appl. Environ. Microbiol.* **72**, 3814–3825
44. Brzuszkiewicz, E., Brüggemann, H., Liesegang, H., Emmerth, M., Ölschläger, T., Nagy, G., Albermann, K., Wagner, C., Buchrieser, C., Emödy, L., Gottschalk, G., Hacker, J., and Dobrindt, U. (2006) How to become a uropathogen: Comparative genomic analysis of extraintestinal pathogenic *Escherichia coli* strains. *Proc. Natl. Acad. Sci.* **103**, 12879–12884
45. Hancock, V., Vejborg, R. M., and Klemm, P. (2010) Functional genomics of probiotic *Escherichia coli* Nissle 1917 and 83972, and UPEC strain CFT073: comparison of transcriptomes, growth and biofilm formation. *Mol. Genet. Genomics.* **284**, 437–454
46. Creutz, C. (1981) Complexities of ascorbate as a reducing agent. *Inorg. Chem.* **20**, 4449–4452
47. Millis, K. K., Weaver, K. H., and Rabenstein, D. L. (1993) Oxidation/reduction potential of glutathione. *J. Org. Chem.* **58**, 4144–4146

48. Song, B., Aebischer, N., and Orvig, C. (2002) Reduction of [VO₂(ma)₂]- and [VO₂(ema)₂]- by Ascorbic Acid and Glutathione: Kinetic Studies of Pro-Drugs for the Enhancement of Insulin Action†. *Inorg. Chem.* **41**, 1357–1364
49. Stoyanovsky, D. A., Wu, D., and Cederbaum, A. I. (1998) Interaction of 1-Hydroxyethyl Radical With Glutathione, Ascorbic Acid and α -Tocopherol. *Free Radic. Biol. Med.* **24**, 132–138
50. Olakanmi, O., Britigan, B. E., and Schlesinger, L. S. (2000) Gallium Disrupts Iron Metabolism of Mycobacteria Residing within Human Macrophages. *Infect. Immun.* **68**, 5619–5627
51. Hubbard, J. A. M., Lewandowska, K. B., Hughes, M. N., and Poole, R. K. (1986) Effects of iron-limitation of *Escherichia coli* on growth, the respiratory chains and gallium uptake. *Arch. Microbiol.* **146**, 80–86
52. Chitambar, C. R., Matthaues, W. G., Antholine, W. E., Graff, K., and O'Brien, W. J. (1988) Inhibition of leukemic HL60 cell growth by transferrin-gallium: effects on ribonucleotide reductase and demonstration of drug synergy with hydroxyurea [see comments]. *Blood.* **72**, 1930–1936
53. Bernstein, L. R. (1998) Mechanisms of Therapeutic Activity for Gallium. *Pharmacol. Rev.* **50**, 665–682
54. Emery, T. (1986) Exchange of iron by gallium in siderophores. *Biochemistry (Mosc.)*. **25**, 4629–4633
55. Benov, L. T., and Fridovich, I. (1994) *Escherichia coli* expresses a copper- and zinc-containing superoxide dismutase. *J. Biol. Chem.* **269**, 25310–25314

56. Imlay, K. R., and Imlay, J. A. (1996) Cloning and analysis of *sodC*, encoding the copper-zinc superoxide dismutase of *Escherichia coli*. *J. Bacteriol.* **178**, 2564–2571
57. Grass, G., and Rensing, C. (2001) CueO Is a Multi-copper Oxidase That Confers Copper Tolerance in *Escherichia coli*. *Biochem. Biophys. Res. Commun.* **286**, 902–908
58. Roberts, S. A., Wildner, G. F., Grass, G., Weichsel, A., Ambrus, A., Rensing, C., and Montfort, W. R. (2003) A Labile Regulatory Copper Ion Lies Near the T1 Copper Site in the Multicopper Oxidase CueO. *J. Biol. Chem.* **278**, 31958–31963
59. Parsons, M., Convery, M., Wilmot, C., Yadav, K., Blakeley, V., Corner, A., Phillips, S., McPherson, M., and Knowles, P. (1995) Crystal structure of a quinoenzyme: copper amine oxidase of *Escherichia coli* at 2 Å resolution. *Structure.* **3**, 1171–1184
60. Minagawa, J., Mogi, T., Gennis, R. B., and Anraku, Y. (1992) Identification of heme and copper ligands in subunit I of the cytochrome bo complex in *Escherichia coli*. *J. Biol. Chem.* **267**, 2096–2104
61. Chaturvedi, K. S., and Henderson, J. P. (2014) Pathogenic adaptations to host-derived antibacterial copper. *Front. Cell. Infect. Microbiol.* **4**, 3
62. Outten, F. W., Huffman, D. L., Hale, J. A., and O'Halloran, T. V. (2001) The independent *cue* and *cus* systems confer copper tolerance during aerobic and anaerobic growth in *Escherichia coli*. *J Biol Chem.* **276**, 30670–7
63. Franke, S., Grass, G., Rensing, C., and Nies, D. H. (2003) Molecular analysis of the copper-transporting efflux system CusCFBA of *Escherichia coli*. *J. Bacteriol.* **185**, 3804–3812
64. Sun, T.-S., Ju, X., Gao, H.-L., Wang, T., Thiele, D. J., Li, J.-Y., Wang, Z.-Y., and Ding, C. (2014) Reciprocal functions of *Cryptococcus neoformans* copper homeostasis machinery during pulmonary infection and meningoencephalitis. *Nat. Commun.* **5**, 5550

65. Ding, C., Yin, J., Tovar, E. M. M., Fitzpatrick, D. A., Higgins, D. G., and Thiele, D. J. (2011) The Cu regulon of the human fungal pathogen *Cryptococcus neoformans* H99: Cuf1 activates distinct genes in response to both Cu excess and deficiency. *Mol. Microbiol.* **81**, 1560–1576
66. Helbig, K., Bleuel, C., Krauss, G. J., and Nies, D. H. (2008) Glutathione and Transition-Metal Homeostasis in *Escherichia coli*. *J. Bacteriol.* **190**, 5431–5438
67. Thrower, A. R., Byrd, J., Tarbet, E. B., Mehra, R. K., Hamer, D. H., and Winge, D. R. (1988) Effect of mutation of cysteinyl residues in yeast Cu-metallothionein. *J. Biol. Chem.* **263**, 7037–7042
68. Robinson, N. J. (2008) A bacterial copper metallothionein. *Nat. Chem. Biol.* **4**, 582–583
69. Tottey, S., Harvie, D. R., and Robinson, N. J. (2005) Understanding How Cells Allocate Metals Using Metal Sensors and Metallochaperones. *Acc. Chem. Res.* **38**, 775–783
70. Osman, D., Patterson, C. J., Bailey, K., Fisher, K., Robinson, N. J., Rigby, S. E., and Cavet, J. S. (2013) The copper supply pathway to a *Salmonella* Cu,Zn-superoxide dismutase (SodCII) involves P(1B)-type ATPase copper efflux and periplasmic CueP. *Mol. Microbiol.* **87**, 466–77

CHAPTER FIVE

Conclusions, Perspectives and Implications

5.1 Summary of the Thesis

This thesis describes the interactions between the yersiniabactin siderophore system and metal ions in the context of uropathogenic *Escherichia coli* (UPEC) pathogenesis in the urinary tract. Yersiniabactin (Ybt) confers a gain-of-function to UPEC through its interactions with both iron and copper ions during infection, and Ybt's interaction with copper has been shown to protect UPEC against host copper ions as well as oxidative stress (1, 2). However it has been unclear whether UPEC imports Cu(II)-Ybt complexes similar to Fe(III)-Ybt, and how Ybt transport impacts UPEC pathogenesis.

We investigated the interactions of Ybt with other physiologic transition metals and whether non-ferric metal-Ybt complexes were transport substrates of FyuA, the Fe(III)-Ybt outer membrane importer (3). Using a constant neutral loss LC-MS/MS screen, we showed Ybt complexes with nickel(II), cobalt(III) and chromium(III), in addition to previously described complexes with iron(III), gallium(III) and copper(II). All stable metal-Ybt complexes were transported through FyuA to the periplasm in TonB-dependent manner. Of these, Cu(II)-Ybt was the only complex not to competitive inhibit Fe(III)-Ybt transport. We next investigated the role of Ybt inner membrane transporters YbtP and YbtQ during UPEC pathogenesis. Using an experimental murine chronic cystitis model, we found that the YbtPQ-deficient strain showed a significant, million-fold competitive defect against the wild type in high titer bladder infections. We next examined the fate of metal-Ybt complexes upon transport through YbtPQ to investigate whether Ybt delivers metal ions in addition to iron. We found that in presence of both FyuA and YbtPQ, Fe(III)-, Cu(II)- and Ni(II)-Ybt import leads to the metal being released from Ybt and the resulting metal-free *apo*-Ybt recycled.

These findings support a model in which Ybt acts as a metallophore that can deliver select physiologic metal ions to UPEC (**Fig 1**). The Ybt system may therefore be fine-tuned for varying host environments to provide a gain-of-function for UPEC. Overall, studies in this thesis present a unique paradigm for *E. coli* copper transport and homeostasis in the urinary tract.

5.2 Perspectives on metal availability in the urinary tract

For pathogenic bacteria, adaptation to host environments is a vital component for establishing an infection and persisting within the host. To defeat the intruding pathogen, the host can deliberately limit the availability of specific transition metals to prevent pathogens from acquiring these vital cofactors, while also increasing the availability of metals such as copper as an antimicrobial strategy (4–6). Therefore depending on the circumstances, the pathogen must sense and counter these changes in the microenvironment. The experimental cystitis model used in this thesis is characterized by a robust inflammatory response and populations of intracellular UPEC within urothelial cells, macrophages and neutrophils (7, 8). Results from this thesis show Ybt import providing a fitness advantage to UPEC in these conditions, suggesting the acquisition of metals through Ybt is important for overcoming the effects of nutritional immunity by the host. Furthermore, previous works have shown Ybt-mediated protection through sequestration of copper ions and interfering with the reactive oxygen species responses in intracellular compartments (1, 2). The findings in this thesis are consistent with these observations as Fe(III)-Ybt is preferentially imported in high Cu(II)-Ybt conditions to prevent excess copper import while maintaining iron transport (3). By protecting UPEC while selecting for iron transport, Ybt

may allow UPEC survival and persistence within immune cells, which in turn may permit dissemination beyond the urinary tract.

In contrast to the copper-rich environments as described above, there may exist microenvironments with low copper availability that may require copper delivery through Ybt. It is interesting to note that *Cryptococcus neoformans*, an opportunistic fungal pathogen encounters varying copper availability during different stages of infection. Upon dissemination to the brain, *C. neoformans* encounters an environment deprived of copper and in response, expresses copper transporters (9–11). Although it is unclear whether UPEC encounters a similar host environment, it does suggest a potential strategy used by the host where copper availability is limited as opposed to in excess. Further studies investigating the metal availability and host responses within urinary tract environments will allow better understanding of Ybt's role in UPEC pathogenesis.

5.3 Implications and outcomes of metallophore transport

The process of siderophore import and metal acquisition requires multiple steps (12–14). The data presented in this thesis provides new insight into our understanding of Ybt's recognition and transport by membrane transporters as well as its intracellular fate. Although multiple metal-Ybt complexes are recognized and imported by the TonB-dependent outer membrane transporter FyuA, the preference for Fe(III)-Ybt over Cu(II)-Ybt import suggests distinct binding interactions between metal-Ybt complexes and FyuA. This is consistent with theoretical structural modeling data supporting a distinctive Cu(II)-Ybt structure from those of other metal-Ybt complexes including Fe(III)-Ybt (3). Although residues in the core β -barrel domain are

heavily conserved among numerous TonB-dependent transporters (TBDT), the extracellular loops are essential for distinct cargo recognition (12). Furthermore, binding of a siderophore to these receptors transduces a signal that may trigger conformational changes and reveal new binding sites (15, 16). Structural analyses investigating the interactions between different metal-Ybt complexes and FyuA could provide insight to FyuA's Cu(II)-Ybt-specificity. TBDT have been the subject of numerous structural investigations to engineer transport substrates that specifically target Gram-negative pathogens (12, 17). Novel binding sites by metal-Ybt complexes may therefore act as targets for future TBDT-dependent inhibitors.

In addition to FyuA, iron acquisition using Ybt requires the inner membrane transporters YbtP and YbtQ (18). The findings in this thesis support a model in which metal-Ybt transport through FyuA and YbtPQ results in metal release and Ybt recycling. Overall, FyuA has been studied in greater detail compared to YbtPQ, in terms of both infection and mechanistic studies. As such, there are several unanswered questions regarding YbtPQ and the fate of metal-Ybt complexes that may provide further insight to this system. Compared to other siderophore systems in *E. coli* such as enterobactin, enzymes associated with metal release from Ybt have yet to be identified (19, 20). Results from this thesis show metal reduction as a potential mechanism of metal release from Ybt. Reduction of Fe(III) to Fe(II) is a proposed model of iron release for several siderophore systems in Gram-negative bacteria, including pyoverdine in *Pseudomonas aeruginosa* and mycobactin in *Mycobacterium tuberculosis* (21, 22). Recent work describing a novel siderophore reductase YqjH in *E. coli* that can release iron from hydrolyzed enterobactin and other catecholate siderophores suggest specific reductases may exist for structurally similar siderophores (20). It is unclear whether yersiniabactin, a phenolate siderophore, is a substrate of

YqjH. Furthermore, as several Gram-negative pathogens including uropathogenic *E. coli*, *Klebsiella pneumonia* and *Yersinia pestis* synthesize yersiniabactin (1, 14, 23), it will be of interest to investigate whether a putative Ybt reductase is conserved in these pathogens away from the *Yersinia* high pathogenicity island. Identification of a Ybt reductase that is conserved among these pathogens may provide an additional therapeutic target.

The intracellular dissociation of Fe(III)-, Cu(II)- and Ni(II)-Ybt complexes results in an intact Ybt molecule and a metal ion. Due to the reactive properties of these metals, they may be rapidly bound to chaperones upon release from Ybt. In the case of iron, the classic cargo for siderophores, previous works have shown glutathione or phosphorylated sugar derivatives as the Fe(II) chaperone prior to transfer to the iron storage protein ferritin or to iron-dependent enzymes (24, 25). However as for copper and nickel, the mechanisms of storage and distribution to metalloproteins is unclear. *E. coli* have several copper defense mechanisms that are extremely sensitive to changes in intracellular copper levels (5, 26, 27). Therefore UPEC must have mechanisms to maintain balance of intracellular copper. Similar to Fe(II), glutathione has also been proposed as a cytoplasmic copper chelator (28). Recent discovery of metallothioneins in *Mycobacterium tuberculosis* suggest these efficient copper chelators, previously studied in eukaryotes models, may also be present in bacteria (10, 29, 30). From these chelators, it is unclear how copper is delivered to *E. coli* cuproenzymes, which are to date, all periplasmic or embedded in the inner membrane (31–33). Recent work suggesting copper efflux ATPases as copper delivery pumps for the *Salmonella* Cu, Zn-superoxide dismutase, suggests novel pathways for copper delivery from the cytoplasm to periplasmic or inner membrane

cuproenzymes (34). Investigating mechanisms of copper acquisition and incorporation by these cuproenzymes would expand our understanding of bacterial copper homeostasis and transport.

The metabolic cost that goes into synthesizing siderophores may be significant during an infection where pathogens are under stress to survive. Recycling of intact siderophores, including Ybt, allows pathogens to conserve scarce resource without constantly synthesizing new siderophore molecules (35, 36). In the case of UPEC, which can encode several siderophore systems, Ybt recycling could perhaps be an additional pathogenic gain-of-function in contrast to enterobactin, which is hydrolyzed prior to iron release. Siderophores as common goods within a bacterial community may suggest these class of recyclable siderophores to benefit the entire bacterial population with relatively minor initial costs. However the evolution of cheater strains as well as counter measures to prevent siderophore piracy suggest a strong relationship between siderophores and bacteria resource management (37, 38). Further investigations comparing the metabolic costs of virulence-associated siderophore systems as well as the prevalence of siderophore cheater strains in polymicrobial infections would expand our understanding of the process of acquiring new siderophore systems or losing components of existing ones by pathogens.

5.4 Methodology development and applications

The methodologies developed in this thesis provide new approaches to unanswered questions in the siderophore field and other areas. The constant neutral loss screen developed by *Chaturvedi* et al., and expanded in this thesis, allow an effective screen to identify stable metabolites with known fragmentation properties that may interact with different metal ions (1, 3). Using the

constant neutral loss screen, we were able to identify novel metal-siderophore complexes and characterize Ybt's metal profile. Taking these newly identified stable metal-siderophore complexes, we developed a quantitative multiple reaction monitoring method to accurately detect and quantify these complexes. This could be applied to numerous conditions that require sensitive detection such as urine or controlled culture conditions. Metabolite profiling and comparisons between clinical isolates using mass spectrometric techniques can provide novel insight to the pathogenicity of numerous pathogens (39–41).

Previous works investigating siderophore transport and metal acquisition have utilized radiolabeled metals or the fluorescent properties of the siderophore (42–45). The quantitative mass spectrometric approach developed in this thesis allows direct comparisons between different metal-bound complexes using non-radioactive metals. Furthermore by specifically quantifying both metal-bound and *apo*-siderophore complexes in the same medium, we could track the siderophore as opposed to the metal to describe new mechanisms in siderophore localization, dissociation and recycling. This in combination with radiolabeling approaches as done in this thesis allow comparisons between the fate of the siderophore and the released metal. While the mass spectrometric techniques allow further investigation of mechanisms of siderophore dissociation, radioactive metals can also be used as sensitive tools for identifying novel co-factors or protein that interact with the imported metal.

5.5 Concluding remarks

The diversity and physiological functions of small metabolites secreted by pathogenic bacteria are areas of great unknowns and interest. This dissertation expands our understanding of the

multi-functional properties of bacterial metabolites in the context of metal homeostasis in the host-pathogen interface. Examining the balance between metal requirements and availability by pathogens may provide a better understanding of the strategies used by pathogens to survive in diverse host environments. This thesis also presents an improved understanding of siderophore systems and raises new questions on the mechanisms of bacterial metalloenzymes, which remain largely uncharacterized (46, 47). With global concerns for rapidly growing antibiotic resistance (48), further examination of the relationship between metabolites and microbial systems may yield novel functions and therapeutic potentials.

CHAPTER FIVE: FIGURES

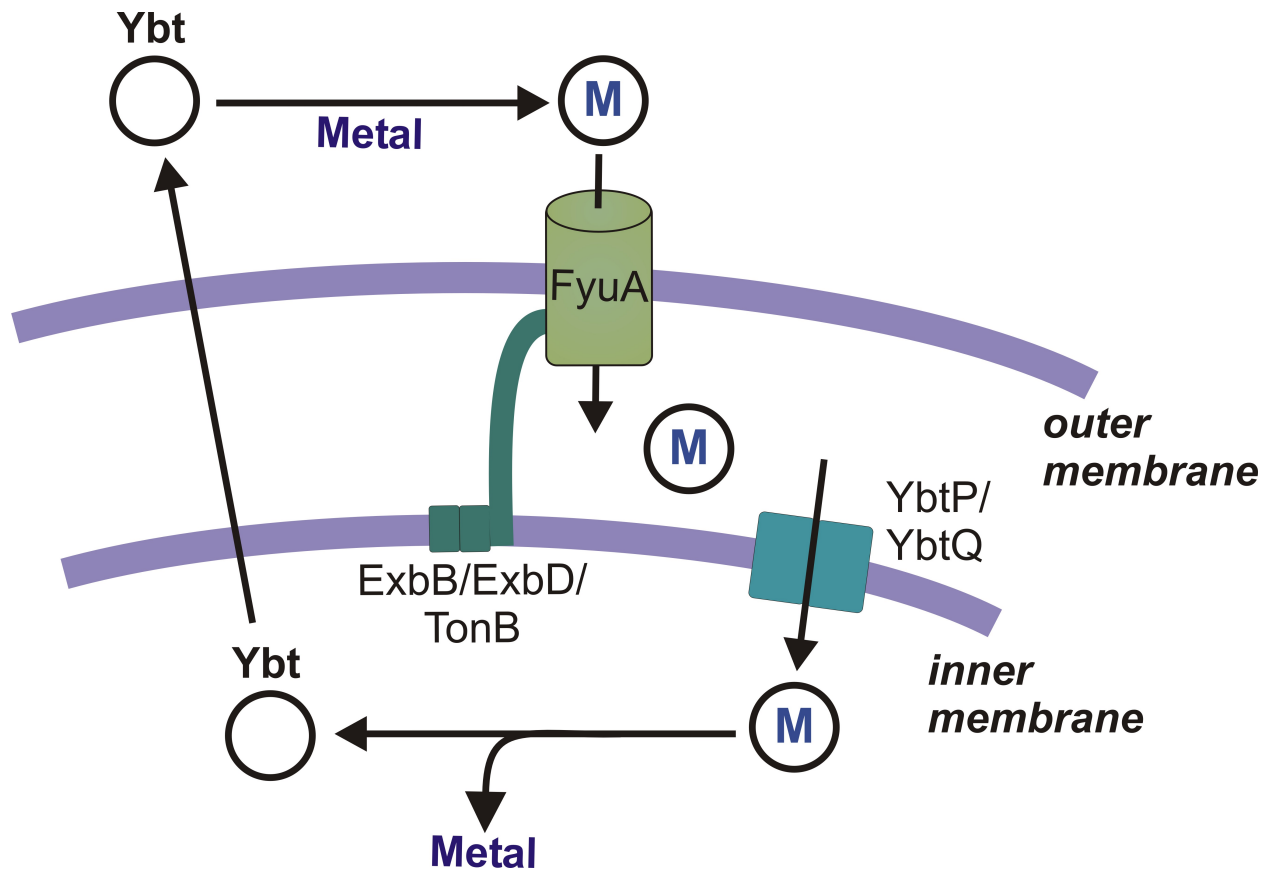


Figure 1. Metal transport and delivery by the yersiniabactin metallophore system.

Extracellular *apo*-Ybt interacts with select transition metals (light blue). Stable metal-Ybt complexes are transported through the TonB-dependent outer membrane receptor, FyuA, and ATP-binding cassette inner membrane transporters, YbtP and YbtQ. Select metal ions are released from intracellular metal-Ybt complexes and *apo*-Ybt is subsequently recycled to the extracellular matrix.

CHAPTER FIVE: REFERENCES

1. Chaturvedi, K. S., Hung, C. S., Crowley, J. R., Stapleton, A. E., and Henderson, J. P. (2012) The siderophore yersiniabactin binds copper to protect pathogens during infection. *Nat. Chem. Biol.* 10.1038/nchembio.1020
2. Chaturvedi, K. S., Hung, C. S., Giblin, D. E., Urushidani, S., Austin, A. M., Dinauer, M. C., and Henderson, J. P. (2013) Cupric Yersiniabactin Is a Virulence-Associated Superoxide Dismutase Mimic. *ACS Chem. Biol.* **9**, 551–561
3. Koh, E.-I., Hung, C. S., Parker, K. S., Crowley, J. R., Giblin, D. E., and Henderson, J. P. (2015) Metal selectivity by the virulence-associated yersiniabactin metallophore system. *Metallomics.* **7**, 1011–1022
4. Hood, M. I., and Skaar, E. P. (2012) Nutritional immunity: transition metals at the pathogen–host interface. *Nat. Rev. Microbiol.* **10**, 525–537
5. Chaturvedi, K. S., and Henderson, J. P. (2014) Pathogenic adaptations to host-derived antibacterial copper. *Front. Cell. Infect. Microbiol.* **4**, 3
6. Prentice, A. M., Ghattas, H., and Cox, S. E. (2007) Host-Pathogen Interactions: Can Micronutrients Tip the Balance? *J. Nutr.*
7. Schwartz, D. J., Chen, S. L., Hultgren, S. J., and Seed, P. C. (2011) Population dynamics and niche distribution of uropathogenic *Escherichia coli* during acute and chronic urinary tract infection. *Infect. Immun.* **79**, 4250–9
8. Hannan, T. J., Mysorekar, I. U., Hung, C. S., Isaacson-Schmid, M. L., and Hultgren, S. J. (2010) Early Severe Inflammatory Responses to Uropathogenic *E. coli* Predispose to Chronic and Recurrent Urinary Tract Infection. *PloS Pathog.*

9. Sun, T.-S., Ju, X., Gao, H.-L., Wang, T., Thiele, D. J., Li, J.-Y., Wang, Z.-Y., and Ding, C. (2014) Reciprocal functions of *Cryptococcus neoformans* copper homeostasis machinery during pulmonary infection and meningoencephalitis. *Nat. Commun.* **5**, 5550
10. Ding, C., Yin, J., Tovar, E. M. M., Fitzpatrick, D. A., Higgins, D. G., and Thiele, D. J. (2011) The Cu regulon of the human fungal pathogen *Cryptococcus neoformans* H99: Cuf1 activates distinct genes in response to both Cu excess and deficiency. *Mol. Microbiol.* **81**, 1560–1576
11. García-Santamarina, S., and Thiele, D. J. (2015) Copper at the Fungal Pathogen-Host Axis. *J. Biol. Chem.* **290**, 18945–18953
12. Noinaj, N., Guillier, M., Barnard, T. J., and Buchanan, S. K. (2010) TonB-Dependent Transporters: Regulation, Structure, and Function. *Annu. Rev. Microbiol.*
13. Schalk, I. J. (2008) Metal trafficking via siderophores in Gram-negative bacteria: specificities and characteristics of the pyoverdine pathway. *J. Inorg. Biochem.* **102**, 1159–69
14. Perry, R. D., and Fetherston, J. D. (2011) Yersiniabactin iron uptake: mechanisms and role in *Yersinia pestis* pathogenesis. *Microbes Infect. Inst. Pasteur.* **13**, 808–17
15. Cobessi, D., Meksem, A., and Brillet, K. (2010) Structure of the heme/hemoglobin outer membrane receptor ShuA from *Shigella dysenteriae*: heme binding by an induced fit mechanism. *Proteins.* **78**, 286–294
16. Yue, W. W., Grizot, S., and Buchanan, S. K. (2003) Structural evidence for iron-free citrate and ferric citrate binding to the TonB-dependent outer membrane transporter FecA. *J. Mol. Biol.* **332**, 353–368

17. Lukacik, P., Barnard, T. J., Keller, P. W., Chaturvedi, K. S., Seddiki, N., Fairman, James W., Noinaj, N., Kirby, T. L., Henderson, J. P., Steven, A. C., Hinnebusch, B. J., and Buchanan, S. K. (2012) Structural engineering of a phage lysin that targets Gram-negative pathogens. *PNAS*. **109**, 9857–9862
18. Fetherston, J. D., Bertolino, V. J., and Perry, R. D. (1999) YbtP and YbtQ: two ABC transporters required for iron uptake in *Yersinia pestis*. *Mol. Microbiol.* **32**, 289–99
19. Lin, H., Fischbach, M. A., Liu, D. R., and Walsh, C. T. (2005) In Vitro Characterization of Salmochelin and Enterobactin Trilactone Hydrolases IroD, IroE, and Fes. *J Am Chem Soc.* **127**, 11075–11084
20. Miethke, M., Hou, J., and Marahiel, M. A. (2011) The siderophore-interacting protein YqjH acts as a ferric reductase in different iron assimilation pathways of *Escherichia coli*. *Biochemistry (Mosc.)*. **50**, 10951–64
21. Imperi, F., Tiburzi, F., and Visca, P. (2009) Molecular basis of pyoverdine siderophore recycling in *Pseudomonas aeruginosa*. *PNAS*. **106**, 20440–20445
22. Jones, C. M., Wells, R. M., Madduri, A. V. R., Renfrow, M. B., Ratledge, C., Moody, D. B., and Niederweis, M. (2014) Self-poisoning of *Mycobacterium tuberculosis* by interrupting siderophore recycling. *Proc. Natl. Acad. Sci.* **111**, 1945–1950
23. Lawlor, M. S., O'Connor, C., and Miller, V. L. (2007) Yersiniabactin Is a Virulence Factor for *Klebsiella pneumoniae* during Pulmonary Infection. *Infect. Immun.* **75**, 1463–1472
24. Böhnke, R., and Matzanke, B. F. (1995) The mobile ferrous iron pool in *Escherichia coli* is bound to a phosphorylated sugar derivative. *Biometals Int. J. Role Met. Ions Biol. Biochem. Med.* **8**, 223–230

25. Hider, R. C., and Kong, X. L. (2011) Glutathione: a key component of the cytoplasmic labile iron pool. *BioMetals*. **24**, 1179–1187
26. Outten, F. W., Huffman, D. L., Hale, J. A., and O'Halloran, T. V. (2001) The independent cue and cus systems confer copper tolerance during aerobic and anaerobic growth in *Escherichia coli*. *J Biol Chem*. **276**, 30670–7
27. Rensing, C., Fan, B., Sharma, R., Mitra, B., and Rosen, B. P. (2000) CopA: An *Escherichia coli* Cu(I)-translocating P-type ATPase. *Proc. Natl. Acad. Sci. U. S. A.* **97**, 652–6
28. Helbig, K., Bleuel, C., Krauss, G. J., and Nies, D. H. (2008) Glutathione and Transition-Metal Homeostasis in *Escherichia coli*. *J. Bacteriol.* **190**, 5431–5438
29. Thrower, A. R., Byrd, J., Tarbet, E. B., Mehra, R. K., Hamer, D. H., and Winge, D. R. (1988) Effect of mutation of cysteinyl residues in yeast Cu-metallothionein. *J. Biol. Chem.* **263**, 7037–7042
30. Robinson, N. J. (2008) A bacterial copper metallothionein. *Nat. Chem. Biol.* **4**, 582–583
31. Grass, G., and Rensing, C. (2001) CueO Is a Multi-copper Oxidase That Confers Copper Tolerance in *Escherichia coli*. *Biochem. Biophys. Res. Commun.* **286**, 902–908
32. Imlay, K. R., and Imlay, J. A. (1996) Cloning and analysis of *sodC*, encoding the copper-zinc superoxide dismutase of *Escherichia coli*. *J. Bacteriol.* **178**, 2564–2571
33. Minagawa, J., Mogi, T., Gennis, R. B., and Anraku, Y. (1992) Identification of heme and copper ligands in subunit I of the cytochrome bo complex in *Escherichia coli*. *J. Biol. Chem.* **267**, 2096–2104
34. Osman, D., Patterson, C. J., Bailey, K., Fisher, K., Robinson, N. J., Rigby, S. E., and Cavet, J. S. (2013) The copper supply pathway to a *Salmonella* Cu,Zn-superoxide dismutase

- (SodCII) involves P(1B)-type ATPase copper efflux and periplasmic CueP. *Mol. Microbiol.* **87**, 466–77
35. Crosa, J. H., and Walsh, C. T. (2002) Genetics and assembly line enzymology of siderophore biosynthesis in bacteria. *Microbiol. Mol. Biol. Rev.* **66**, 223–249
 36. Lv, H., Hung, C. S., and Henderson, J. P. (2014) Metabolomic analysis of siderophore cheater mutants reveals metabolic costs of expression in uropathogenic *Escherichia coli*. *J. Proteome Res.* **13**, 1397–404
 37. Hancock, V., Vejborg, R. M., and Klemm, P. (2010) Functional genomics of probiotic *Escherichia coli* Nissle 1917 and 83972, and UPEC strain CFT073: comparison of transcriptomes, growth and biofilm formation. *Mol. Genet. Genomics.* **284**, 437–454
 38. Youard, Z. A., Mislin, G. L. A., Majcherczyk, P. A., Schalk, I. J., and Reimann, C. (2007) *Pseudomonas fluorescens* CHA0 produces enantio-pyochelin, the optical antipode of the *Pseudomonas aeruginosa* siderophore pyochelin. *J. Biol. Chem.* **282**, 35546–35553
 39. Henderson, J. P., Crowley, J. R., Pinkner, J. S., Walker, J. N., Tsukayama, P., Stamm, W. E., Hooton, T. M., and Hultgren, S. J. (2009) Quantitative Metabolomics Reveals an Epigenetic Blueprint for Iron Acquisition in Uropathogenic *Escherichia coli*. *PLoS Pathog.*
 40. Bachman, M. A., Oyler, J. E., Burns, S. H., Caza, M., Lepine, F., Dozois, C. M., and Weiser, J. N. (2011) *Klebsiella pneumoniae* yersiniabactin promotes respiratory tract infection through evasion of lipocalin 2. *Infect. Immun.* **79**, 3309–16
 41. Crouch, M.-L. V., Castor, M., Karlinsey, J. E., Kalthorn, T., and Fang, F. C. (2008) Biosynthesis and IroC-dependent export of the siderophore salmochelin are essential for virulence of *Salmonella enterica* serovar Typhimurium. *Mol. Microbiol.* **67**, 971–983

42. Braud, A., Geoffroy, V., Hoegy, F., Mislin, G. L., and Schalk, I. J. (2010) Presence of the siderophores pyoverdine and pyochelin in the extracellular medium reduces toxic metal accumulation in *Pseudomonas aeruginosa* and increases bacterial metal tolerance. *Environ. Microbiol. Rep.* **2**, 419–25
43. Braud, A., Hannauer, M., Mislin, G. L., and Schalk, I. J. (2009) The *Pseudomonas aeruginosa* pyochelin-iron uptake pathway and its metal specificity. *J. Bacteriol.* **191**, 3517–25
44. Emery, T. (1971) Role of ferrichrome as a ferric ionophore in *Ustilago sphaerogena*. *Biochemistry (Mosc.)*. **10**, 1483–8
45. Ecker, D. J., and Emery, T. (1983) Iron uptake from ferrichrome A and iron citrate in *Ustilago sphaerogena*. *J. Bacteriol.* **155**, 616–22
46. Cvetkovic, A., Menon, A. L., Thorgersen, M. P., Scott, J. W., Poole, F. L., 2nd, Jenney, F. E., Jr., Lancaster, W. A., Praissman, J. L., Shanmukh, S., Vaccaro, B. J., Trauger, S. A., Kalisiak, E., Apon, J. V., Siuzdak, G., Yannone, S. M., Tainer, J. A., and Adams, M. W. (2010) Microbial metalloproteomes are largely uncharacterized. *Nature*. **466**, 779–82
47. Waldron, K. J., and Robinson, N. J. (2009) How do bacterial cells ensure that metalloproteins get the correct metal? *Nat. Rev. Microbiol.* **7**, 25–35
48. World Health Organization (2014) *Antimicrobial resistance: global report on surveillance 2014*, World Health Organization

Eun-Ik Koh

Curriculum Vitae

- Education** Ph.D. in Molecular Microbiology and Microbial Pathogenesis
Washington University in St. Louis May 2016
- B.S. in Molecular and Cellular Biology
University of Illinois at Urbana-Champaign May 2010
- Research Experience** Washington University in St. Louis
Graduate Student March 2011 to December 2015
Advisor: Jeffrey P. Henderson, M.D., Ph.D.
Metal selectivity and acquisition by the yersiniabactin metallophore system in uropathogenic Escherichia coli
- University of Illinois at Urbana-Champaign
Undergraduate Thesis Researcher May 2007 to May 2010
Advisors: Steven R. Blanke, Ph.D., Manfredo J. Seufferheld, Ph.D.
Biochemical characterization of Helicobacter pylori acidocalcisome-like granules
- Publications** Koh, E., Hung, C. S., Parker, K. S., Crowley, J. R., Giblin, D. E., and Henderson, J. P., (2015) Metal selectivity by the virulence-associated yersiniabactin metallophore system. *Metallomics*, 7, 1011-1022
- Koh, E., and Henderson, J. P., (2015) Microbial copper-binding siderophores at the host-pathogen interface. *Journal of Biological Chemistry*, 290 (31), 18967-18974
- Chandrasekaran, S., Ghosh, J., Port, G., Koh, E., and Caparon, M. G., (2013) Analysis of polymorphic residues reveals distinct enzymatic and cytotoxic activities of the Streptococcus pyogenes NAD⁺ glycohydrolase. *The Journal of biological chemistry*, 288(27): p. 20064-20075.
- Koh, E., Hung, C. S., and Henderson, J. P., The yersiniabactin-associated ATP binding cassette transporters YbtP and YbtQ enhance *E. coli* fitness during high titer cystitis. (Under review)

Koh, E., Bandara, N., Tran, H. D., Rogers, R. E., and Henderson, J. P., Metal acquisition by the virulence-associated yersiniabactin metallophore system. (In preparation)

Teaching Experience Washington University in St Louis
Teaching Assistant Spring 2012
Principles of Biology I

Honors Francis and Harlie Clark Research Excellence Award in Microbiology 2010
Francis and Harlie Clark Research Award in Microbiology 2009
Biology Open House Best Poster Award 2009
Dean's List, University of Illinois at Urbana-Champaign 2006

Conference Abstracts Koh, E., Hung, C. S., Parker, K. S., Crowley, J. R., Giblin, D. E., and Henderson, J. P., Metal selectivity by the virulence-associated Yersiniabactin metallophore system. Gordon Research Conference on Cell Biology of Metals, Mount Snow, VT, July 2015. Poster Presentation

Koh, E., Hung, C. S., Parker, K. S., Crowley, J. R., Giblin, D. E., and Henderson, J. P., Metal selectivity by the Yersiniabactin metallophore system in Uropathogenic Escherichia coli. 21th Annual Midwest Microbial Pathogenesis Conference, Chicago, IL, September 2014. Poster Presentation

Koh, E., Hung, C. S., Crowley, J. R., and Henderson, J. P., Gatekeeping: Metal selectivity by the Yersiniabactin siderophore system in Uropathogenic Escherichia coli. 20th Annual Midwest Microbial Pathogenesis Conference, Columbus, OH, September 2013. Poster Presentation

Koh, E., Hung, C. S., Crowley, J. R., and Henderson, J. P., Gatekeeping: Metal selectivity by the Yersiniabactin siderophore system in Uropathogenic Escherichia coli. William H. Danforth Scientific Symposium, St Louis, MO, November 2013. Poster Presentation

Invited talks "Metal selectivity by the virulence-associated Yersiniabactin metallophore system". 2015 Molecular Microbiology & Microbial Pathogenesis Retreat, St. Louis, MO, September 2015.

Professional Memberships Korean-American Scientists and Engineers Association
American Society for Microbiology